

**SURFACE SOIL MOISTURE
RETRIEVAL OVER HETEROGENEOUS
AGRICULTURAL PLOTS USING SAR
OBSERVATIONS**

Thesis

Submitted in partial fulfilment of the requirements for the degree of

DOCTOR OF PHILOSOPHY

by

**PUNITHRAJ G
165079AM16F10**



**DEPARTMENT OF WATER RESOURCES & OCEAN
ENGINEERING
NATIONAL INSTITUTE OF TECHNOLOGY KARNATAKA
SURATHKAL, MANGALORE – 575 025
DECEMBER 2022**

**SURFACE SOIL MOISTURE
RETRIEVAL OVER HETEROGENEOUS
AGRICULTURAL PLOTS USING SAR
OBSERVATIONS**

Thesis

Submitted in partial fulfilment of the requirements for the degree of

DOCTOR OF PHILOSOPHY

by

PUNITHRAJ G

165079AM16F10

Under the guidance of

Dr. Pruthviraj U
Assistant Professor

Prof. Amba Shetty
Professor



**DEPARTMENT OF WATER RESOURCES & OCEAN
ENGINEERING
NATIONAL INSTITUTE OF TECHNOLOGY KARNATAKA
SURATHKAL, MANGALORE – 575 025
DECEMBER 2022**

D E C L A R A T I O N

By the Ph.D. Research Scholar

I hereby declare that the Research Thesis entitled "**SURFACE SOIL MOISTURE RETRIEVAL OVER HETEROGENEOUS AGRICULTURAL PLOTS USING SAR OBSERVATIONS**", which is being submitted to the **National Institute of Technology Karnataka, Surathkal** in partial fulfilment of the requirements for the award of the Degree of **Doctor of Philosophy** in the **Department Of Water Resources & Ocean Engineering** is a bonafide report of the research work carried out by me. The material contained in this Research Thesis has not been submitted to any University or Institution for the award of any degree.



165071AM16F10, PUNITHRAJ G

(Register Number, Name & Signature of the Research Scholar)

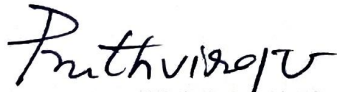
Department of Water Resources and Ocean Engineering
National Institute of Technology Karnataka, Surathkal


Place: NITK-Surathkal

Date: 06/14/2022

C E R T I F I C A T E

This is to certify that the Research Thesis entitled "**SURFACE SOIL MOISTURE RETRIEVAL OVER HETEROGENEOUS AGRICULTURAL PLOTS USING SAR OBSERVATIONS**" submitted by **PUNITHRAJ G** (Register Number: 165071 AM16F10) as the record of the research work carried out by him, is accepted as the Research Thesis submission in partial fulfilment of the requirements for the award of degree of **Doctor of Philosophy**.


Dr. PRUTHVIRAJ U
Assistant Professor
Research Guide


Prof. AMBA SHETTY
Professor
Research Guide


Prof. B. M. Dodamani

Chairman (DRPC)
Chairman - DRPC
Dept. of Water Resources & Ocean Engineering



Department of Water Resources and Ocean Engineering
National Institute of Technology Karnataka, Surathkal

ACKNOWLEDGEMENT

With deep sense of gratitude, I express my heartfelt thanks to my research supervisor Dr. Pruthviraj U, Assistant Professor, and Prof. Amba Shetty, Professor, Department of Water Resources and Ocean Engineering, NITK for their invaluable guidance, encouragement and motivation throughout my research work. I am indebted to them for their wholehearted interest and keenness in every phase of research work and thesis preparation. Their moral support, guidance, interactions, discussions and precious suggestions have greatly helped me to complete this research work. It has been my greatest opportunity and pleasure to work under them. Their crucial comments have guided me to publish my research work in acclaimed International Journals. I would also thank Prof. Y. S Rao, Professor, Indian Institute of Technology Bombay for their valuable inputs in processing SAR images and technical suggestions. I would also like to convey my sincere thanks to my Research Progress Assessment Committee members, Prof. Lakshman Nandagiri, Department of Water Resources and Ocean Engineering, and Dr. Suresha S.N, Department of Civil Engineering for providing valuable suggestions, comments and encouragement at various stages of this research work.

I would like to thank Prof. Dodamani B M, Head of the Department of Civil Engineering and the former Heads Prof. Amba Shetty, Prof. A. Mahesha and Prof. Dwarakish G S, for all the support throughout my stay at NITK campus. I am also thankful to all faculty and staff of Water Resources and Ocean Engineering Department for their help and support.

My special thanks to Mr. Balakrishna, GIS Lab, who made sure that laboratory facilities were working fine all the time and helped me out whenever in trouble. My sincere thanks to Mr. Seetharam, and Mr. Anil Kumar Water Resources and Ocean Engineering Department for their help in procuring data and department facilities. I am grateful for the help and co-operation rendered by non-teaching staff and office staff of Water Resources and Ocean Engineering Department.

My special thanks to Narayanswamy, Mahadevanna, and Mahesh, farmers of Malavalli for allowing to collect the field data from their respective agricultural fields during the study period. I gratefully acknowledge Tammayya, Sidhanna and Lingraju who helped me to collect field data.

I am forever grateful to my father Sri. Gururaj M D, mother Smt. Pushpalatha P R, and my brother Mr. Naveenraj G, who provided me the best education and encouraged in all my endeavors motivating me in this journey with moral support and cooperation.

I lovingly acknowledge the moral support and help extended by my research colleagues during this journey. Their informal support and encouragement has been very crucial. I am grateful to everybody who helped and encouraged me during this research work.

Punithraj G

Dedication

I dedicate this thesis to my beloved parents,

&

Along with those close to my heart

Family members and Friends

ABSTRACT

Soil moisture is a basic component of meteorological cycle and in the determination of agricultural crop yield. Spatial information about soil moisture over agricultural crops is required for efficient irrigation, which in turn helps in saving water and increases the crop yield. However, capturing spatiotemporal field measurement of soil moisture is time consuming and not a practical approach. Synthetic Aperture Radar (SAR) remote sensing is a valuable tool for retrieving surface soil moisture over agricultural fields owing to its great sensitivity to surface soil moisture.

The objective of the research is retrieval surface soil moisture over typical heterogeneous agricultural plots of a semi-arid region of India using C and L band polarized SAR data. A methodology is developed to retrieve surface soil moisture over different agricultural fields at different crop stages. To implement the methodology, a typical agriculture-dominated landscape has been selected. For the study, different agricultural plots of Malavalli village in Karnataka, were selected. Agricultural crops include; crops like Paddy, Tomato, Maize, Sugarcane and a reference bare field. Agricultural plots of size 1 acre approximately, were selected and sampling grids were made according to SAR ground resolutions. Field measured data like surface soil moisture, surface roughness, soil texture, vegetation height and vegetation water content were collected from every grid of the agricultural plots in synchronization with satellite pass. Sentinel-1a, C-band data and ALOS PALSAR-2, L-band SAR data products are used to retrieve surface soil moisture. The developed models were compared with existing models and validated using field measure values.

Surface soil moisture was retrieved using L-band SAR across agricultural plots at two distinct crop stages. Initially, processed SAR images are decomposed using Freeman Durden, Yamaguchi and Van-Zyl decomposition techniques to know the major scattering components (like surface, dihedral, and volume scattering). In vegetative crop stage, surface scattering (>34%) is dominating scattering component, which shows less interaction of vegetation with radar backscattering energy.

Surface scattering component of Yamaguchi decomposition has dependence on field measured surface soil moisture with $R^2 > 0.5$ good correlation. Multilinear regression (MLR) is carried out in which soil moisture (M_v) is a dependent variable and $\sigma_{surface}^{\circ}$, σ_{VH-VV}° and $\sigma_{Dihedral}^{\circ}$ are considered as independent variables and validated. To assess the resilience of the developed models, it is compared with existing models like Oh 1992, Oh 2004, X-Bragg and WCM. RMSE of developed model varies from 0.82 to 2.51 cm^3/cm^3 for two distinct crop stages. Whereas, in case of sugarcane at grand growing stage none of models performed well (RMSE= 3.64~4.7 % gm/cm^3). X-Bragg model is underestimating surface soil moisture in two distinct crop stages of paddy, maize, tomato and sugarcane field plots (RMSE= 1.21~4.23 % gm/cm^3).

In the same way, surface soil moisture is retrieved using C-band SAR across above mentioned agricultural plots for whole crop cycle of each crop at an interval of 12 days. Each crop cycle is divided into vegetative, maturity, yield formation stage and surface soil moisture of each crop stage is estimated. The relationship between backscattered energy and soil moisture, roughness and vegetation parameter (RVI) is analyzed and MLR analysis is carried out to develop semi empirical model (SEM) and validated against grid sampled field data (RMSE= 1.3~8.1 % gm/cm^3). The developed model found to be better when compared with Oh model, 1994. In grand growing stage of sugarcane and yield formation stage of maize and sugarcane, the RMSE values were found to 4.1~8.1 % gm/cm^3 . Which shows the vegetation attenuation increased as the crop matures and affecting soil moisture retrieval beneath it.

Performance of C-band dual polarized data with L-band quad polarized data at two different crop stages were compared for surface soil moisture retrieval. Quad polarized data is found to performing better than dual polarized data. At various crop stages, the proposed semi-empirical model for retrieving surface soil moisture functions effectively. In future, the developed model can be simplified by introducing constant parameters based on crop stage and type of crop. This study helps to understand the spatial variation of soil moisture within the small plots thus helping marginal farmers and local irrigation departments for better allocation of water resources.

Keywords: Soil moisture; SAR; backscattering model; PolSAR; Oh model; X-Bragg

TABLE OF CONTENTS

Description	Page no
ABSTRACT	i-ii
TABLE OF CONTENTS	iii-v
LIST OF FIGURES	vi-x
LIST OF TABLES	xi-xii
ABBREVIATIONS	xiii-xv
NOMENCLATURE	xiv

Chapter no.	Title	Page no.
1	INTRODUCTION	1-8
1.1	BACKGROUND	1
1.2	SOIL MOISTURE MEASUREMENT BY REMOTE SENSING	3
1.3	STATEMENT OF THE PROBLEM AND RESEARCH SCOPE	5
1.4	RESEARCH OBJECTIVES	7
1.5	THESIS OUTLINE	7
2	MICROWAVE REMOTE SENSING	9-18
2.1	INTRODUCTION	9
2.2	DIFFERENT WAVELENGTHS AND POLARIZATION OF SAR	9
2.3	ACTIVE MICROWAVE REMOTE SENSING	11
2.4	PASSIVE MICROWAVE REMOTE SENSING	11
2.5	FACTORS INFLUENCING SOIL MOISTURE RETRIEVAL USING MICROWAVE REMOTE SENSING	12
2.5.1	Dielectric constant	13
2.5.2	Thermal sampling depth	13
2.5.3	Surface roughness	14
2.5.4	Vegetation effects	14
2.6	PAST AND CURRENT MICROWAVE SPACE BORNE-SENSORS	15
3	LITERATURE REVIEW	19-50
3.1	INTRODUCTION	19

3.2	SURFACE SOIL MOISTURE RETRIEVAL USING EMPIRICAL AND SEMI EMPIRICAL MODELS	20
3.3	SURFACE SOIL MOISTURE RETRIEVAL USING THEORETICAL MODELS	31
3.4	SURFACE SOIL MOISTURE MODELS COMPARATIVE STUDIES	39
3.5	SUMMARY OF LITERATURE REVIEW AND RESEARCH GAPS	49
4	MATERIALS AND RESEARCH METHODOLOGY	51-62
4.1	INTRODUCTION	51
4.2	STUDY SITE AND ITS SALIENT FEATURES	51
	4.2.1 Topography	53
	4.2.2 Climate	53
	4.2.3 Geology and soil	54
4.3	DATA PRODUCTS AND TOOLS	54
	4.3.1 Sentinel-1a	54
	4.3.2 ALOS PALSAR-2	55
	4.3.3 SRTM	56
	4.3.4 Google earth data	56
	4.3.5 Soil and Vegetation data	56
	4.3.6 Rainfall data	57
4.4	TOOLS	57
4.5	RESEARCH METHODOLOGY	58
4.6	SURFACE SOIL MOISTURE MODELS	59
5	DATA COLLECTION, PROCESSING AND ANALYSIS	63-86
5.1	RECONNAISSANCE SURVEY	63
5.2	SAMPLING LOCATIONS IDENTIFICATION	63
	5.2.1 Sampling locations for Sentinel-1a data	64
	5.2.2 Sampling locations for ALOS PALSAR-2 data	71
5.3	SAMPLING COLLECTION AND TRANSPORT	72
5.4	EXPERIMENTAL MEASUREMENTS	74
	5.4.1 Gravimetric soil moisture	74
	5.4.2 Volumetric soil moisture	74
	5.4.3 Vegetation water content	75
5.5	IMAGE PROCESSING	75
	5.5.1 Sentinel-1a image	75
	5.5.2 ALOS PALSAR-2 image	77
5.6	SENTINEL-1A DATA ANALYSIS	78
	5.6.1 Bare field	78

5.6.2	Maize field	79
5.6.3	Paddy field	80
5.6.4	Tomato field	82
5.6.5	Sugarcane field	83
5.7	ALOS PALSAR-2 DATA ANALYSIS	85
5.8	Crop height	89
5.9	Vegetation water content	90
6	RESULTS AND DISCUSSION	91-134
6.1	INTRODUCTION	91
6.2	SPATIO-TEMPORAL VARIATION OF SURFACE SOIL MOISTURE	91
6.3	SURFACE SOIL MOISTURE RETRIEVAL USING SAR	92
6.3.1	Surface soil moisture retrieval using quad-pol, L-band SAR	92
6.3.1.1	Model development	99
6.3.1.2	Regression analysis	101
6.3.1.3	Semi empirical modelling	117
6.3.1.4	Validation	119
6.3.2	Surface soil moisture retrieval using dual-pol, C-band SAR	121
6.3.2.1	Model development	122
6.3.2.2	Semi empirical modelling	130
6.3.2.3	Validation	133
6.4	COMPARISON OF QUAD AND DUAL-POL SURFACE SOIL MOISTURE	134
7	SUMMARY AND CONCLUSIONS	135-138
7.1	Summary	135
7.2	Conclusions	136
7.3	Limitations of the work	137
7.4	Scope of the future work	137
	REFERENCES	139-156
	PUBLICATIONS	157-158

LIST OF FIGURES

Figure No.	Description	Page No.
4.1	Location of the study area	52
4.2	Google Earth View of Study area	53
4.3	Research methodological framework of the study	58
5.1A	Sampling locations of bare field for Sentinel-1a acquisitions	64
5.1B	Sampling locations of maize field for Sentinel-1a acquisitions	65
5.1C	Sampling locations of paddy field for Sentinel-1a acquisitions	65
5.1D	Sampling locations of sugarcane field for Sentinel-1a acquisitions	66
5.1E	Sampling locations of tomato field for Sentinel-1a acquisitions	66
5.2A	Field photographs of Maize crop during field data acquisition	67
5.2B	Field photographs of Paddy crop during field data acquisition	68
5.2C	Field photographs of Sugarcane crop during field data acquisition	70
5.2D	Field photographs of Tomato crop during field data acquisition	71
5.3A	Sampling locations of bare field and sugarcane field for ALOS PALSAR-2 acquisitions	71
5.3B	Sampling locations of paddy and tomato field for ALOS PALSAR-2 acquisitions	72
5.3C	Sampling locations of maize field for ALOS PALSAR-2 acquisitions	72
5.4	Pre-processing steps of Sentinel-1a	76
5.5	Pre-processing steps of ALOS PALSAR-2	78
5.6	Spatio-temporal variation of VV and VH backscattered energy within the bare field during Sentinel-1a pass	79
5.7	Spatio-temporal variation of soil moisture within the bare field during Sentinel-1a pass	79
5.8	Spatio-temporal variation of VV and VH backscattered energy within Maize field during Sentinel-1a pass	80
5.9	Spatio-temporal variation of soil moisture within Maize field during Sentinel-1a pass	80
5.10	Spatio-temporal variation of VV and VH backscattered energy within Paddy field during Sentinel-1a pass	81

5.11	Spatio-temporal variation of soil moisture within Paddy field during Sentinel-1a pass	82
5.12	Spatio-temporal variation of VV and VH Backscattered Energy within Tomato Field during Sentinel-1a pass	83
5.13	Spatio-temporal variation of soil moisture within tomato field during Sentinel-1a pass	83
5.14	Spatio-temporal variation of VV backscattered energy within sugarcane field during Sentinel-1a pass	84
5.15	Spatio-temporal variation of VH backscattered energy within sugarcane field during Sentinel-1a pass	84
5.16	Spatio-temporal variation of soil moisture within sugarcane field during Sentinel-1a pass	84
5.17	Spatio-temporal variation of backscattered energy within barren field during ALOS PALSAR-2 pass	85
5.18	Spatio-temporal variation of soil moisture within barren field during ALOS PALSAR-2 pass	85
5.19	Spatio-temporal variation of backscattered energy within paddy field during ALOS PALSAR-2 pass	86
5.20	Spatio-temporal variation of soil moisture within paddy field during ALOS PALSAR-2 pass	86
5.21	Spatio-temporal variation of backscattered energy within tomato field during ALOS PALSAR-2 pass	87
5.22	Spatio-temporal variation of soil moisture within tomato field during ALOS PALSAR-2 pass	87
5.23	Spatio-temporal variation of backscattered energy within sugarcane field during ALOS PALSAR-2 pass	87
5.24	Spatio-temporal variation of soil moisture within sugarcane field during ALOS PALSAR-2 pass	88
5.25	Spatio-temporal variation of backscattered energy within maize field during ALOS PALSAR-2 pass	88
5.26	Spatio-temporal variation of soil moisture within maize field during ALOS PALSAR-2 pass	88
5.27	Crop height variation of paddy, sugarcane, tomato and maize crops during Sentinel-1a pass	89
5.28	VWC variation of paddy, sugarcane, tomato and maize crop during Sentinel-1a pass	90
6.1	Mean surface soil moisture collected from time series in situ data for each agricultural plots	91
6.2	Surface soil moisture maps of 23/07/2018 derived using Oh 1992 (a), Oh 2004 (b) and X-Bragg (c) models	93,94,95

6.3	Surface soil moisture maps of 01/10/2018 derived using Oh 1992 (a), Oh 2004 (b) and X-Bragg (c) models	96,97,98
6.4	Proportion analysis of three polarization decomposition techniques of Maize	100
6.5	Proportionality of three scattering components on 23/07/2018 of paddy, Tomato, sugarcane and fallow field	101
6.6	Proportionality of three scattering components on 01/10/2018 of paddy, Tomato, sugarcane and fallow field	101
6.7	Relationship between polarization (HH, HV, VV & VH), surface scattering component, dihedral component and field-measured soil moisture at growing stage of maize (23/07/2018) (FD3-Freeman Durden; Y4- Yamaguchi and VZ4-Van Zyl polarimetric decomposition technique)	103
6.8	Relationship between polarization (HH, HV, VV & VH), surface scattering component, dihedral component and field-measured soil moisture at vegetative stage of paddy (23/07/2018) (FD3-Freeman Durden; Y4- Yamaguchi and VZ4-Van Zyl polarimetric decomposition)	105
6.9	Relationship between polarization (HH, HV, VV & VH), surface scattering component, dihedral component and field-measured soil moisture at vegetative stage of paddy (01/10/2018) (FD3-Freeman Durden; Y4- Yamaguchi and VZ4-Van Zyl polarimetric decomposition)	107
6.10	Relationship between polarization (HH, HV, VV & VH), surface scattering component, dihedral component and field-measured soil moisture at vegetative stage of Tomato field (23/07/2018) (FD3- Freeman Durden; Y4- Yamaguchi and VZ4-Van Zyl polarimetric decomposition)	109
6.11	Relationship between polarization (HH, HV, VV & VH), surface scattering component, dihedral component and field-measured soil moisture at first harvest stage of Tomato field (01/10/2018) (FD3- Freeman Durden; Y4- Yamaguchi and VZ4-Van Zyl polarimetric decomposition)	111
6.12	Relationship between polarization (HH, HV, VV & VH), surface scattering component, dihedral component and field-measured soil moisture at vegetative stage of Sugarcane field (23/07/2018) (FD3- Freeman Durden; Y4- Yamaguchi and VZ4-Van Zyl polarimetric decomposition)	112

6.13	Relationship between polarization (HH, HV, VV & VH), surface scattering component, dihedral component and field-measured soil moisture at grand growing stage of Suagarcane field (01/10/2018) (FD3- Freeman Durden; Y4- Yamaguchi and VZ4- Van Zyl polarimetric decomposition)	114
6.14	Relationship between polarization (HH, HV, VV & VH), surface scattering component, dihedral component and field-measured soil moisture of bare field (23/07/2018) (FD3- Freeman Durden; Y4- Yamaguchi and VZ4- Van Zyl polarimetric decomposition)	115
6.15	Relationship between polarization (HH, HV, VV & VH), surface scattering component, dihedral component and field-measured soil moisture of bare field (01/10/2018) (FD3- Freeman Durden; Y4- Yamaguchi and VZ4- Van Zyl polarimetric decomposition)	117
6.16	Relationship between depolarization ratio and surface roughness height of Maize (a), Paddy (b), Tomato (c) and bare field (d) of 23/07/2018	118
6.17	Relationship between depolarization ratio and surface roughness height of Tomato (a) and bare field (b) of 01/10/2018	118
6.18	Relationship between soil moisture and radar signal VV and VH polarization at seedling (a), vegetative (b) and yield stage (c) of Maize field	122
6.19	Relationship between radar signal (VV and VH polarization) and RVI at vegetative (a) and yield (b) stage of Maize field	123
6.20	Relationship between soil moisture and radar signal VV and VH polarization at vegetative (a), maturity (b) and yield stage (c) of paddy field	124
6.21	Relationship between radar signal (VV and VH polarization) and RVI at maturity (a) and yield (b) stage of paddy field	125
6.22	Relationship between soil moisture and radar signal VV and VH polarization at vegetative (a), maturity (b) and yield stage (c) of Tomato field	126
6.23	Relationship between radar signal (VV and VH polarization) and RVI at maturity (a) and yield (b) stage of tomato field	127
6.24	Relationship between soil moisture and radar signal VV polarization at early growth (a) vegetative (b) grand growing (c) and yield stage (d) of sugarcane	128
6.25	Relationship between soil moisture and radar signal VH polarization at early growth (a) vegetative (b) grand growing (c) and yield stage (d) of sugarcane field	128

6.26	Relationship between radar signal (VV and VH polarization) and RVI at Early growth stage of sugarcane	129
6.27	Relationship between soil moisture and radar signal VV and VH polarizations of bare field	130
6.28	Relationship between RVI and radar signal VV and VH polarizations of bare field	130
6.29A	Relationship between depolarization ratio and surface roughness height of bare (a), Maize (b) and Sugarcane (c) at vegetative stage.	131
6.29B	Relationship between depolarization ratio and surface roughness height of Tomato at vegetative (a) and maturity stage (b)	131
6.29C	Relationship between depolarization ratio and surface roughness height of Paddy at vegetative (a) and maturity stage (b)	132

LIST OF TABLES

Table No.	Description	Page No.
1.1	Methods for estimating soil moisture by remote sensing	4
2.1	Various bands and wavelengths of microwave remote sensing	10
2.2	Microwave remote sensing sensors	16
3.1	Summary of surface soil moisture retrieval using empirical and semi empirical models	27
3.2	Summary of surface soil moisture retrieval using theoretical models	35
3.3	Summary of comparative evaluation of surface soil moisture retrievals	43
3.4	Comparison of various SAR based surface soil moisture models	47
4.1	Salient features of Study area	51
4.2	Characteristics of each test plots	52
4.3	Data characteristics of Sentinel-1a	54
4.4	Sentinel-1a data acquisitions over the study area during the study period	55
4.5	ALOS PALSAR-2 data information	55
5.1	Crop height during ALOS PALSAR-2 pass	89
5.2	VWC during ALOS PALSAR-2 pass	90
6.1	WCM model parameter	99
6.2	Details of developed Semi-Empirical Model (SEM) of 23/07/2018 for various crops	119

6.3	Details of developed Semi-Empirical Model (SEM) of 01/10/2018 for various crops	119
6.4	Accuracy assessment of surface soil moisture models of L-band SAR	120
6.5	Details of developed Semi-Empirical Model (SEM) at crop stages	132
6.6	Validation results of surface soil moisture models of C-band SAR	133

ABBREVIATIONS

Abbreviation	Description
AE _{max}	:Maximum Absolute Error
AIRSAR	:Airborne Synthetic Aperture Radar
ALOS PALSAR	:Advances Land Observation Satellite Phased Array L-band Synthetic Aperture Radar
AMSR-E	:Advanced Microwave Scanning Radiometer
AOI	:Area Of Interest
ASI	:Agenzia Spaziale Italiana
BM	:Bench Mark
CONAE	:Comisión Nacional de Actividades Espaciales
CSA	:Canadian Space Agency
DEM	:Digital Elevation Model
DLR	:German Aerospace Center
DTDC	:Dual Temporal Dual Channel
EO	:Earth Observation
ERS	:Earth Remote Sensing Satellite
ESA	:European Space Agency
EVI	:Enhanced Vegetation Index
EW	:Extra-Wide Swath
FAO	:Food Agricultural Organization
GPS	:Global Positioning System
GRD	:Ground Range Detected
IEM	:Integral Equation Method
IRS	:Indian Remote sensing Satellite
IS	:Indian Standard
ISA	:Israel Space Agency
ISRO	:Indian Space Research Organization
IST	:Indian Standard Time
IW	:Interferometric Wide Swath

JAXA	:Japan Aerospace Exploration Agency
JERS	:Japanese Earth Resources Satellite
JPL	:Jet Propulsion Laboratory
KA	:Kirchhoff Approximation
KARI	:Korea Aerospace Research Institute
KSNDMC	:Karnataka State Natural Disaster Monitoring Centre
LAI	:Leaf Area Index
LMA	:Levenberg Marquardt Algorithm
LPM	:Laser Profile Meter
LUT	:Look Up Table
MIMICS	:Michigan Microwave Canopy Scattering
MLR	:Multi Linear Regression
MSMR	:Multi-frequency Scanning Microwave Radiometer
MULESME	:Multi-temporal Least Square Moisture Estimator
NABARD	:National Bank for Agriculture and Rural Development
NASA	:National Aeronautics and Space Administration
NDVI	:Normalized Difference Vegetation Index
NISAR	:NASA-ISRO Synthetic Aperture Radar
NRSCC	:National Remote Sensing Center Of China
PALS	:Passive-Active L and S-band Sensor
Pol	:Polarization
RBFANN	:Radial Basis Function Artificial Neural Network
RCS	:Radar Cross Section
RISAT	:Radar Imaging SATellite – 1
RMS	:Root Mean Square
RMSE	:Root Mean Square Error
RRI	:Radar Roughness Index
RVI	:Radar VegeataionIndex
SAR	:Synthetic Aperture Radar
SEM	:Semi-Empirical Model
SIR C	:Space-borne Imaging Radar-C

SLC	:Single Look Complex
SM	:Soil Moisture
SM	:Strip Map
SMAP	:Soil Moisture Active Passive
SMOS	:Soil Moisture and Ocean Salinity
SNAP	:Sentinel Application Platform
SOI	:Survey Of India
SPM	:Small Perturbation Model
SRTM	:Shuttle Radar Topography Mission
SSR	:Soil Surface Roughness
TDR	:Time Domain Reflectometry
VWC	:Vegetation Water Content
WCM	:Water Cloud Model
X-Bragg	:Extended Bragg

NOMENCLATURE

T_b	:Brightness temperature
e_s	:Smooth-surface emissivity
e_r	:Rough surface emissivity
R_s	:Smooth-surface reflectivity
u	:Incidence angle
ϵ_b	:Bulk dielectric constant
(ϵ)	:Dielectric constant
ϵ_a	:Dielectric constant of air
ϵ_s	:Dielectric constant dry soil
ϵ_w	:Dielectric constant water
h	:Empirical roughness parameter
l	:Correlation length
σ°	: Backscattered energy
ω	: Single scattering albedo
Γ	:Transmissivity
T_S	:Physical temperatures of soil
T_C	:Physical temperatures of canopy
τ	:Optical depth
s	:Vertical surface roughness
k	:Wave number
θ_i	:Incidence angle
Γ_0	: Fresnel reflectivity
[T]	:Total coherence matrix
P_S	:Surface component scattering power
P_D	:Dihedral component scattering power
P_V	:Volume component scattering power
δ	: Depolarization

CHAPTER 1

INTRODUCTION

1.1. BACKGROUND

A thin layer of soil on the earth gives plants mechanical support and substance when combined with the right amounts of air and water. Despite its ephemeral nature and the extent to which it fills the pore space. Water is a crucial component of soil and often controls the dynamic qualities of soil (Petropoulos et al., 2015). Soil moisture is the quantity of water stored in pore space (Dobson et al., 1985). A large portion of the land surface hydrology is integrated by soil moisture, which is also crucial for the dynamics of ecosystems and biochemical cycles. A key element affecting runoff, infiltration, redistribution, groundwater movement, storage, and drainage is moisture close to the soil surface. (Kornelsen and Coulibaly 2013; Peng and Loew 2017). Soil moisture also plays a vital role in the functioning of ecosystems. Surface soil moisture is a basic component of the meteorological cycle and in determining agricultural crop yield (Walker and Houser, 2004). Soil moisture is a critical state of variation that determines the response of soil-plant system to water input and monitoring of soil moisture is of significance in irrigation management (Saux-Picart et al. 2009; El Hajj et al. 2016).

Information about soil moisture can be obtained through point measurements or remote sensing techniques. Point-based measurements of soil moisture, which are categorized as ground-based measurements, produce accurate information but sampling such data is costly and time consuming. Point-based measurement methods can be further divided into direct and indirect methods. For direct measurements, a sample of soil is taken and the water is removed by either evaporation or a chemical process and measured. The thermogravimetric method, the standard direct method of measuring volumetric soil moisture content, removes water from the soil sample by evaporating the sample at 105°C using an oven. Direct point-based measurement is simple, inexpensive and the soil moisture can be easily calculated. However, this method is also destructive and it is not possible to repeatedly carry out the point-based measurement at the same

location. Indirect methods are non-destructive and monitor soil properties that are a function of water content. The use of Time Domain Reflectometry (TDR) probes is based on the measurement of the dielectric properties of soil. Indirect methods normally involve inserting instruments into the soil or placing them on the surface. This method promises in-situ measurements of soil moisture and can be repeated at the same location a number of times, although it requires one-time calibration for the same location to determine soil moisture (Garg et al. 2016).

The disadvantage of using point-based measurement is this type of measurement is rarely representative of the spatial distribution of moisture required for mapping large areas. This is because accurate spatial estimates of soil moisture require samples that are closely spaced relative to the correlation length of the spatial soil moisture fields, meaning that this method is impractical for determining the large-scale areal estimation of soil moisture.

Remote sensing, on the other hand, provides a means of measuring soil moisture in both higher spatial and temporal dimensions and can provide readings for the top few centimeters of soil for areas with moderate to low vegetation cover. Platforms supporting remote sensing instruments can be either ground-based, aircraft-based or space-based. The optimal solution in terms of mapping large areas and long-term repetition coverage involves space-borne satellite systems (Engman, 1992). Remote sensing methods offer rapid data collection over large areas on a repetitive basis within the top 7-8 cm of the soil. On the other side, remote sensing measurements do not provide as accurate or as deep a measurement of the soil moisture as can be obtained by conventional in-situ measurements at a point. Moreover, the remote sensing measurements are often restricted by the sensor configuration like the spatial resolution, incidence angle, frequency and land characteristics like surface roughness and vegetation cover. Therefore, an integrated system should be designed to capitalize on the advantages and minimize the disadvantages (Schmugge et al., 1980).

1.2. SOIL MOISTURE (SM) MEASUREMENT BY REMOTE SENSING

The measurement of soil moisture using the electromagnetic spectrum (frequency dependence) is classified as follows:

Visible and Infrared: Electromagnetic Spectrum: Reflected radiation in the visible region of the electromagnetic spectrum has been demonstrated to have an excellent correlation with moisture content but limited to top few millimeters of soil surface. At these wavelengths, the penetration is small and because of cloud cover, the sensitivity rapidly decreases within the first few millimeters of the soil surface. In addition, the electromagnetic interaction with different dry and wet soil varies widely. Major sources causing uncertainty are surface roughness and surface cover. Therefore, establishing a relationship between these two demands a prior knowledge of soil characteristics (Carlson et al., 1995b; Venturini et al., 2004).

Thermal Infrared Method: It has also been demonstrated that thermal radiation from surface measurements in the thermal infrared range (10–12 μm) correlates well with the amount of moisture present on the soil's surface. Although this method seems to be able to detect moisture at a deeper level than is possible with visible spectrum measurements, it is constrained by the slightest vegetation cover. In addition, both optical reflectance and thermal emission models for estimating soil moisture require knowledge of solar radiation (irradiance and insolation), which is not always available (Hassan et al., 2007).

Microwaves: Microwaves refer to the electromagnetic radiations of frequencies ranging from approximately 300 MHz to 300 GHz. Applications of microwaves have been put to various uses depending on the frequencies range. They have certain distinct advantages over other frequencies, e.g. they propagate through ionosphere with a minimum loss, hence most suited for space-bound communications and satellite remote sensing. Atmosphere is entirely transparent to these radiations. They can also penetrate deep into the soils. Hence, multi-frequency and multi-polarization approaches are possible (Schmugge, 1984). The sensitivity of microwave response to soil moisture variation and their relative atmosphere transparency (>90%) makes microwave sensors

well suited for soil moisture remote sensing. Also, with proper choice of frequency, incidence angle and polarization, the effect of surface roughness can be minimized. Lower frequency end of microwave spectrum offers a significant advantage in measurement of soil moisture. At these frequencies, penetration of vegetative cover is significant and the sampling depth of the measurement may be several centimeters depending on soil moisture content. Sampling depth is the maximum depth at which the moisture can be measured.

Measurement programs in the microwave region have followed two distinct approaches: (a) employing passive radiometric measurement and (b) using active radar backscattering measurement. Both approaches have demonstrated excellent correlation with soil moisture content. However, the resolution and penetration capability of active and passive is different and makes significant differences in retrieving surface soil moisture resolution, vegetation penetration capability and sampling depth. The volumetric soil moisture can be considered as a monotonically decreasing function of the emissivity of bare soil. It has been shown that both active and passive microwave remote sensors can be used to monitor soil moisture over land surfaces (Wang et al., 1981) depending upon applicability. The details of soil moisture methods based on remote sensing technique is presented in Table 1.1.

Table 1.1 Methods for estimating soil moisture by remote sensing

Remote Sensing	Characteristics	Advantage	Disadvantage
Optical	Soil reflection	High spatial resolution; Wide coverage	Limited surface penetration; Atmospheric effects; many other noises
Thermal Infrared	Soil surface temperature	High spatial resolution; Wide coverage, Physically well understood	Limited surface penetration; atmospheric effects; affected by meteorological events

Passive Microwave	Brightness temperature, Dielectric properties and soil temperature	Less atmospheric effect; moderate surface penetration; Coarse spatial resolution; physical well understood	Low spatial resolution; effected by surface roughness & vegetation
Active Microwave	Backscatter coefficient, dielectric properties and Surface scattering components	Less atmospheric effect; moderate surface penetration; Fine spatial resolution; physical well understood	Limited swath width; effected by surface roughness & vegetation

1.3. STATEMENT OF THE PROBLEM AND RESEARCH SCOPE

Surface soil moisture differentiates between surface and sub-surface flow. However, percentage of water in soil moisture is less compared to other hydrological parameters of hydrological cycle. Still, it plays a vital role in many hydrological and agricultural studies. In the early days of research, surface soil moisture is measured over bare fields using scatterometer (passive microwave) or single channel SAR data. Later, these studies extended towards vegetated areas like grasslands and cropland using dual and quad polarimetric data. Three approaches are used to retrieve surface soil moisture namely, physical or theoretical approaches, empirical approaches and change detection or time series approaches.

Physical approach rely on scattering models to forecast microwave backscatter based on sensor characters like frequency, incidence angle and field characters like surface roughness, and dielectric constant. This approach is most suitable for non-vegetated areas. With the addition of vegetation component, the approach becomes more complex. Integral Equation model (IEM) and Small Perturbation Model (SPM) are most commonly used physical models. The empirical approach is used to retrieve surface soil moisture directly from backscattered SAR energy. This method needs extensive field information, to evaluate the effect of soil moisture, roughness and vegetation on backscattered energy. Oh et al. (1992), Oh (2004), Dubois et al. (1995) and Baghdadi et al. (2004) are examples for empirical approach. Change detection or

time series approach is a different approach, which require multiple SAR imageries to calculate surface soil moisture. This approach focuses more on qualitative soil moisture in terms of indices rather than quantitative soil moisture. This approach does not give any discrete value of soil moisture, it only denotes low and high relative soil moisture index.

All these approaches and models are tested on agricultural, bare, wetlands and grasslands all across the globe. Majority of these investigations carried out based on political or watershed boundary, which are in few square kilometers or hectares. Which are more suitable and effective to the countries with homogeneous cropping over larger agricultural fields. Nevertheless, in India, it is a different case, where agricultural field is much smaller and heterogeneous in cropping (different crops). For example, the average farmland size in the United States is approximately 450ha while that in India is 1.16ha (MacDonald et al. 2013; NABARD, India). So, there is need to explore utility of surface soil moisture models at field/plot/regional scale using microwave remote sensing. This will be helpful to marginal farmers to detect patches having crop water stress and to determine irrigating areas for stable crop production.

The main scope of this work is to answer the following scientific questions.

- Which surface parameters are most significant to retrieve soil moisture from plot scale bare and agricultural fields?
- Is real space-borne data useful for soil moisture estimation in plot scale fields? If yes, what accuracy can we achieve for bare and agricultural fields?
- Which model is good for soil moisture inversion for a given test site?
- Which SAR frequency (C or L band) is good to retrieve soil moisture at various crop stages?
- Is it possible retrieve surface soil moisture at agricultural field grid level?
- Does different crop stages have impact on accuracy of surface soil moisture models?

1.4. RESEARCH OBJECTIVES

The main objective of the study is to retrieve surface soil moisture over bare and agricultural plots at different crop stages using active microwave remote sensing. In mandate to achieve this, the following objectives are framed.

1. To investigate the surface soil moisture variation across crop stages and crops in semi-arid tropical region.
2. To develop surface soil moisture model and comparison of its performance with existing models.
3. To study the potential of dual and quad-pol SAR data in surface soil moisture retrieval over heterogeneous agricultural plots.

1.5. THESIS OUTLINE

To achieve the proposed objectives and to answer scientific questions, this thesis is organized in to seven chapters as follows:

Chapter 2 describes the basics of microwave remote sensing like different wavelength, and polarization along with the soil and vegetation parameters affecting backscattered energy is discussed.

Chapter 3 reviews the literature based on various surface soil moisture approaches like physical or theoretical and empirical or semi-empirical approach using SAR. It also explains the identified literature gaps.

Chapter 4 describes salient features of the study area, data products and framework of research methodology adopted to achieve the objectives.

Chapter 5 presents the field data collection, experimental studies, analysis and remote sensing data processing.

Chapter 6 discusses results obtained by evaluating surface soil moisture models. First section discuss about the spatio-temporal soil moisture variation during crop period. Second section discusses about the polarization decomposition and surface soil moisture retrieval using L band SAR during two different crop growth stage. Third section

discuss surface soil moisture retrieval using C band SAR at different crop stages using existing and developed model. Finally validating and comparing developed model with existing model.

Chapter 7 summarizes the research work of the thesis section by section. The subsequent conclusions drawn from the results. Finally, the limitations and future scope of the research work are presented.

The next chapter presents the brief overview of microwave remote sensing and its factors influencing surface soil moisture retrieval.

MICROWAVE REMOTE SENSING

2.1 INTRODUCTION

Microwave remote sensing uses electromagnetic radiation with a wavelength between 1 cm and 1 m (commonly referred as microwaves) as a measurement tool. Due to the longer wavelength compared to visible and infrared radiation, microwaves exhibits the important property of penetrating clouds, fog, etc. This important property makes this technique virtually suitable to work in any weather condition or environment. In addition, microwave remote sensing provides unique information on soil moisture, biomass, oil spills, rainfall, wind direction, sea wind and wave direction, which are derived from frequency characteristics, Doppler effect, polarization, back scattering etc. that cannot be achieved from optical remote sensing. The advantages of microwave are,

- All weather capability (penetration capability through clouds).
- Day and night capability (independent of intensity and sun illumination angle).
- Penetration through vegetation, soil sand and dry snow to a certain extent.
- Sensitivity to surface roughness, dielectric properties and moisture (in liquid or vapor forms).
- Sensitive to wave polarization and frequency.
- Volumetric analysis.
- Better analysis of inaccessible areas.

2.2 DIFFERENT WAVELENGTHS AND POLARIZATION OF SAR

SAR data is available in various bands, including the Ka, Ku, X, C, L, and P bands, and has a range of azimuth and range resolutions. These bands have their own advantages and disadvantages concerning to its applications. The various bands, wavelength and their applications are shown in the Table 2.1.

Table 2.1 Various bands and wavelengths of microwave remote sensing

Band	Wavelength (cm)	Applications
Ka	0.75-1.1	Communication and Military purposes
Ku	1.67-2.4	Communication and Military purposes
X	2.4-3.8	Military mapping, Surveillance and surface change studies.
C	3.8-7.5	Penetration capability is limited though vegetation, soil moisture, glacier and cryosphere studies
S	7.5-15	Used for medium-range Metrological applications.
L	15-30	Penetrates through vegetation to some extent used in vegetation, soil moisture, glacier and cryosphere studies
P	30-100	Used for research and experimental applications with significant penetration capability.

Microwave polarization refers to the orientation of the electric field vector of the transmitted beam with respect to the horizontal direction. If the electric field vector oscillates along a direction parallel to the horizontal direction, the beam is said to be "H" polarized. On the other hand, if the electric field vector oscillates along a direction perpendicular to the horizontal direction, the beam is "V" polarized (Woodhouse, 2009). The four combinations SAR data polarizations Electro-Magnetic Radiation (EMR) is: (1) HH: horizontal transmitted and horizontal received (2) HV: horizontal transmitted and vertically received. (3) VH: vertically transmitted and horizontally received. (4) VV: vertically transmitted and vertically received.

There are two types of microwave remote sensing namely, active and passive. The active type has its own source of energy, emits the EMR and receives the backscattering energy, which is incident on the ground surface. Passive systems collect the radiation that is naturally emitted by the earth surface. In fact, objects emit energy

at the microwave frequencies, although sometimes in an extremely small amount and generally characterized by relatively low spatial resolutions.

2.3 ACTIVE MICROWAVE REMOTE SENSING

Radar systems are basically categorized into three classes: imaging radar, scatterometer, and altimeter. Imaging radar is the most commonly used radar in remote sensing applications. Scatterometers and space-borne altimeters are used for specialized applications such as wind measurements at sea and ocean monitoring, respectively. Imaging radar is an active illumination system. An antenna transmits a radar signal in a side-looking direction towards the earth's surface. The reflected signal, known as the echo, is backscattered from the surface and received a fraction of a second later at the same antenna. Intensity, or amplitude, of this received echo is measured and recorded and the data are then used to construct an image. For coherent radar systems such as Synthetic Aperture Radar (SAR), the phase of the received echo is also measured and used to construct an image. Single frequency radar uses a single frequency for illumination, therefore there is no color associated with raw radar imagery.

2.4 PASSIVE MICROWAVE REMOTE SENSING

Passive microwave remote sensing is based on measuring thermal radiation in the centimeter wavelength of the electromagnetic spectrum, referred to as brightness temperature. This radiation is mainly determined by the radiating body's physical temperature and emissivity and can be approximated by using Eq. 2.1.

$$T_{b(P)} \approx e_{s(P)} * T \quad (2.1)$$

Where

T_b = Observed brightness temperature

T = Physical temperature of the emitting layer

P = refers to vertical or horizontal polarization

$e_{s(P)}$ = Smooth-surface emissivity.

This emissivity is further defined as

$$e_{s(P)} = (1 - R_{s(P)}) \quad (2.2)$$

Where R_s is the smooth-surface reflectivity for a homogeneous soil with a smooth surface, the reflectivities at vertical and horizontal polarizations, $R_{s(V)}$ and $R_{s(H)}$, are given by the Fresnel expressions as:

$$R_{sV} = \left| \frac{k \cos u - \sqrt{k - \sin^2 u}}{k \cos u + \sqrt{k - \sin^2 u}} \right| \quad (2.3)$$

$$R_{sH} = \left| \frac{\cos u - \sqrt{k - \sin^2 u}}{\cos u + \sqrt{k - \sin^2 u}} \right| \quad (2.4)$$

where u is the incidence angle (relative to the surface normal) and k is the absolute value of the soil bulk dielectric constant (ϵ_b), which is a measure of the response of the soil to an electromagnetic wave and is determined mainly by the volumetric soil water content. From the Fresnel equations, it can be seen that the absolute magnitude of the soil emissivity is somewhat lower at horizontal polarization, but the sensitivity to changes in surface moisture, and vegetation, is significantly greater than at vertical polarization. The reverse is true for temperature.

For bare soil, the measured brightness temperature is almost directly related to soil water content and the physical temperature of the emitting layer. However, when vegetation is present, it profoundly influences the measured brightness temperature. Vegetation may attenuate or scatter the soil's radiation but will also emit its own radiation. Further influence on the brightness temperature is caused by surface roughness.

2.5 FACTORS INFLUENCING SOIL MOISTURE RETRIEVAL USING MICROWAVE REMOTE SENSING

The major parameters which affect the backscattered energy and brightness temperature are,

- Dielectric Constant
- Thermal Sampling Depth
- Surface roughness

- Vegetation effects

2.5.1 Dielectric constant

Dielectric constant can be stated as the ability of the material to get depolarized when electromagnetic field is applied (Hallikainen, 2014). The dielectric constant is a characteristic quantity of a given dielectric substance, sometimes called the relative permittivity. The dielectric constant (ϵ) is a measure of the response of soil to an electromagnetic wave. This response is composed of two parts (real and imaginary), which determine the wave velocity and energy losses respectively. In a non-homogeneous medium such as soil, the soil bulk dielectric constant (ϵ_b) is a combination of individual dielectric constants of its components, (i.e. air, water, dry soil, etc.), but it is not a weighted average. The wide contrast between the dielectric constant of air ($\epsilon_a \sim 1$), dry soil ($\epsilon_s \sim 4$), and water ($\epsilon_w \sim 80$) results in a range in ϵ_b from 4 to 40. This wide range in ϵ_b can be directly related to volumetric soil water content, and is further influenced by soil texture, frequency, temperature and salinity. The direct relation between soil bulk dielectric constant and volumetric soil water content is not straight forward. Many empirical and theoretical dielectric models have been suggested to describe this relationship.

The frequency dependence in the range up to 5 GHz is little because there is only little variability in the real part of the dielectric constant. The marked frequency dependence of the small imaginary part in this range influences only the penetration depth, with smaller penetration depths for higher frequencies (Njoku and Entekhabi, 1996). The temperature dependence of dielectric constant is weak, and it may be ignored for the range of temperatures encountered in nature (Topp et al., 1980; Njoku and Entekhabi, 1996).

2.5.2 Thermal sampling depth

Microwave energy originates from entire soil depth, but much of this energy is absorbed in higher soil layers. As a consequence, the contribution of each soil layer to actually emitted microwave energy decreases rapidly with depth. The thickness of surface layer that provides most of the measurable energy contribution is defined as thermal sampling

depth (De Jeu, 2003). This layer is thought to be only several tenths of a wavelength thick. However, this thickness varies according to its moisture content, wavelength, polarization, and incidence angle. As the average moisture content of this layer decreases, its thickness increases. It is combined dielectric properties of this layer that determine observed emissivity or reflectivity, and it is the representative temperature of this layer that should be used to interpret measured brightness temperature or backscattered energy.

2.5.3 Surface roughness

Surface roughness increases the apparent emissivity or reflectivity due to increase in surface area of the emitting surface. In order to modify reflectivity or emissivity for rough surfaces, an empirical roughness model was developed by Choudhury et al. 1979 and is described in Eq. 2.5

$$e_r = 1 - R \exp(-h \cos 2u) \quad (2.5)$$

Where e_r the rough surface emissivity, h is an empirical roughness parameter, related to the root mean square height variation of the surface and the correlation length, and u is the incidence angle of the observation. This model is a modification of Eq. 2.2. The effect of surface roughness is considered to be minimal at most locations at satellite scale, except in areas with extreme relief.

A more elaborate formulation that includes a polarization mixing parameter (Q) has been proposed by Wang and Choudhury 1981. This model may be appropriate at smaller wavelengths than L-band but its implementation is still very difficult.

2.5.4 Vegetation effects

Like soil, vegetation emits its own microwave energy, and it may attenuate or scatter the radiation emitted by the soil. The brightness temperature (T_b) or backscattered energy (σ°) measured above the canopy therefore contains not only information on soil moisture, but also on vegetation characteristics. In order to differentiate between different components of the measured brightness temperature or backscattered energy is necessary to simplify the vegetation to a canopy model. Numerous canopy models have been developed for this purpose. Mo. et al 1982 is a simple method but physically

based model that can effectively estimate the radiation by the soil surface even under vegetation (Owe et al., 2001). This is given in Eq. 2.6.

$$T_{b(P)} = T_S e_{r(P)} \Gamma_{(P)} + (1 - w_{(P)}) T_C (1 - \Gamma_{(P)}) + (1 - e_{r(P)}) (1 - w_{(P)}) T_C (1 - \Gamma_{(P)}) \Gamma_{(P)} \quad (2.6)$$

Where

T_S and T_C physical temperatures of the soil and canopy respectively;

ω = single scattering albedo;

e_r = Rough surface emissivity;

Γ = transmissivity;

P = horizontal or vertical polarization.

The first term in this equation defines the radiation from the soil that is weakened by the overlying vegetation. The second term accounts for the upward radiation directly from the vegetation, and the third term defines the downward radiation from the vegetation, reflected upward by the soil and again weakened by the canopy (Owe et al. 2001). The single scattering albedo describes the scattering of the emitted radiation by the vegetation, and is a function of plant geometry. The transmissivity (Γ) is further defined in terms of the optical depth (τ) is described in equation 2.7.

$$\Gamma = \exp(-\tau / \cos u). \quad (2.7)$$

The optical depth is related to the vegetation density and frequency. With increasing optical depth, the sensitivity of the above-canopy brightness temperature to soil emissivity decreases. This is because the vegetation weakens soil emission and emission from vegetation forms a larger part of the signal with increasing optical depth. The threshold value of optical depth at which above-canopy signal becomes totally saturated varies with frequency and soil moisture content. In dry conditions, this threshold occurs sooner.

2.6 PAST AND CURRENT MICROWAVE SPACE BORNE-SENSORS

The past, current and future space borne microwave remote sensing sensors are briefly summarized in the Table 2.2

Table 2.2 Microwave remote sensing sensors

Sensor	Operation	Frequency Band	Polarization	Institution, Country
SeaSAT	1978	L	HH	NASA/JPL,USA
ERS 1/2	1991-2000 1995-2011	C	VV	ESA, Europe
JERS-1	1992-1992	L	HH	JAXA, Japan
Radarsat-1	1995-	C	HH	CSA, Canada
Radarsat-2	2007-Today	C	Quad	
SRTM	Feb-2000	C and X	HH+VV VV	NASA, USA DLR, Germany ASI, Italy CSA, Canada
ALOS PALSAR	2006-2011	L	Quad	JAXA, Japan
TerraSAR- X/Tandem-X	2007-Today 2010-Today	X	Quad	DLR/Astrium, Germany
Cosmo- Skymed-1/4	2007 and 2010-Today	X	Dual	ASI, Italy

Table 2.2 (Cont...)

Sensor	Operation	Frequency Band	Polarization	Institution, Country
RISAT-1	2012-2016	C	Quad	ISRO, India
RISAT-2	2009-Today	X	Dual	ISRO, India ISA, Israel
HJ-1C	2012-Today	S	VV	NRSCC, China
Kompsat-5	2013-Today	X	Dual	KARI, Korea
ALOS PALSAR-2	2013-Today	L	Quad	JAXA, Japan
Sentinel 1a/1b	2014-Today 2016-today	C C	Dual Dual	ESA, Europe
SAOCOM-1a	2018	L	Quad	CONAE, Argentina
Radarsat-3	2018	C	Quad	CSA, Canada
SMOS	2009-2021	L	HH	ESA, Europe
SMAP	2015-Today	L	VV, HH	NASA, USA
RISAT-1a	2022- Today	C	Quad and Circular	ISRO, India
NISAR	2023	L & S	Quad	NASA, USA

With this knowledge as background, next chapter reviews the past studies on application of active microwave remote sensing in the field of surface soil moisture retrieval.

CHAPTER 3

LITERATURE REVIEW

3.1 INTRODUCTION

An overview of the current state of investigations in the fields of soil moisture retrieval using microwave remote sensing are presented in this chapter. For detailed history and evolution of radar and SAR systems and its applications in earth remote sensing techniques may be referred to Ulaby et al., 1981, 1982, and 1986. SAR remote sensing is an important tool for geo-physical parameter extraction from natural and man-made features. To retrieve soil moisture from plot scale fields, literature reviews has been classified into 3 themes. (i) Surface soil moisture retrieval using empirical and semi empirical models. (ii) Secondly literature regarding surface scattering and theoretical surface soil moisture models. Finally, comparative studies carried out on surface soil models are discussed.

Research in soil moisture remote sensing began in the mid 1970's shortly after the surge in satellite development. Quantitative soil moisture measurements in the surface layer of soil were carried out using microwave remote sensing. Soil moisture content is commonly expressed in gravimetric or volumetric units. Ulaby and Batlivala (1976) experimentally determined the radar response to soil moisture content at three bare soil fields, which is having different surface roughness by using eight different frequencies varying from 2-8 GHz for HH and VV polarizations using truck, mounted sensor. They found that incidence angle with 10° and frequency 4.7 GHz had very good correlation. Schmugge (1980) concluded the brightness temperature varies mainly due to its dielectric properties. There is large difference between dielectric constants of wet ($\cong 80$) and dry (3~5) soils which shows strong correlation with soil moisture but this is effected by soil texture and surface roughness. Wang and Choudhury (1981) and Schmugge (1984) have proved significant dependence of dielectric constant on soil texture keeping the same volumetric soil moisture content. This is evident from the experiment conducted by Hallikainen et al., (1985) on the plot having sandy loam soil.

The larger variation in the regression curve was found for the plot having real dielectric constant (ϵ') with varying bulk density and suggested to express soil moisture in volumetric units.

3.2 SURFACE SOIL MOISTURE RETRIEVAL USING EMPIRICAL AND SEMI EMPIRICAL MODELS

Oh et al. (1992) have conducted field tests in bare soils using Scatterometer, Laser Profile Meter (LPM), Dielectric probe to develop empirical model at L, C and X band frequencies at various incidence angles with accurate measurements of rms surface height, correlation length, and dielectric constant. The model found very good agreement with backscattering measurements in bare soils and by inverting this model soil moisture and surface roughness can be retrieved from multi-polarized radar observations.

Dubois et al. (1995) have developed an empirical model to estimate surface roughness and soil moisture from scatterometer data and cross-verified with AIRSAR and SIR C data. The model performs better in bare soil and vegetated lands, which is having NDVI less than 0.4 and surface roughness less than 2.5. This model's drawback is that it does not account for topography or surface correlation length.

Engman and Chauhan (1995) and Wang (1997) discussed the requirement of model and software to retrieve soil moisture over discontinuous vegetation and investigate the potential of polarimetric SAR in soil moisture estimation. Ulaby et al, (1996) found that L-band is good at estimating soil moisture at top 5 cm and also suggested that it is possible to develop a model to estimate soil moisture under vegetation using vegetation parameters. Shi et al, (1997) developed an empirical model to estimate surface soil moisture and surface roughness using L band SAR data over well-maintained Oklahoma watershed and found an RMSE of 3.4%, which is acceptable. Wang et al, (1997) compared two semi empirical models on bare fields of little Washita watershed and found Shi et al, 1997 model is performing better than Dubois et al, 1995 model. Neusch and Sties (1999) used Dubois model to estimate soil moisture and results are well within range they suggested incorporate incidence angle and vegetation coverage parameters to model.

De Roo et al. (2001) measured backscatter over fields of Soybean using C, L band AIRSAR and scatterometer data. They have used modified 'oh' model to study soil moisture and Michigan Microwave canopy scattering (MIMICS) model to study canopy structure to differentiate the backscatter values from canopy volume scattering. Authors studied the backscattered values in four parameters two from the canopy, one from the rough ground and the other one surface roughness and found that L band VV polarization gives better results for canopy scatter modelling as well as soil moisture measurements.

Wigneron et al. (2003) reviewed the soil moisture retrieval algorithms for AMSR-E and SMOS satellites working on passive microwave remote sensing. Vegetation effects on soil moisture are taken into account and classified them into statistical technique; forward model inversion and explicit inversion are explained. Srivastava et al (2003) explored the use of multi incidence angle in measuring surface roughness and soil moisture using C band Radarsat images. The author estimated the surface roughness without actual field data by taking ratio of high and low incidence angles, incorporating it with the soil moisture model, and got good results. The limitation is that soil moisture change must be negligible while taking two incidence images and should be examined over a large area. Zribi and Dechambre (2003) introduced a new parameter called surface roughness parameter (z) which is function of surface height and correlation length to develop new empirical model to calculate the surface soil moisture using C band Radarsat and ERASME (airborne) data over three test fields of France and got better results compared to the RMSE height of the soil surface. Singh et al. (2005) attempted to estimate volumetric soil moisture for the whole Indian sub-continent using multi-frequency scanning microwave radiometer (MSMR) sensors onboard Indian remote sensing satellite (IRS) P4 Oceansat-1. They tried to study the variability of soil moisture throughout the Indian sub-continent and found that soil moisture is high during the period of June-July and low during April-May. They also found that coastal India has more soil moisture compared to other regions. This study was biased due to presence of low and high dense vegetation.

Holah et al, (2005) and Baghdadi et al, (2008) analyzed the sensitivity of surface parameters to radar backscatter energy and found that surface roughness is more

sensitive to higher incidence angle (43°) and lower the incidence angle minimizes effect on soil moisture. Zhan et al, (2006) and developed empirical surface soil moisture model over various land use like grassland, cereal, harvested crop and root crop fields. The developed model gave good results when compared with field values at better spatial resolution and temporal frequency. Baup et al, (2007) and Koyama et al, (2010) used modified algorithm based on Dubois et al, (1995) and estimated surface soil moisture averaging by upscaling at different scales varying from catchment to field. They found modified algorithm results are acceptable when compared field values.

Prakash et al. (2011) attempted fusion approach of SAR data and optical data for estimation of soil moisture in bare and vegetation cover fields. ALOS PALSAR L band data was used to estimate surface roughness and MODIS data was used to extract the NDVI values of the study area. Authors have developed semi empirical relationship between NDVI and backscattering coefficients such that the relation considers vegetated land as bare soil and soil moisture is retrieved using Dubois model. The author validated his semi empirical approach with other images and got good results. Barrett et al. (2013) checked the suitability of Envisat and ALOS PALSAR for Differential interferometric synthetic aperture radar soil moisture change detection over agricultural fields of study area. In this study, the author found that C band surface displacement in HV polarization correlates more with soil moisture changes over both barley and potato crop fields than L band surface displacement. Even though L band has better penetration power C band has given better results. The limitation of the study is that data used is of poor temporal resolution so daily and weekly soil moisture changes cannot be estimated. In contrast, future satellites with more repetivity can overcome this.

Balenzano et al. (2013) showed the capability of multi temporal X and L band SAR data to map temporal changes of soil moisture content under agricultural crops with in a small revisit time. In this study, two crops were considered winter wheat and winter rape below which soil moisture is retrieved. They found that C band is influenced by canopy structure whereas L band HH polarization is sensitive to soil moisture combined use of these bands help in change detection of soil moisture.

Bertoldi et al. (2014) analyzed the surface soil moisture spatial patterns in pastures of Italian Alps. Soil moisture is estimated using fixed and ground sensors, GEOTop (hydrological model) and SAR images. Soil moisture under meadows and pasture can be successfully evaluated using the support vector regression technique with additional NDVI, DEM and land cover data.

Kousik Das and Prabir kumar paul (2015) demonstrated that RISAT 1 data products are highly sensible for the variations in the soil roughness, dielectric constant and soil moisture. It showed that σ° has relationship with right circular horizontal and vertical polarizations and a semi-empirical model was built for Bankura district region with the help of 23 plots, which is used for ground truth measurements. Narvekar et al. (2015) developed an algorithm for surface soil moisture mapping using L-band radar observations. This was designed to be free from any ancillary information on surface roughness and vegetation. In this study author as considered smooth bare soil, rough bare soil and vegetation cover and as part of ancillary data radar vegetation index (RVI) and radar roughness index (RRI) are taken into account. RVI and RRI mainly depends on the radar back scattering observations. Kim et al (2015) tried to check feasibility of using airborne Synthetic aperture radar (SAR) to validate space borne SAR along with ground PALS scatterometer. This was used to provide more confidence in calibration of SMAP (Soil moisture Active and Passive) sensor and this work is called as SMAP validation experiment 2012 (SMAPVEX 12). In this study, they collected the data on wetland, grassland, pasture, fallow, oats, corn and forest using all 3 means of SAR. They compared between the UAV and PALS data and concluded that the effect of incidence angle θ will be minimal if the land cover within the PALS footprint is homogeneous.

Upender (2015) have compared two approaches namely 1) Modified water cloud model (WCM) 2) Microwave/optical synergy method. Author has noticed that by incorporating the vegetation effects into the model, the RMSE has decreased considerably in soil moisture estimation using PALSAR L band data. Soil moisture shown better correlation with the modified water cloud model around Roorkee region. Bai et al (2016) have attempted to enhance the Dubois model to retrieve soil moisture over prairie regions of 2 study areas with different climatic conditions in china using

synergy of optical and Synthetic aperture radar (SAR) data. Four different vegetation parameters are considered namely Leaf area index (LAI), Vegetation Water Content (VWC), Normalized Difference Vegetation Index (NDVI), and Enhanced Vegetation Index (EVI) are parameterized with Dubois model to check their efficiency. Finally, the author found that EVI and LAI performs better compared to other two methods. The limitation of this study is that it mainly depends upon the type of vegetation, slope and wavelength of SAR data. It requires large field tests around the globe to improvise it.

Fieuzal and Baup (2016) tried to improvise the performance of semi empirical Oh and Dubois model using multi frequency SAR data. Author had used X band Terra SAR, C band Radarsat and L band ALOS PALSAR data to reduce the errors in the existing models. Authors attempted correct the residues in the models and found that modified Dubois models fits better to X and C band whereas modified Oh 2004 model fits to L band. They noticed in modified models RMSE was reduced below 2dB for X and C bands for L band it reduced below 1 dB. Kerr et al. (2016) have widely discussed the techniques and limitations of measuring soil moisture from space. They have given the information regarding the L band satellites, which are meant mainly for soil moisture estimation and their limitations. They found that L band synthetic aperture radiometer is promising by providing better results over low vegetation as well as forest regions. The only issue encountered was Radio frequency interference and spatial resolution. Han et al. (2017) analyzed the relationship between back scattered coefficients of SAR with soil physical properties. Field soil test were conducted for the physical properties like texture, penetration resistance, saturated hydraulic conductivity, field capacity, permanent wilting point, and porosity. Cross-polarized back scattered coefficient found correlated with most of the soil physical properties except texture i.e. clay fraction.

Ouellette et al. (2017) have extended alpha method to estimate soil moisture from time series L band SMAP data under vegetation canopy. It was difficult to retrieve soil moisture over canopy because of its complexity but this model gave some promising results. This model is based on the SMAPVEX 12 field campaign studies. This model did not require any priori information of vegetation because of its change detection approach. The limitation of this model is that it does not perform well if vegetation water content (VWC) is more than 3.69kg/sq. m. Hosseini and McNairn (2017) used C

and L band data of SAR to estimate biomass and retrieve soil moisture from wheat fields of Canada. They used fully polarized data as input to coupled water cloud model (WCM) and Ulaby soil moisture model. Whereas water cloud model estimates the total back scattering coefficients knowing the effect of vegetation and soil on backscatter. Very good results are obtained for both biomass and soil moisture even though L band accuracy is less due to comparable temporal coverage changes. El Hajj et al, (2017) aimed to map high resolution surface soil moisture at plot scale using Sentinel 1 & 2. They combined the water cloud model with the integral equation model to generate synthetic backscattering coefficient and used it to train neural networks and calculate soil moisture.

Rawat et al, (2018) retrieved surface soil moisture by developing semi empirical model over bare fields by carrying out sensitivity analysis between field soil moisture and backscattering coefficients of RISAT and found that difference in hybrid polarization improves model accuracy. Bousbih et al (2018) aimed to retrieve surface soil moisture at regional scale of bare and cereal fields. Firstly, they correlated between backscattered energy with soil and vegetation parameters. They found VV polarization has good correlation with soil moisture rather than VH polarization and mapped soil moisture at high resolution using inversion approach. Li and Wang (2018) used Radar Vegetation Index (RVI) as vegetation descriptors in WCM instead of Normalized Difference vegetation Index (NDVI) and Leaf Area Index (LAI) and found that RVI improved the results making model more feasible in different conditions. Pulvirenti et al (2018) developed an automated surface soil moisture mapping plugin and implemented in MULESME (Multi-temporal Least Square Moisture Estimator) software for whole Italy using sentinel-1 SAR data and estimates are accurate in bare field and decreases with increase vegetation density.

Yang et al, (2019) has used single, dual and polarimetric parameters to retrieve soil moisture by linear and non-linear regression methods and found with increase in polarimetric parameters soil moisture estimates are better. Xing et al, (2019) modified the water cloud model and retrieved the surface soil moisture over agricultural field of soyabean and wheat, which are in growing conditions. They found modified model with addition of vegetation fraction has improved the soil moisture estimates.

El Hajj et al, (2019) and Sekertekin et al (2020) compared the accuracy of soil moisture estimates of C and L band SAR and stated with increase in NDVI ($NDVI > 0.7$) C- band gets attenuated whereas L-band performs well. Dave et al, (2019) modified the Dubois model to for estimating surface soil moisture using single channel (HH) SAR data and gave good results at initial stage of crop cycle but poor outcomes are observed as crops reach maturity stage.

Tripathi and Tiwari (2020) used synergy of SAR and optical data developed cost effective surface soil moisture model using regression equations and indices and results are appreciable. Zhang et al, (2021) analyzed the relation between SAR polarimetric channels with field values (soil and vegetation) and used them as constants of WCM to retrieve soil moisture at different growing stages of wheat and it gave better results with accuracy. Fan et al, (2021) developed a dual-temporal dual-channel (DTDC) algorithm to estimate soil moisture over croplands. They utilized the ancillary field information and assumed there will be no change in surface roughness during crop period. The proposed model performed well with temporal soil moisture change with RMSE 0.06%. Bhogapurapu et al, (2022) introduced new dual-pol radar vegetation index based on GRD SAR data to retrieve surface soil moisture over wheat and canola crop lands at different phenological stages. Found that developed DpRVic is better vegetation descriptor than RVI and NDVI. Summary of surface soil moisture retrieval using empirical and semi empirical models is presented in Table 3.1.

Table 3.1 Summary of surface soil moisture retrieval using empirical and semi empirical models

Sl. No.	Author	Study area	Model	Inference
1	Oh et al (1992)	In-situ experiment	Experimental using Scatterometer	Developed a model to calculate Dielectric constant on bare fields.
2	Dubois et al (1995)	Michigan	Dubois model	Developed an empirical model to estimate SM and verified with SIR-C data The model performed better in bare soils and vegetation with NDVI less than 0.4
3	De Roo et al (2001)	Hickory Corners, Michigan	Oh model	Modified Oh model and incorporated canopy scattering model to retrieve the soil moisture over vegetation. Found that L band VV polarization gives better results for canopy scatter modelling as well as soil moisture measurements.
4	Zribi and Dechambre (2003)	Orgeval, Pays de Caux and Alpilles of France	Empirical model	Introduced a new parameter called surface roughness parameter (z) which is function of surface height and correlation length to develop new empirical model using C band.

Table 3.1 (Cont...)

Sl. No.	Author	Study area	Model	Inference
5	Holah et al (2005)	Touch catchment, Toulouse	Semi empirical model	Analyzed the sensitivity of surface parameters to radar backscatter energy and found that surface roughness is more sensitive to higher incidence angle (43°) and lower the incidence angle minimizes effect on soil moisture.
6	Bourgeau-Chavez et al (2007)	Delta junction and Anderson of Alaska	Semi empirical model	Developed empirical surface soil moisture model over various land use like grassland, cereal, harvested crop and root crop fields. The developed model gave good results when compared with field values at better spatial resolution and temporal frequency.
7	Koyama et al, (2010)	River Rur, Germany	Dubois model	Modified algorithm based on Dubois et al, (1995) and estimated surface soil moisture averaging by upscaling at different scales varying from catchment to field. They found modified algorithm results are acceptable when compared field values.

Table 3.1 (Cont...)

Sl. No.	Author	Study area	Model	Inference
8	Prakash et al (2011)	Roorkee, (Uttarakhand, India)	Dubois model	Attempted synergetic approach to estimate SM over bare and vegetation lands using Modis NDVI data and got good results.
9	Bertoldi et al. (2014)	Italian Alps	Support vector regression	Soil moisture is estimated using fixed and ground sensors, GEOTop (hydrological model) and SAR images. Soil moisture under meadows and pasture can be successfully estimated using support vector regression technique with additional NDVI, DEM and land cover data.
10	Das and Paul (2015)	Bankura district, west Bengal	Topp model, Semi empirical model	Developed the semi empirical model and compared results with top model.
11	El Hajj et al, (2017)	Agricultural plot one in France and Tunisia	Water cloud model	Mapped surface soil moisture at plot scale using Sentinel 1 & 2. They combined WCM with IEM to generate synthetic backscattering and used it train neural networks and calculated soil moisture.

Table 3.1 (Cont...)

Sl. No.	Author	Study area	Model	Inference
12	Hosseini and McNairn (2017)	Canada	Semi empirical model, and WCM	Explored the use of C and L band SAR for soil moisture over wheat fields and found C band is good at temporal moisture changes.
13	Rawat et al, (2018)	Rewari district, Haryana, India	Semi empirical model	Developed semi empirical model over bare fields by carrying out sensitivity analysis between field soil moisture and backscattering energy of RISAT and found that difference in Hybrid polarization improves model accuracy.
14	Dave et al, (2019)	Khambhat region, Gujarat, India	Dubois model	Modified the Dubois model for estimating surface soil moisture using single channel SAR data and gave good results at initial stage of crop cycle but poor results are observed as crops reach maturity stage.
15	Zhang et al, (2021)	Hebei Province, China	Water cloud model	Analyzed the relation between SAR polarimetric channels with field values (soil and vegetation) and used them as constants of WCM to retrieve soil moisture at different growing stages of wheat and it gave better results with accuracy.

Table 3.1 (Cont...)

Sl. No.	Author	Study area	Model	Inference
16	Fan et al, (2021)	North eastern Thailand	Dual-Temporal Dual-Channel (DTDC) algorithm	Developed an algorithm to estimate soil moisture over croplands. They utilized the ancillary field information and assumed there will be no change in surface roughness during crop period. The proposed model performed well with temporal soil moisture change with RMSE 0.06%.
17	Bhogapurapu et al, (2022)	Carman test site, Canada and Demmin test site, Germany	Water cloud model	Introduced new dual-pol radar vegetation index based on GRD SAR data to retrieve surface soil moisture over wheat and canola crop lands at different phenological stages. Found that developed DpRVic is better vegetation descriptor than RVI and NDVI.

3.3 SURFACE SOIL MOISTURE RETRIEVAL USING THEORETICAL MODELS

There is no general model that can account for backscattered energy throughout the full frequency range as well as naturally occurring surface conditions. Therefore, it is difficult to have common model performing on all terrain conditions. The theoretical models are developed based on electromagnetic wave scattering from different earth surface (vegetation and soil). Theoretical models basically work on certain

assumptions made on target properties for simplification. The basic theoretic modes are Kirchhoff Approximation (KA) and the Small Perturbation Model (SPM). SPM is also called as Bragg surface scattering model to apply this surface should satisfy Bragg resonance condition. The applicability range of SPM is evaluated by Engman and Wang. (1987) and Borgeaud and Noll, (1994).

The Integral Equation Model (IEM) was presented by Fung et al, (1992) as a backscattering model based on pair of integral equations for tangential surface fields. However, this model requires more number of input parameters along with assumption according to field surface. Altese et al, (1996) developed inversion approach based on IEM to retrieve surface soil moisture over 2 different bare fields. It was seen that sensitivity of SAR backscatter energy is much more to surface roughness rather than soil dielectric constant. So, small error in measuring roughness can induce error in soil moisture estimates. *Shi et al. (1997)* conducted field tests based on single scattering integral equation method to estimate soil moisture and surface roughness over bare field and short vegetated fields using L band SIR C and AIRSAR data. They applied this new algorithm on time series data sets and found the good agreement between estimated and measured soil moisture. Bindlish and Barros (2000) investigated IEM applicability in sparse vegetated land using multi frequency and multi polarization SAR data. They found even though IEM was developed for bare fields it performed well in vegetated areas at low incidence angles.

IEM is improved and modified over a period by introducing various vegetation scattering parameters like vegetation water content, leaf area index, NDVI etc., and roughness scattering parameters like roughness correlation length and roughness emissivity model (Bindlish and Barros, 2001; Shi et al, 2002). Baghdadi et al, (2002) introduced semi empirical calibration of surface roughness to IEM in case of bare fields. Since, measurement of correlation length in field is very difficult. The calibrated version of IEM gave good agreement between backscatter energy and soil moisture. In continuation Baghdadi et al, (2004) extended his semi empirical calibrated IEM to agricultural fields. They tested the calibration parameters with various radar configuration like polarization, incidence angle and frequency using experimental data and validated on independent field data. Notarnicola et al, (2006) introduced probability

distribution function (pdf) and Bayesian theorem in parametrization of vegetation and surface roughness respectively and later used in inversed IEM algorithm found good agreement between calibrated version and backscattering coefficient of different radar system and got improved results in both C and L-band. Dash and Prusty (2007) aimed to stimulate the backscattering coefficients at various SAR incidence angle like steep and shallow into IEM algorithm over 2 different Indian bare fields. It is noted model results gave good agreement measured backscattered data. Song et al, (2009) proposed change in IEM and called as Empirically Adopted IEM (EA-IEM) which considered soil dielectric constant as function of backscattered energy. Tested EA-IEM over bare fields and found analysis improved model results. In the same way, they also suggested another modification and called as Multilayer Soil IEM (MS-IEM) which considered surface and volume scattering of soil as effective parameter (Song et al, 2010).

Joseph et al. (2010) conducted field tests to retrieve soil moisture using L band Radar data with different incidence angle over corn fields. The author measured soil moisture over few plots and derived surface roughness by inverting the integral equation model (IEM). By simulating these surface roughness retrieved soil moisture over the entire study area. The retrieval method correlates well with soil moisture depending on the incidence angle, polarization and vegetation water content. *Baghdadi et al, (2011)* in continuation to *Baghdadi et al, (2004)* replaced the correlation length by fitting or calibration parameter and found IEM is better than previous one. *Lievens et al, (2011)* tested the IEM model over large agricultural fields which differ in incidence angle and soil roughness are parametrized and found fairly accurate soil moisture for both C and L band. *Guo et al. (2013)* developed a new soil moisture retrieval algorithm for bare surface using the L-band radiometer dual-polarization measurements. The newly developed algorithm was a simple semi-empirical model by analyzing Advanced Integral Equation Model (AIEM) under SMAP sensors and validated with SMOS data. They also found that the surface roughness parameters at different polarizations can be directly eliminated from the microwave observations. This leads to a new bare surface soil moisture algorithm using dual measurements without surface roughness information. *Ponnurangam et al, (2015)* proposed new model based on compact decomposition technique. After removal of vegetation scattering component, surface

scattering component is used to retrieve soil moisture and compared it with existing theoretical models like X-Bragg and IEM. The developed model is tested in both bare agricultural fields including all crop phenological stages and found acceptable results. Bai et al, (2015) described bare surface soil moisture using forward advanced IEM. Author used 4 different indices to reduce effect vegetation on model by empirical ratio method and recommended LAI as best vegetation descriptor.

Gupta et al. (2016) conducted field test to calculate soil moisture using scatterometer (dual polarized) on bare soils. Author noticed 25° is suitable incidence angle to estimate soil moisture using Radial basis function artificial neural network (RBFANN) model. RBFANN model showed better correlation with VV polarization than HH polarization to soil moisture. *Tao et al. (2016)* used the Integral equation model to estimate soil moisture using both L band ALOS and C band Radarsat data over four Beijing, China test fields. They estimated soil moisture over bare soils and low vegetation and found that VV polarization is more sensitive to soil moisture than HH polarization. They have introduced combined roughness parameter which is function of RMS surface heights and correlation length to estimate soil moisture.

Ghafouri et al, (2017) found difficulty in retrieving surface roughness RMS height which does not include surface height dispersion in IEM model inversion. So, author introduced random fractal geometry using the power law roughness spectrum which enhanced surface roughness calculation by 10% thus, improving the IEM soil moisture. In the same way Yang et al, (2017) and Tao et al, (2017) introduced Gaussian function and Fresnel reflection to develop combined surface roughness parameter. Which, improved the agreement between IEM simulations and SAR observations. Zhang et al, (2018) developed a methodology to retrieve soil moisture from multi source SAR images. They also developed a Look Up Table (LUT) which does not need any prior information about surface roughness and retrieved soil moisture using IEM over various bare fields. Meyer et al, (2018) and Huang et al, (2019) used AIEM based on numerical simulation analysis to retrieve surface soil moisture over bare and sparsely vegetated areas. They found correlation between simulated and calculated soil moisture from AIEM are better in vegetative conditions. Zhang et al, (2020) utilized the surface roughness rms and empirical correlation length to reduce error in surface roughness

parameter to retrieve bare field moisture using AIEM and found this empirical model is feasible when incidence angle is 33.5° to 26.3° at C-band. Zhang et al, (2021) changed roughness parameter by using effective and combined roughness form in AIEM to improve accuracy of soil moisture retrieved by AIEM and to reduce uncertainty in roughness measurement. Summary of surface soil moisture retrieval using theoretical models is presented in Table 3.2.

Table 3.2 Summary of surface soil moisture retrieval using theoretical models

Sl. No.	Author	Study area	Model	Inference
1	Fung et al, (1992)	Experimental setup at University of Texas at Arlington.	Integral Equation Model (IEM)	Developed backscattering model based on pair of integral equations for tangential surface fields. However, this model requires more number input parameters along with assumption according to field surface.
2	Shi et al, (1997)	Oklahoma	Integral Equation Model (IEM)	Developed an empirical model to estimate surface soil moisture and surface roughness using L band SAR data over well maintained Oklahoma watershed and found an RMSE of 3.4% which is acceptable.

Table 3.2 (Cont...)

Sl. No.	Author	Study area	Model	Inference
3	Njoku et al. (2000)	Oklahoma, Georgia, Arizona, and Idaho	Iterative forward model	Demonstrated AMSR-E has better capability in soil moisture retrieving over MSMR and SSM/I
4	Baghdadi et al, (2002)	Pays de Caux region and Rhone valley, France	IEM	Introduced semi empirical calibration of surface roughness to IEM in case of bare fields. Since, measurement of correlation length in field is very difficult. The calibrated version of IEM gave good agreement between backscatter energy and soil moisture.
5	Vecchia et al. (2007)	Les Landes forest,	Radiative transfer model	Developed a model which is incorporated with litter effects to estimate brightness temperature.
6	Joseph et al (2010)	Beltsville, U.S	IEM	Conducted field tests to retrieve soil moisture over corn fields.

Table 3.2 (Cont...)

Sl. No.	Author	Study area	Model	Inference
7	Wang et al (2011)	Heihe River Basin	IEM	Followed two step retrieval method first calculated surface roughness by using this inverting soil moisture is estimated
8	Balenzano et al (2013)	Demmin site, Germany	Radiative transfer model	Checked the capability of X and L band SAR data to map SM over agricultural land and found that L band HH polarization is performing well.
9	Tao et al. (2017)	Beijing, China	IEM	Found that VV polarization gives better results than HH polarization over low vegetated fields.
10	Ghafouri et al, (2017)	Ilam and Dehloran, Iran	IEM	Found difficulty in retrieving surface roughness RMS height which does not include surface height dispersion in IEM model inversion. So, author introduced random fractal geometry using power law roughness spectrum which enhanced surface roughness calculation by 10%

Table 3.2 (Cont...)

Sl. No.	Author	Study area	Model	Inference
11	Zhang et al, (2018)	Hebei, China	IEM	They developed a Look Up Table (LUT) which does not need any prior information about surface roughness and retrieved soil moisture using IEM over various bare fields.
12	Huang et al, (2019)	Ugan-Kuqa River Delta Oasis, China	AIEM	AIEM based on numerical simulation analysis to retrieve surface soil moisture over bare and sparsely vegetated areas. They found that the correlation between simulated and calculated soil moisture from AIEM is better in vegetative conditions.
13	Zhang et al, (2021)	Linze County, China	AIEM	Roughness parameter is replaced by using effective and combined roughness form in AIEM to improve accuracy of soil moisture retrieved by AIEM and to reduce uncertainty in roughness measurement.

3.4 SURFACE SOIL MOISTURE MODELS COMPARATIVE STUDIES

In the early 1990's researchers concentrated on developing algorithms to retrieve surface soil moisture using SAR. So, there is no much studies based on comparing the models. In fact researchers compared results of SAR retrieved soil moisture with land processed models (Hallikainen et al, 1985; McLaughlin, 1995; Houser et al, 1998; Bach and Mauser et al, 2003).

It was seen that IEM is performing better but this model requires more data and the analogy is quite complex. Boisvert et al., (1997) conducted field test to know the impact of gradients on soil moisture estimation using SAR. They noticed that the integral equation model (IEM) performs better than the 'oh' model. Author had coupled the scattering models with penetration depth models to check the impact of gradient. A fixed mean depth gave good correlation when there was no moisture gradient but even IEM over estimated backscattered energy during the gradients. So, the authors noticed that moisture gradients have impact over backscatter models. Oevelen and Hoekman (1999) compared semi empirical Oh model with numerical inversion IEM over two test sites of the study and found that IEM has better agreement with field measured soil moisture values. Narayanan and Hegde (2000) compared two inversion models based on regression and neural network for three bands of SAR energy. They found that neural network has better results than regression analysis but both model show comparable errors. So, both models have unique advantageous over other.

Narayanan and Hirsave (2001) compared the three semi empirical soil moisture modelling approaches namely, linear regression, linear statistical inversion and neural network models using SIR-C images of X, C and L bands. Linear statistical inversion technique performs well but underestimates higher soil moisture. Neural network technique works well but overestimates lower soil moisture. Romshoo et al, (2002) time series SAR data is used to retrieve surface soil moisture (Dubois model) over agricultural fields. Compared the SAR extracted soil moisture values with three hydrological models at field scale and found that the estimates are matching reasonably well. Sahebi et al, (2003) compared two empirical models developed by Ji et al, (1995) and Champion (1996) and found that there is a need for recalculation of constants. So,

another model proposed based new constants which gave better results than previous models. Thoma et al, (2004) compared the IEM theoretical model with a newly developed delta index to estimate soil moisture. IEM performed very poorly because of rocky terrain surface. The index was also simple to use and implicitly took into consideration both rock pieces and surface roughness. Thoma et al, (2006) compared IEM, semi empirical model with newly developed delta to estimate soil moisture at watershed scale. IEM performed poorly, semi empirical used field data and gave good results whereas delta index performed well at this scale too. Baghdadi and Zribi (2006) tested Oh, Dubois and IEM over bare fields using different experimental observations. Oh model performed well but underestimated the values HV polarization. In the same way IEM model also overestimated at HH polarization and major errors are seen in VV polarization. Dubois gave good results only if soil moisture is more than 30% if not it over estimated it.

Baghdadi et al, (2011) compared Oh, Dubois and IEM using TerraSAR-X over bare fields and found that IEM is giving best results if it is calibrated with exponential correlation function instead of Gaussian function. Oh model correctly stimulated backscattered values when compared to Dubois model in VV and HH polarizations. Wang *et al.* (2011) attempted to estimate surface roughness and soil moisture by satellite products without using any ancillary products. Authors followed two step retrieval method in the first step he used multi incidence angle to estimate surface roughness and correlation length by integral equation method. In the second step advanced integral equation method was used to estimate surface soil moisture with help surface roughness derived from first step. One of the major problem is vegetation cover but it was overcome by using water cloud model. Khabazan *et al.* (2013) compared the semi empirical Oh, Dubois and theoretical Integral equation method to estimate soil moisture using L and C band AIRSAR data. They found that Dubois model is over estimating soil moisture in both bands whereas Oh and IEM models over estimated in L band and under estimated in C band. They found the best correlation when soil depth is between 3 cm with NDVI less than 0.2. Panciera et al, (2013) compared the Oh, Dubois and IEM soil moisture models using L-band SAR and found that Oh model is performing well compared to other two models. Also, calibrated the surface roughness

correlation of IEM and improved the miss match between observed and estimated values. Palosica et al, (2013) compared the two layer artificial neural network and IEM over agricultural fields of experimental study. Found that ANN produced slightly better soil moisture estimates than IEM. Al-Bakri et al, (2014) investigates the performance of Oh model and Semi empirical model to predict soil moisture and found that semi empirical model suits any field by using field data but empirical model needs to be corrected during scaling up the moisture values. Zhang et al, (2015) compared empirical and semi empirical models over bare field and found modified Dubois model gave comparable results to empirical model independent of surface roughness. MirMazloumi and Sahebi (2016) compared Oh, Dubois and IEM for C, L and P bands over agricultural fields. Oh model has best results in C-band however Dubois and IEM look accurate in L band. They also found that Oh model is good in estimating soil moisture whereas IEM is good in surface roughness.

Choker et al, (2017) compared the Oh, Dubois, IEM, AIEM and IEM modified by Baghdadi model (Baghdadi et al, 2002) using large set of experimental filed data along various SAR observations in X, C and L band. In comparison between empirical models Oh model works to better model in HH and VV polarization. Dubois model gave poor agreement with field moisture values in HH polarization but quite better for VV polarization. In comparison with theoretical models IEM and AIEM simulated backscattered energy found better performing when Gaussian correlation function was replaced by exponential function. Overall, IEM by Baghdadi was the most adequate model to estimate soil moisture and roughness. Wang et al, (2017) compared three polarimetric decomposition techniques to get surface scattering parameters and estimated surface soil moisture over various agricultural fields. Results showed soil moisture based on each decomposition has its own advantage depending upon its crop type and crop phenological stage. Freeman-Durden decomposition worked well in wheat and corn fields whereas, Van-Zyl decomposition worked in canola fields. Overall comparison at phenological stage is done, found that enhanced surface scattering gave good surface parameter to retrieve surface soil moisture.

Zribi et al, (2019) analyzed five different backscattering SAR models to estimate surface soil moisture over bare and vegetated fields. Compared AIEM, IEM-Baghdadi,

Oh'92, Dubois, and Baghdadi models over turmeric, marigold, and sorghum fields. Results showed Baghdadi models are performing well on prior information of field. The soil moisture estimation errors observed in the HV polarization are higher than in the HH polarization, for all three crops. Kumar et al, (2019) compared various semi-empirical approaches like random forest regression (RFR), support vector regression (SVR) and artificial neural network regression (ANNR) to estimate soil moisture over crop covered area. ANNR gave poor estimates compared SVR and RFR. Results also showed VV polarization works better than VH polarization. Ezzahar et al, (2019) evaluated Support vector regression, Oh and IEM soil moisture models and found that Oh model performs better than IEM in agriculture fields. SVM results are close to estimates of IEM. So, SVM can be relied when there is difficulty measuring surface roughness. Zhang et al, (2020) analyzed two semi empirical models (modified water cloud model (MWCM) and ANN) to retrieve soil moisture during corn growing stage. Results showed ANN has potential in mapping soil moisture over corn fields at early growing stage. Whereas MWCM gave better results in overall corn growing stage. Chen et al, 2022 studied the different scattering models combining with Calibrated IEM (CIEM) and Dubois model and found this approach gave good results with CIEM. Summary of comparative evaluation of surface soil moisture retrieval is given in Table 3.3. The comparison of various models along with their advantages are given in Table 3.4.

Table 3.3 Summary of comparative evaluation of surface soil moisture retrievals

Sl. No.	Author	Study area	Model	Inference
1	Boisvert et al (1997)	Along Lethbridge, Canada	Semi empirical and IEM model	Conducted Field test to know the impact of gradients on SM and found IEM performed well. Noticed gradients have impact over backscatter models
2	Oevelen and Hoekman (1999)	EFEDA-Spain'91 and HAPEX-Sahel'92 experiment area	Oh and IEM	Compared semi empirical model with numerical inversion model over two test sites of the study and found that IEM has better agreement with field measured soil moisture values.
3	Narayanan and Hirsave (2001)	New Hampshire, USA	Linear regression, Linear statistical inversion and Neural network	Compared the three semi empirical soil moisture modelling approaches using SIR-C images of X, C and L bands. Linear statistical inversion technique performs well but underestimates higher soil moisture. Neural network technique works well but overestimates lower soil moisture.

Table 3.3 (Cont...)

Sl. No.	Author	Study area	Model	Inference
4	Thoma et al, (2004)	Walnut Gulch Experimental Watershed, Arizona	IEM and Delta index	Compared theoretical model with newly developed index to estimate soil moisture. IEM performed very poorly because of rocky terrain surface. The index was also simple to use and implicitly took into consideration both rock pieces and surface roughness.
5	Baghdadi and Zribi (2006)	Pays de Caux, Rhone valley, Orgeval site, Villamblain and Toulouse of France Chateauguay River basin, and Brochets River basin of Canada	Oh, Dubois and IEM	Tested three models over bare fields using different experimental observations. Oh model performed well but underestimated the values HV polarization. In same way IEM model also overestimated at HH polarization and major errors are seen in VV polarization. Dubois gave good results only if soil moisture is more than 30% if not it over estimated it.

Table 3.3 (Cont...)

Sl. No.	Author	Study area	Model	Inference
6	Baghdadi et al, (2011)	Orgeval, Villamblain, Mauzac, Garons, Versailles, Thau and Seysses of France and Kairouam of Tunisia	Oh, Dubois and IEM	Compared three soil moisture models using TerraSAR-X over bare fields and found that IEM is giving best results if it is calibrated with exponential correlation function instead of Gaussian function. Oh model correctly stimulated backscattered values when compared to Dubois model in VV and HH polarizations.
7	Khabazan et al (2013)	Oklahoma	Oh, Dubois and IEM model	Found that Oh and IEM models are performed well whereas Dubois overestimated SM.
8	MirMazloui and Sahebi (2016)	Little Washita Experimental Watershed, Oklahoma	Oh, Dubois and IEM	Compared three models for C, L and P bands over agricultural fields. Oh model has best results in C-band however Dubois and IEM look accurate in L band. They also found that Oh model is good in estimating soil moisture whereas IEM is good in surface roughness.

Table 3.3 (Cont...)

Sl. No.	Author	Study area	Model	Inference
9	Choker et al, (2017)	Agricultural sites in France, Italy, Germany, Belgium, Luxembourg, Canada and Tunisia	Oh, Dubois, IEM, AIEM and IEM by Baghdadi model	Compared five soil moisture models using large set of experimental filed data using various SAR observations in X, C and L band. In comparison between empirical models, Oh model works to better model in HH and VV polarization. In comparison with theoretical models IEM and AIEM simulated backscattered energy found better performing In overall, IEM by Baghdadi found to be most adequate model to estimate soil moisture and roughness.
10	Zribi et al, (2019)	Berambadi watershed, Karnataka, India	AIEM, IEM- Baghdadi , Oh'92, Dubois, and Baghdadi models	Compared five different backscattering SAR models to estimate surface soil moisture over turmeric, marigold, and sorghum fields. Results showed Baghdadi models are performing well on prior information of field. The soil moisture estimation errors observed in the HV polarization are higher than in the HH polarization, for all three crops.

Table 3.3 (Cont...)

Sl. No.	Author	Study area	Model	Inference
11	Zhang et al, (2020)	Heihe watershed, China	MWCM and ANN	MWCM and ANN to retrieve soil moisture during corn growing stage. Results showed ANN has potential in mapping soil moisture over corn fields at early growing stage. Whereas MWCM gave better results in overall corn growing stage.
12	Gharechelou et al, (2021)	Northern Iran	Oh, Dubois and Delta index model	Compared the Oh and Dubois model in bare and sparsely vegetated areas of arid region and found Oh model to be better than Dubois. Also, author claimed the model performance varies with land characteristics and effects the model accuracy.

Table 3.4 Comparison of various SAR based surface soil moisture models

Sl. No.	Models	Validity range	Advantage	Disadvantage
1	Oh, 1992	$0.1 < k_s < 6.0$; $2.6 < k_l < 19.7$ and $20^\circ < \theta < 50^\circ$	Wide range of incident angle	Valid only for bare to sparsely vegetated area.
2	Kirchhoff's approximation	$k_l > 6$; $l^2 > 2.76k_s$	Easy inversion model	Valid for rough surface

Table 3.4 (Cont...)

Sl. No.	Models	Validity range	Advantage	Disadvantage
3	Small perturbation model (Bragg model)	$k_s < 0.3$ and $k_l < 3$	Forward inversion	Applicable for slight rough surface
4	Fung, 1992 (Integral Equation Model (IEM))	$k_s < 3$	Valid for extensive range of roughness	Too many data is required and complex.
5	Dubois, 1995	$K_s \leq 2.5$; $2.5 < k_l < 20$ and $20^\circ \leq \theta < 65^\circ$	Easy inversion model	Valid only for bare fields
6	Shi, 1997	$0.2 < s < 3.6$; $2.5 < l < 35$	Surface roughness spectrum considered	Valid for sparsely vegetated area
7	Hajnsek, 2003 (X-Bragg model)	$k_s < 1$ and $k_l < 6$	Forward inversion	Valid for sparsely vegetated area
8	Oh, 2004	$k_s < 3.5$; $20^\circ < \theta < 50^\circ$	Volumetric soil moisture inversion	Valid for bare fields to light vegetated field

*s-vertical surface roughness, l-horizontal surface roughness, k-wave number, θ -Incidence angle

3.5 SUMMARY OF LITERATURE REVIEW AND RESEARCH GAPS

The extensive literature review shows that active microwave remote sensing is suitable for retrieving surface soil moisture. Research studies also explained the various bands of SAR remote sensing and its advantages in estimating surface soil moisture over bare and vegetated fields. Shorter wavelengths (X-band, 3 cm) are sensitive to the upper surface such as vegetation canopy. Intermediate wavelengths (C-band, 10 cm) sensible to soil moisture studies in sparsely vegetated areas whereas, longer wavelengths (L-band, 24 cm) retrieves soil moisture in moderately vegetated areas such as agricultural fields (Baghdadi et al., 2008; Kim et al., 2017). Polarizations and decomposition techniques also plays a vital role in retrieving surface soil moisture. The literature review also showed the various empirical, semi-empirical and theoretical models' advantages and disadvantages depending on the surface and vegetation conditions.

From the literature review, it is evident that Oh model is more utilized and applied in various land surface and vegetation conditions. On the other hand, IEM performed well in most of the comparative studies but requires a lot of information about the field and is complex. In case of vegetated fields, Water Cloud Model (WCM), a semi empirical radiative transfer model has performed well in both bare and vegetated land by using model and vegetation derived parameters. Literature review also show cased that majority of the studies are carried out at large scale areas and in case agricultural fields most of the studies are carried out on homogeneous cropping pattern. In case of agricultural field surface soil moisture retrieval most of the studies concentrated for well-defined single day not on whole crop cycle. Limited studies are seen in evaluating surface soil moisture models and bands for phenological stages of crop (crop cycle).

The primary issue in the Indian sub-continent agricultural fields is that they are smaller in size than other western countries. For example, the average farmland size in the United States is approximately 450ha while that in India is 1.16ha (MacDonald et al 2013; NABARD, India). Very limited number of studies are found targeting surface soil moisture retrieval at plot/regional scale. Previous surface soil moisture studies are backed by random sampling field information. Few studies are supported by gridded field sampled soil moisture information and based on it mapped. This thesis intends to address the above mentioned research gaps.

The upcoming chapter discusses about the characteristics of study area, data products and formulated methodology to achieve defined objects.

MATERIALS AND RESEARCH METHODOLOGY

4.1 INTRODUCTION

This chapter explains the characteristics of study area, data products and methodology followed to achieve the pre-defined objectives and it is organised under the following sections,

- i. Study area and its salient features
- ii. Data products and tools
- iii. Research methodology

4.2 STUDY SITE AND ITS SALIENT FEATURES

The study area has primarily heterogeneous cropping pattern typically seen in the Indian context. The study plots/sites considered for this study falls in Malavalli, which is in Mandya district of Karnataka, India. Which extends between 12.22°N to 12.50°N and 77.00°E to 77.20°E which falls in 57D Survey of India (SOI) toposheet. The study area is classified as tropical semi-arid region according to Koppen and Geiger classification and the study area is agricultural based town thus study regrading surface soil moisture is significant and comes under Cauvery basin. The field selected to study surface soil moisture retrieval using SAR without vegetation effects is bare land and for with vegetation effects are crops like Paddy, Sugarcane, Maize, and Tomato. The location of agricultural plots in the study area is presented in Figure 4.1. Figure 4.2 shows the google earth view of the agricultural plots selected, and the salient features of the study area and characteristics of each study plot are presented in Table 4.1 and Table 4.2 respectively.

Table 4.1 Salient features of study area

Sl. No.	Title	Description
1	Location	12.22°N to 12.50°N and 77.00°E to 77.20°E
2	Geology	80% covered by Gneiss and by Granite rocks

3	Soil	Sandy Loam to Sandy Clayey Loam.
4	Rainfall	Average annual rainfall is 700-900 mm.
5	Temperature	Varies from 16° C to 32° C.
6	Altitude	600 m
7	Irrigation Source	Canal from Shimsha river and Groundwater

Table 4.2 Characteristics of each test plots

Sl. No.	Crop	Area (acres)	Crop Breed	Crop period (months)	Crop month	Soil type
1	Paddy	0.51	Omkar	6	July-Dec	Clayey loam
		0.48				
2	Tomato	1	Arka Saurabh	4	July-Oct	Sandy loam
3	Sugarcane	1	Nayana	11	April-Feb	Sandy loam
4	Maize	1	Ganga-11	3	Jun-Aug	Sandy loam
5	Bare land	1.3	-----	-----	-----	Sandy loam

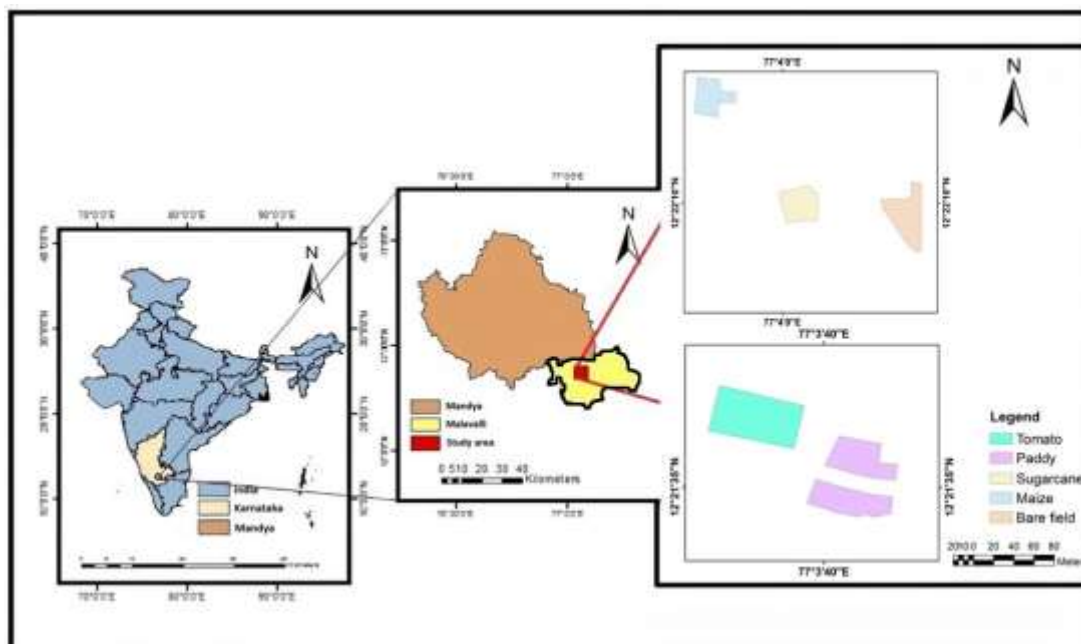


Figure 4.1 Location of the study area



Figure 4.2 Google Earth View of Study Area

4.2.1 Topography

The study area falls into deccan plataue region of India. So the terrain is almost flat with altitude variation of 600-700m above mean sea level. Study area falls under cauvery basin. The major portion agricultural land is irrigated by canal water from an anicut (or dam) built across shimsha river, a tributary of river Cauvery. Nearly 44% of study area is under cultivation using tanks, canal and wells. Paddy and Sugarcane are the two major crops grown in this region.

4.2.2 Climate

Study area experinces tropical semi-arid type of climate. The average annual rainfall is 740mm of which more than 50% of rainfall occurs during southwest monsoon with average number of rainy days are 73. The temperature varies from 18° C to 32° C with higher rate of evapo-transpiration during summer compared winter and rainy days.

4.2.3 Geology and soil

The peninsular Gneisses covers almost 80% of the study area, including few patches of porphyritic granite. The soil ranges from red sandy loams to clay loam very thin at ridges og higher elevation and comparatively thick at valley regions.

4.3 DATA PRODUCTS AND TOOLS

Remote sensing data and In-situ/ field data are the two different types of data used in this study. Remote sensing data involves Sentinel-1a, ALOS PALSAR-2, SRTM DEM and Google earth data. In-situ data involves soil, vegetation and rainfall data.

The details of the Remote sensing data products used are described below.

4.3.1 Sentinel-1a

Sentinel-1a is a Synthetic Aperture Radar (SAR) in C band (center frequency: 5.405 GHz), that provides continuous imagery (day, night and all weather). It provides dual polarization capability, very short revisit times and rapid product delivery. For each observation, precise measurements of spacecraft position and attitude are available. The data characteristics of Sentinel-1a is explained in Table 4.3. The data acquisition period is shown in Table 4.4. Various data acquisitions modes of Sentinel-1a are as follows

- Strip Map (SM): 80 km swath, 5 x 5 m spatial resolution
- Interferometric Wide Swath (IW): 250 km swath, 15 x 20 m spatial resolution
- Extra-Wide Swath (EW): 400 km swath, 20 x 40 m spatial resolution
- Wave (WV): 20 x 20 km, 5 x 5 m spatial resolution

Table 4.3 Data characteristics of Sentinel-1a

Satellite/Sensor	Sentinel-1a
Frequency (GHz)	5.405
Frequency Band	C Band
Polarization	VV and VH (Dual-pol)
Orbit direction	Ascending
Incidence angle (°)	23

Resolution (m)	15*20
Resampled Resolution	10*10
Swath (km)	250
Period	2014- Present
Repetivity	12 days

Table 4.4 Sentinel-1a data acquisitions over the study area during the study period

	Sentinel-1a
Data acquisition Dates	05/05/2018, 17/05/2018, 29/05/2018, 10/06/2018, 22/06/2018, 04/07/2018, 16/07/2018, 28/07/2018, 09/08/2018, 21/08/2018, 02/09/2018, 14/09/2018, <u>26/09/2018*</u> , 08/10/2018, 20/10/2018, <u>01/11/2018*</u> , 07/12/2018, 31/12/2018, <u>12/01/2019*</u> , 24/01/2019, 05/02/2019

*Field samples are not collected due to rain in study area.

4.3.2 ALOS PALSAR-2

Advanced Land Orbiting Satellite (ALOS) Phased Array L- Band Synthetic Aperture Radar (PALSAR)-2 is a Japanese L band, quad Polarized data which means the data consists of all possible polarization combinations ((VV, VH, HH & HV). ALOS PALSAR-2 has five different acquisition modes with four different levels of data products. In the present study, Single Look Complex (SLC) products are used which are acquired in high sensitive strip mode. Two quad polarimetric images of ALOS PALSAR-2 are acquired over the study area with beam no FP6-3 and 2. The detailed image information of the satellite data is presented in Table 4.5.

Table 4.5 ALOS PALSAR-2 data information

Sensor	PALSAR-2
Date of acquisition	23/07/2018 & 01/10/2018
Band	L
Beam mode	FP6-2 & FP6-3
Mode of acquisition	High sensitive quad polarized data

Polarization	VV, VH, HH and HV
ENL	2
Incidence angle	27.79°
Ground resolution	6 m
Swath	30*70 km

4.3.3 SRTM (Shuttle Radar Topography Mission)

SRTM data (30 m resolution) is downloaded from earth explorer for the study area to check the SAR limitations like Foreshortening, shadow and layover. Since the study area did not have much variation in altitude. So, it overwhelmed the limitations of SAR.

4.3.4 Google earth data

Google Earth is a computer program that renders a 3D representation of Earth based on primary satellite imagery. The program maps the Earth by superimposing satellite images, aerial photography, and GIS data onto a 3D globe. In the present study, Google earth is used to conduct an initial field survey and check the accessibility of fields for sample collection.

The details of the In-situ/field data products used are described below

4.3.5 Soil and Vegetation data

The two types of soil samples were collected from the each field. One set of surface soil from each grid to calculate surface soil moisture and another set was collected using core cutter to analyze the bulk density (According to IS 2720-4, 1965). The surface soil samples (of weight 40-60gm) for surface soil moisture estimation from agricultural plots were collected in the plastic bags and sealed it with labelling. Initial weight of the samples was measured in the field itself and for soil moisture, bulk density and texture analysis collected samples were transferred to laboratory. Roller chain method was used to measure soil surface roughness and it is measured in both directions of the field (along and across ridge).

Vegetation Water Content (VWC) data is collected using destructive sampling method i.e., from each crop field 0.5*0.5m of vegetation was cut and collected in the sealed plastic bag with initial weight measurement. Later on these samples also transferred to laboratory. Crop height of field was measured using metallic scale and staff during all field visits.

4.3.6 Rainfall data

Rainfall data is collected from the Karnataka State Natural Disaster Monitoring Centre (KSNDMC). The daily data for this station is available through an online portal (https://www.ksndmc.org/Weather_info.aspx). Rainfall collected data were used to check whether the study area has been affected by rainfall or not prior to the days of sampling. It is found that rainfall has occurred during 26/09/2018, 01/11/2018 and 12/01/2019, and samples are not collected on those days.

4.4 TOOLS

Sentinel Application Platform 7.0 (SNAP), PolSARPro 5.1.3, Arc GIS 10.1 and R studio 1.1.423 are the tools or software used in this study to achieve desired objectives. The following technical advancements make the SNAP architecture appropriate for Earth Observation (EO) processing and analysis. Extensibility, portability, modular rich client platform, generic EO data abstraction, tiled memory management, and graph processing framework. It is most appropriate in processing and analysing sentinel 1a data. PolSARpro is a tool for high-level radar polarimetry teaching as well as supporting scientific use of polarimetric SAR data. The programme includes a set of well-known algorithms and tools, lays the groundwork for the use of polarimetric methods in scientific study, and encourages research and application creation utilising Pol-SAR, Pol-InSAR, Pol-TomoSAR, and Pol-TimeSAR data. Arc GIS is a geographic information system used to analyse the remote sensing data and to develop interactive maps. R studio, a programming language for statistical calculation and graphical visuals. It is used to extract backscattered energy corresponding to field sampled points from SAR data.

4.5 RESEARCH METHODOLOGY

A systematic research methodology has been made to achieve the objectives of this study. Which includes field/in-situ data collection, lab experiments, data analysis, SAR image processing and retrieval of surface soil moisture using various models over small/plot scale agricultural plots at different crop stages. Figure 4.3 provides the research methodology followed to achieve the pre-defined objectives of the study

Next chapter gives details about the field data collection, lab experiments, and systematic explanation of SAR image processing and data analysis.

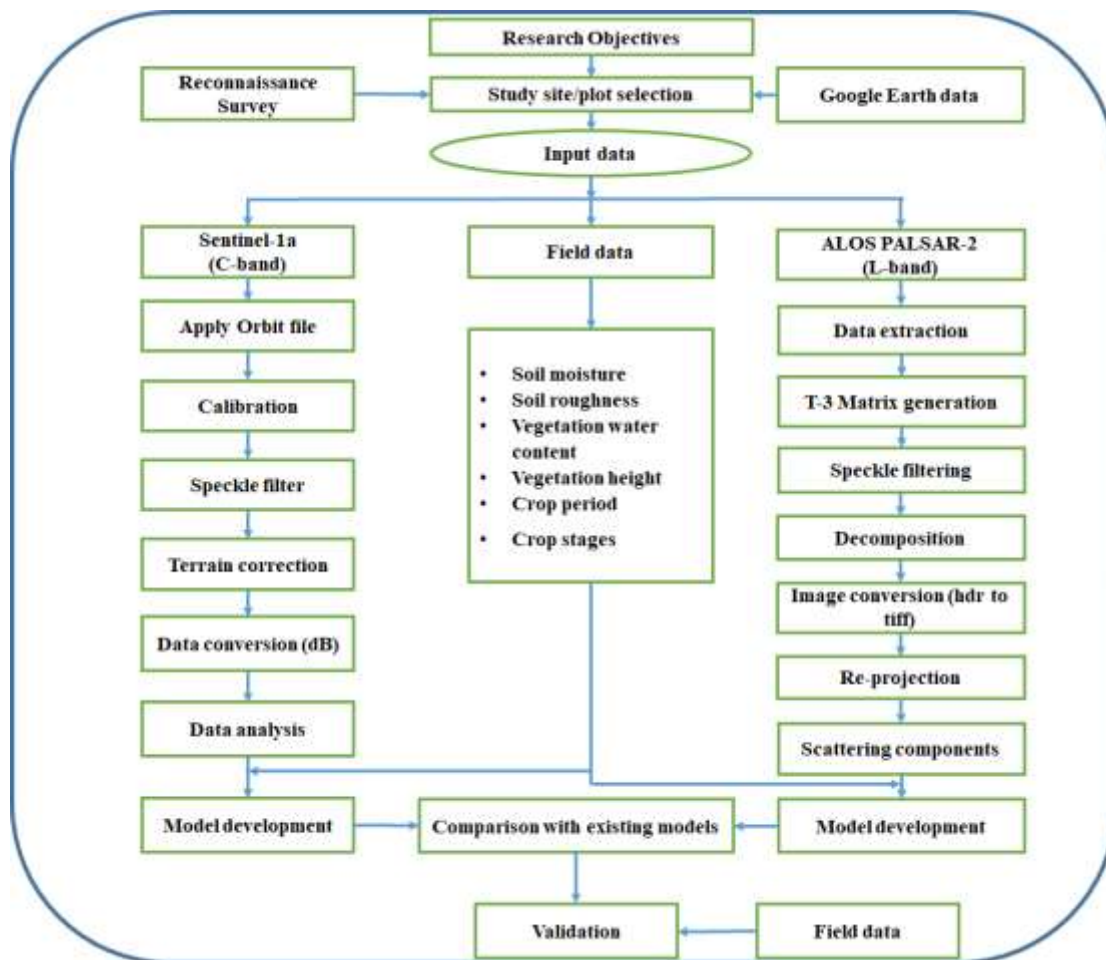


Figure 4.3 Research methodological framework of the study

4.6 SURFACE SOIL MOISTURE MODELS

Oh model

Oh model is an empirical method of retrieving surface soil moisture using multi-polarized data like VV, VH, HH and HV (Oh et al., 1992). Using the multi-polarized radar signal and considering the co-polarized and cross-polarized ratio, this model could predict the r.m.s height (cm) of the surface and soil moisture. The initial Oh model, 1992 is presented in equation (4.1) to (4.3).

$$p = \frac{\sigma_{HH}^{\circ}}{\sigma_{VV}^{\circ}} = \left[1 - \left(\frac{\theta}{90^{\circ}} \right)^{\frac{1}{3\Gamma}} e^{-k.r.m.s} \right]^2 \quad (4.1)$$

$$q = \frac{\sigma_{HV}^{\circ}}{\sigma_{VV}^{\circ}} = 0.23\sqrt{\Gamma_{\circ}}(1 - e^{-k.r.m.s}) \quad (4.2)$$

$$\Gamma_{\circ} = \left| \frac{1-\sqrt{\epsilon_r}}{1+\sqrt{\epsilon_r}} \right|^2 \quad (4.3)$$

Where, (θ) is incident angle, (k) wave number, (r.m.s) soil surface roughness and Fresnel reflectivity of the surface at nadir (Γ_0). The parameters p and q are derived by empirical fitting to the ground-based measurements of σ_{HH}° , σ_{VV}° and σ_{HV}° . Then Oh model is modified to cross-polarization and further updated to retrieve soil moisture and surface roughness. The modified Oh model, 2004 is given in equation (4.4).

$$k.r.m.s(\theta, M_v, \sigma_{VHM}^{\circ}) = \left[-3.125 \ln \left\{ 1 - \frac{\sigma_{VHM}^{\circ}}{0.11M_v^{\circ}(\cos\theta)^{2.2}} \right\} \right]^{0.556} \quad (4.4)$$

X-Bragg model

Extended Bragg scattering model is the modified version of the Bragg scattering model. The Bragg model is suitable only to smooth surface and longwave bands that cannot explain cross-polarization power. Hajnsek et al., 2000 developed X-Bragg model to overcome depolarization and to remove non-zero cross-polarization power. It is also reported that surface scattering power is maximum when $\delta=\pi/6$ and most stable with real field conditions (Hajnsek et al., 2009).

$$\begin{aligned}
[T] = P_S \begin{bmatrix} 1 & \beta^* \text{sinc}(2\delta) & 0 \\ \beta \text{sinc}(2\delta) & \frac{1}{2} |\beta|^2 (1 + \text{sinc}(4\delta)) & 0 \\ 0 & 0 & \frac{1}{2} |\beta|^2 (1 - \text{sinc}(4\delta)) \end{bmatrix} + \\
P_D \begin{bmatrix} |\alpha|^2 & \alpha^* & 0 \\ \alpha & 1 & 0 \\ 0 & 0 & 0 \end{bmatrix} + P_V \begin{bmatrix} 2 & 0 & 0 \\ 0 & 1 & 0 \\ 0 & 0 & 1 \end{bmatrix} \quad (4.5)
\end{aligned}$$

Where, T is the total coherence matrix; P_S, P_D, and P_V are surface, dihedral and volume components scattering power; δ is depolarization; α and β are dihedral and surface scattering parameters.

Water cloud model (WCM)

Attema and Ulaby (1978) developed Water Cloud Model by considering the vegetation canopy as clouds, in which water droplets are distributed randomly within the canopy. Effect of vegetation, soil, vegetation water content, and two-way attenuation between soil and vegetation on radar backscatter is accounted for estimation of co-polarization, using the incident angle and interaction between soil and vegetation (Baghdadi et al., 2017).

$$\sigma_{PP}^{\circ} = \sigma_{veg}^{\circ} + \sigma_{veg+soil}^{\circ} + (\tau^2) \sigma_{soil}^{\circ} \quad (4.6)$$

In co-polarization radiation, the interaction between vegetation and soil is not a dominating factor, and hence the term $\sigma_{veg+soil}^{\circ}$ is neglected. The modified equation of water cloud model is

$$\sigma_{PP}^{\circ} = \sigma_{veg}^{\circ} + (\tau^2) \sigma_{soil}^{\circ} \quad (4.7)$$

Where τ^2 is the two-way attenuation (transmissivity) of the vegetation, σ_{PP}° is the total backscatter coefficient of the co-polarized signal, σ_{veg}° and σ_{soil}° is the backscatter contribution of the vegetation cover and soil surface, respectively.

$$\sigma_{veg}^{\circ} = AV_1 \cos\theta (1 - \tau^2) \quad (4.8)$$

$$\tau^2 = \exp(-2BV_2 \text{Sec}\theta) \quad (4.9)$$

$$\sigma_{soil}^{\circ} = C + D M_v \quad (4.10)$$

Where A and B are WCM model parameters, C and D are soil parameters, θ is the incident angle, and V_1 , V_2 are vegetation descriptors, and M_v is the field soil moisture. σ_{soil}° is computed by the function of surface roughness (Srivastava et al. 2008) and soil moisture.

DATA COLLECTION, PROCESSING AND ANALYSIS

5.1 RECONNAISSANCE SURVEY

Initially Google earth image data is used to identify the city, water bodies and agricultural fields. Once the agriculture area location is known, a reconnaissance field survey is carried out to select various croplands. Reconnaissance survey also includes interacting with local farmers to know the type of crop they are planning to grow. Based on the interaction and survey few crop fields of Paddy, Sugarcane, Maize and Tomato are selected for the study. The selected crop fields GPS locations are taken during the visit, which was transferred to Google earth later to know the distance between each fields and to check feasibility of data collection between fields within defined time period during satellite pass.

5.2 SAMPLING LOCATIONS IDENTIFICATION

Utilizing the information of the Reconnaissance survey and field accessibility to bare field and agricultural fields like Paddy, Sugarcane, Maize and Tomato crops are selected for the study. Several ground parameters are measured in synchronization with all the above-mentioned satellite overpasses (Table 2.3). To facilitate the periodical data collection during the crop growth period few Bench Mark (BM) objects namely, pump set, big tress and shed corners were used to mark sampling grids. Enough care was taken regarding size and pixel matching of sampling locations. Two different grid sampling is made in each study plot based on sentinel-1a and ALOS PALSAR-2 ground pixel size and field of interest coverage. Extensive ground measurements of soil and vegetation parameters such as soil moisture, soil roughness, soil texture, vegetation height and vegetation water content for four different agriculture crop types (Paddy, Sugarcane, Maize and Tomato) planted on four different fields along with bare field were collected.

5.2.1 Sampling locations for Sentinel-1a data

C-band observations each sample plot is divided into 10*10m plots. The reason behind the plot size of 10*10m was by resolution of resampled sentinel-1a data. The total number of grids in bare, paddy, sugarcane, maize and tomato are 43, 34, 34, 30 and 34 respectively, shown in Figures 5.1A to 5.1E. Field photographs of each field during data acquisition is given in Figure 5.2A to 5.2D. The crop stage classification is done according to FAO guidelines (<https://www.fao.org/land-water/databases-and-software/crop-information>).



Figure 5.1A Sampling locations of bare field for Sentinel-1a acquisitions



Figure 5.1B Sampling locations of maize field for Sentinel-1a acquisitions



Figure 5.1C Sampling locations of paddy field for Sentinel-1a acquisitions



Figure 5.1D Sampling locations of sugarcane field for Sentinel-1a acquisitions



Figure 5.1E Sampling locations of tomato field for Sentinel-1a acquisitions

Seedling stage



10/06/2018



22/06/2018

Vegetative stage



04/07/2018



16/07/2018



28/07/2018

Yield stage



09/08/2018



21/08/2018



30/08/2018

Figure 5.2A Field photographs of Maize crop during field data acquisition

Vegetative stage



16/07/2018



28/07/2018



09/08/2018



21/08/2018



02/09/2018

Maturity Stage



14/09/2018



26/09/2018



08/10/2018

Yield stage



20/10/2018



01/11/2018



07/12/2018

Figure 5.2B Field photographs of Paddy crop during field data acquisition

Early growth stage



05/05/2018



17/05/2018



29/05/2018



10/06/2018



22/06/2018



04/07/2018

Vegetative stage



16/07/2018



28/07/2018



09/08/2018



21/08/2018



02/09/2018



14/09/2018

Grand growth stage



08/10/2018



20/10/2018



07/12/2018

Yield stage



31/12/2018



12/01/2018



24/01/2018



05/02/2018



17/02/2018

Figure 5.2C Field photographs of Sugarcane crop during field data acquisition

Vegetative stage



04/07/2018



16/07/2018



28/07/2018



09/08/2018

Maturity stage



21/08/2018



02/09/2018



14/09/2018

Yield stage



Figure 5.2D Field photographs of Tomato crop during field data acquisition

5.2.2 Sampling locations for ALOS PALSAR-2 data

Once the fields are finalized, each field is divided into grids based on satellite ground pixel size. In the case of ALOS PALSAR-2 each agricultural plot is divided into 6*6m grids using its previous grey scale image. The total number grids in bare, paddy, sugarcane, maize and tomato are 150, 103, 116, 100 and 113 respectively. The grid sampled plots are presented from Figure 5.3A to 5.3C.



Figure 5.3A Sampling locations of bare field and sugarcane field for ALOS PALSAR-2 acquisitions



Figure 5.3B Sampling locations of paddy and tomato field for ALOS PALSAR-2 acquisitions



Figure 5.3C Sampling locations of maize field for ALOS PALSAR-2 acquisitions

5.3 SAMPLING COLLECTION AND TRANSPORT

Sentinel-1a pass over the study area is determined using the European Space Agency (ESA) acquisition calendar, which is in the form of Google Earth .kmz files. For ALOS

PALSAR-2 two different dates are selected and data is ordered at JAXA (Japanese Aerospace eXploration Agency). From this it was known that satellite passing time for sentinel-1a and PALSAR-2 is 6:20 IST AM and 12:40 IST AM over the study area respectively. In the present study soil and vegetation samples were collected from each field grids. Ground data collections are performed on the same day in synchronization with satellite pass (± 1 hours) during the study period mentioned in Table 2.3.

Soil sampling data are collected over all the fields in the time period of $6:30 \pm 1$ hour and $12:30 \pm 1$ hour. Top Soil (5-8 cm) of about 100-150 gm are collected in air tight container and initial weight is taken into in the field itself using Portable weighing instrument. About 500-600 gm of soil using core cutter is collected to measure bulk density in Lab.

The surface roughness (rms) of soil in the study area was measured using a roller chain method (Saleh 1993). This simplest and most convenient way to estimate surface roughness. It is based on the fact that horizontal length decreases as SSR increases when a chain of a given length L_1 is laid on the surface. Therefore, SSR can be calculated using eq. 5.1

$$SSR = \left(1 - \frac{L_1}{L_2}\right) * 100 \quad (5.1)$$

Roughness caused by aggregates (random roughness) was obtained by measuring the SSR in a perpendicular direction to ridges. L_1 is the length of the roller chain and L_2 is the linear distance of chain due to roughness. The statistical parameter explained SSR as root mean square (RMS) height (vertical variation) of soil and calculated using the Eq. 5.2,

$$RMS = \sqrt{\frac{1}{n-1} [\sum (z_i - z)^2]} \quad (5.2)$$

A representative sample of half m^2 of vegetation within the plot of each crop field is collected using destructive sampling technique required to measure Vegetation Water Content (VWC) and its initial weight is measured at the field itself. The collected samples are transferred into polythene bags. The samples of VWC are collected only during early stages of crop. After flowering stage of crops farmers did not agree to go

through destructive sampling method. So, no data has been collected after maturity stage of each crops except from paddy.

The height of the crops are measured in the field using measuring staff of height 4 meter and metallic scale. The two types of collected soil and vegetation samples were transferred to Water Resources and Ocean Engineering (WROE) department, NITK Surathkal for further lab experiments.

5.4 EXPERIMENTAL MEASUREMENTS

5.4.1 Gravimetric soil moisture

The experiments were carried out from the laboratory to estimate soil moisture. They are collected in airtight containers. The soil samples are weighed and dried in an oven for a period of 24 hrs. under 105°C until all the moisture was driven off. After removing from oven, they are cooled slowly to room temperature and weighed again. The difference in weight is amount of moisture in the soil. The ratio weight of soil moisture and the dry weight of the soil gives gravimetric soil moisture.

$$\text{Gravimetric soil moisture} = \frac{\text{Wet weight} - \text{Dry weight}}{\text{Dry weight}} * 100 \quad (5.3)$$

5.4.2 Volumetric soil moisture

Soil sample is taken with a core sampler or with a tube auger whose volume is known. The amount of water present in soil sample is estimated by drying it in the oven and the bulk density of the soil is calculated by eq. 5.4 and the volumetric moisture content is calculated by multiplying the gravimetric moisture content with the bulk density of soil. The unit of volumetric soil moisture content is % gm/cm³.

$$\text{Bulk density of the soil} = \frac{\text{Weight of the Wet Soil}}{\text{Volume of the wet soil}} \quad (5.4)$$

$$\text{Moisture content} = \text{Gravimetric soil moisture} * \text{Bulk density} \quad (5.5)$$

5.4.3 Vegetation water content (VWC)

VWC is collected using destructive sampling method. The sample is transferred to oven and kept at 108°C until all the water content is driven off. After removing from oven, they are cooled slowly to room temperature and weighed again. The difference in weight is the VWC which should be upscaled to 1m. The ratio weight of vegetation and the dry weight of the vegetation gives VWC.

$$\text{VWC} = \frac{\text{Wet weight} - \text{Dry weight}}{\text{Dry weight}} * 100 \quad (5.6)$$

5.5 IMAGE PROCESSING

Radar signals need pre-processing to account for geometric distortions (e.g., layover and foreshortening), and for differences in illumination conditions due to topography and the surface being illuminated to one side of the satellite or aircraft. An additional step is needed to remove noise caused by reflections from undesirable features, e.g. minor irregularities. This is called speckle noise and is removed by a process called speckle filtering. A typical processing sequence applied to SAR data entails radiometric calibration, multi-looking, speckle filtering, terrain illumination correction, etc. The pre-processing steps for Sentinel-1a and ALOS PALSAR-2 are shown in Figures 5.4 and 5.5 respectively.

5.5.1 Sentinel-1a image

Radiometric Calibration: SAR image pixel is associated with a small area of the earth's surface called a resolution cell. Each pixel gives a complex number that carries amplitude and phase information about the microwave field backscattered by all the scatters (rocks, vegetation, buildings, etc.) within the corresponding resolution cell projected on the ground. Thus, Synthetic Aperture Radar data are complex-valued usually. The amount of radar echo from a target is characterized by its Radar Cross Section (RCS) typically in units of square-meters or dBsm. For distributed targets (e.g., grass, dirt, etc.) this value is usually normalized per unit area, that is, square-meters per square-meters, or dBs/sm. RCS per unit area is often called clutter reflectivity. Relating pixel values to either RCS or clutter reflectivity is called radiometric calibration. The

objective of SAR calibration is to provide imagery in which the pixel values can be directly related to the radar backscatter of the scene.

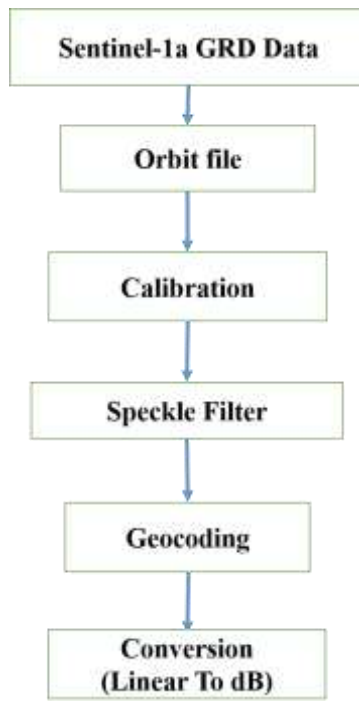


Figure 5.4 Pre-processing steps of Sentinel-1a

Subsetting: Subsetting refers to breaking out a portion of a large file into one or more smaller files. Often, image files contain areas much larger than a particular study area. In these cases, it is helpful to reduce the size of the image file to include only the area of interest (AOI). This eliminates the extraneous data in the file and speeds up processing due to the smaller amount of data to process.

Multi-looking: Multi-look processing refers to the division of the radar beam into several narrower sub-beams. Each sub-beam provides an independent "look" at the illuminated scene, each of these "looks" will also be subject to speckle, but by summing and averaging them together to form the final output image, the amount of speckle will be reduced.

Speckle Filtering: Speckle reduction by spatial filtering is performed on the output image in a digital (i.e., Computer) image analysis environment. Speckle reduction filtering consists of moving a small window of a few pixels in dimension (e.g., 3x3 or

5x5) over each pixel in the image, applying a mathematical calculation using the pixel values under that window (e.g. Calculating the average), and replacing the central pixel with the new value. The window is moved along in both the row and column dimensions one pixel at a time, until the entire image has been covered. By calculating the average of a small window around each pixel, a smoothing effect is achieved and the visual appearance of the speckle is reduced.

Terrain Correction: A characteristic of side-looking SAR image is the so-called foreshortening and layover, a reflected signal from a mountaintop reaches the sensor earlier or at the same time as the signal at the foot of the mountain. This results in the typical look of mountains that seem to have “fallen over” towards the sensor. The freely available SNAP SAR Toolbox terrain-correct SAR images in a fully automatic process. The algorithm takes the DEM and using orbit parameters of the satellite creates a simulated SAR image from this DEM. The simulated and the real SAR image, which will look very similar, are co-registered. Through this simulation, the displacement for each location in the original landscape, the DEM, is known, so if the simulated SAR image is transformed back into the original DEM and the co-registered SAR image along with the pixels of the SAR image will receive their real, geographical location.

5.5.2 ALOS PALSAR-2 image

ALOS PALSAR-2 data was pre-processed using PolSARPro, an open source software including multi-looking, filtering, decomposition and geocoding are performed. Initially the environment is set by providing destination of image file. Data is imported to software based on type of sensor, polarization, processing level and file format. The ALOS PALSAR-2 SLC data was multi-looked twice (multilook is calculated using incidence angle, pixel and line spacing) and Pauli RGB image is created. Refined lee filter with window size 7*7 was used to reduce speckle (noise) in the data. The output .hdr files are transferred ENVI® and georeferenced using and ArcGIS®.

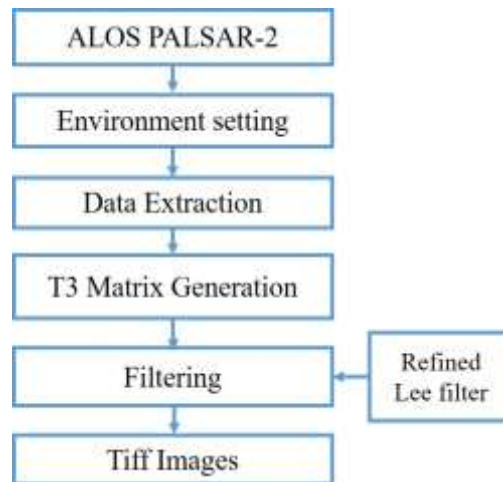
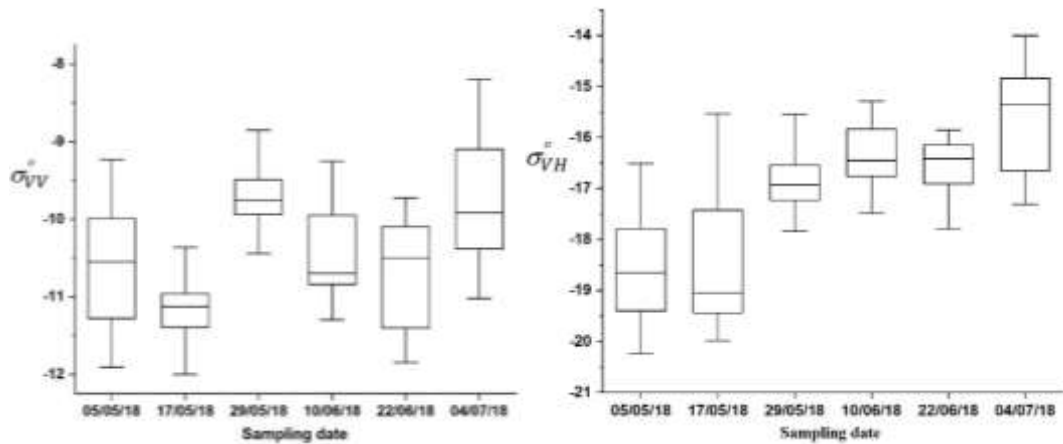


Figure 5.5 Pre-processing steps of ALOS PALSAR-2

5.6 SENTINEL-1A DATA ANALYSIS

5.6.1 Bare field

Bare field is considered to study the effect of soil moisture on backscattered energy without vegetation effects. Forty-three Sampling collection are made within the bare field, which was shown in Fig 5.1A. The data was collected for a period of 05/05/2018 to 04/07/2018 at 12 days interval in synchronization with sentinel-1a pass over study area. The Spatio-Temporal variation (~ 8 to 22gm/cm^3) of backscattered energy and soil moisture within the plot is shown in the Figure 5.6 and 5.7. From the box plot, soil moisture on 04/07/2018 has increased because of the rainfall on 30/06/2018. Since there was no effect of vegetation, it was observed that backscattered energy variation and soil moisture variation within the field followed a same pattern. It showed the direct relationship between soil moisture and backscattered energy in bare fields.



. Figure 5.6 Spatio-temporal variation of VV and VH backscattered energy within the bare field during Sentinel-1a pass

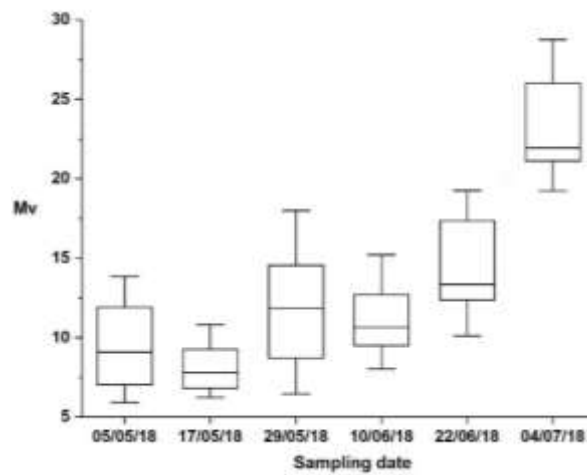


Figure 5.7 Spatio-temporal variation of soil moisture within the bare field during Sentinel-1a pass

5.6.2 Maize field

To study the effect of vegetation in surface soil moisture retrieval Maize crop is selected which is Broadleaf structured. The area considered for the study is of 0.8 acres in 30 sampling locations (Figure 5.1B), which are made of 10*10m. The data is acquired for the period of 10/06/2018 to 21/08/2018 in synchronization with sentinel-1a pass over study area. The cropping period of Maize is 3 months. The Spatio-Temporal Variation of VV, VH backscattered energy and soil moisture are shown in Figure 5.8 and 5.9 respectively. The soil moisture over the field is wet in initial condition whereas in later

stages it went quite low ($\sim 15\text{gm/cm}^3$) because the crop was infected. To avoid the spread of infection irrigation was controlled by farmers. Also, we can observe that as the crop grows the effect of vegetation is sensed by VH backscattered energy is also increasing.

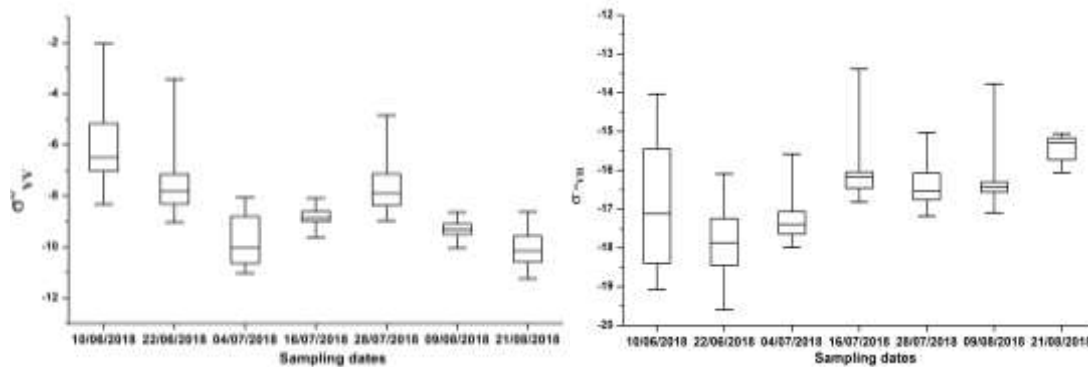


Figure 5.8 Spatio-temporal variation of VV and VH backscattered energy within Maize field during Sentinel-1a pass

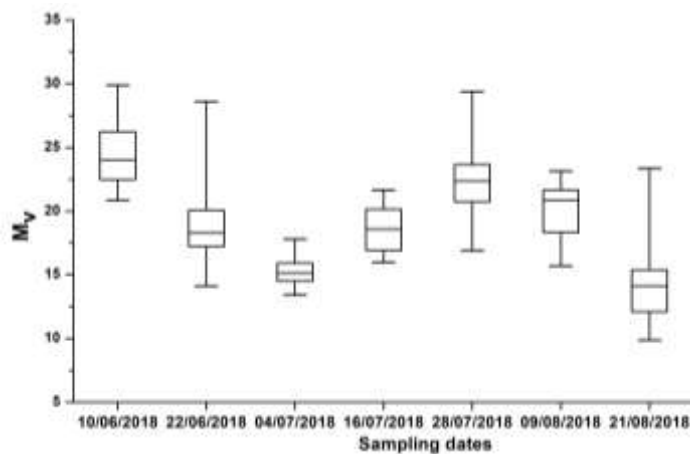
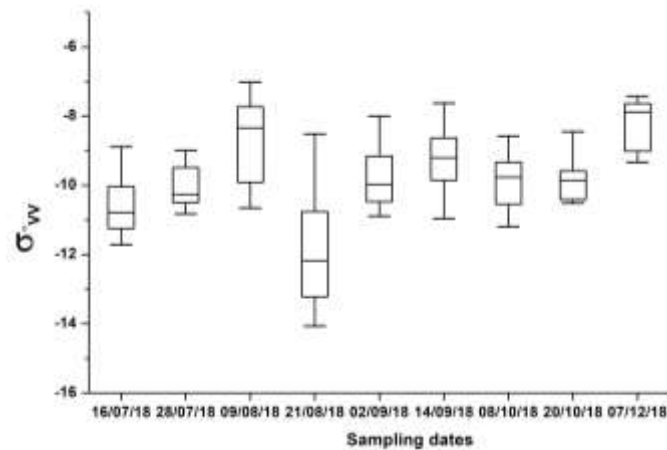


Figure 5.9 Spatio-temporal variation of soil moisture within Maize field during Sentinel-1a pass

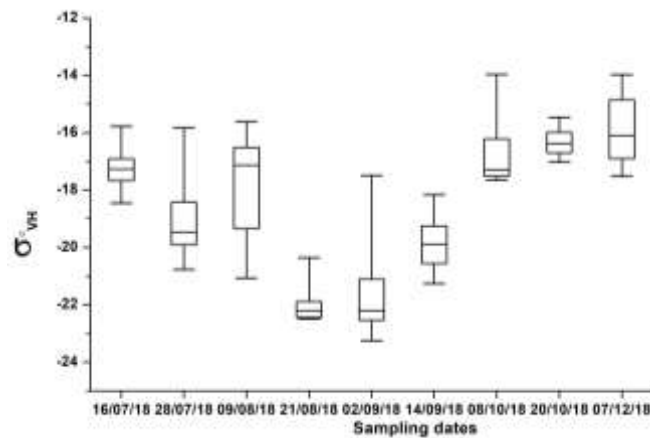
5.6.3 Paddy field

Paddy is another crop which is a narrow leaf structured to study the effect of vegetation in surface soil moisture retrieval of area 1 acre land. Since the same breed paddy is not available in the field two paddy plots are selected, which has already shown in Figure 5.1C. Total 30 sampling fields of which 18 from plot-1 and 16 from plot-2 were

collected. The sampling data is acquired for the period of 16/07/2018 to 07/12/2018 in synchronization with sentinel-1a pass over the study area. The spatiotemporal variation soil moisture of too varying within the Field (Figure 5.10 & 5.11). We can observe that as the crop grows the effect of vegetation is sensed by VH backscattered energy whereas VV backscattered energy doesn't show much variation and it's a kind of same (Figure 5.11 & 5.12).



(a)



(b)

Figure 5.10 Spatio-temporal variation of VV (a) and VH (b) backscattered energy within Paddy field during Sentinel-1a pass

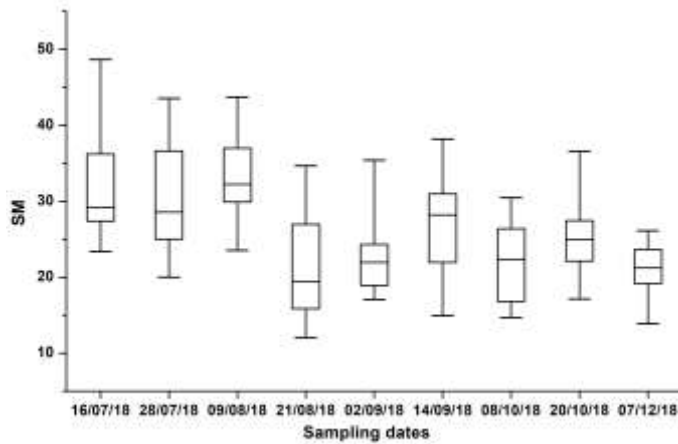
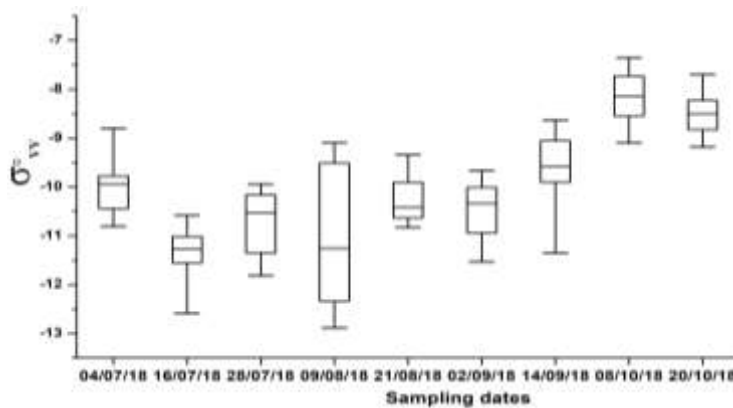


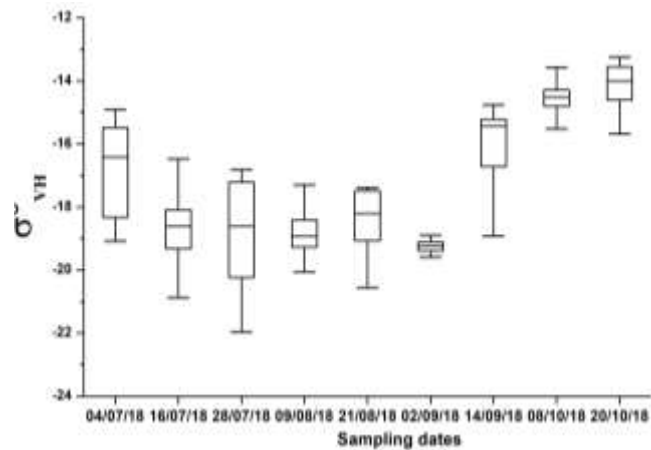
Figure 5.11 Spatio-temporal variation of soil moisture within Paddy field during Sentinel-1a pass

5.6.4 Tomato field

Tomato is one more broadleaf structured crop selected to study surface soil moisture retrieval over agricultural fields of 1 acre land. 34 sampling locations are selected from tomato field which is divided into 10*10m grid, which should match pixels of sentinel-1a. The data is acquired for the period of 16/07/2018 to 07/12/2018 in synchronization with sentinel-1a pass over the Tomato fields. The crop period of Tomato is 4 months. The soil moisture over the field is dry in the initial condition, whereas in later stages, it was almost uniform (Figure 5.13). Also, we can observe that as the crop grows the effect of vegetation is sensed by VH backscattered energy (Figure 5.12).



(a)



(b)

Figure 5.12 Spatio-temporal variation of VV (a) and VH (b) backscattered energy within Tomato Field during Sentinel-1a pass

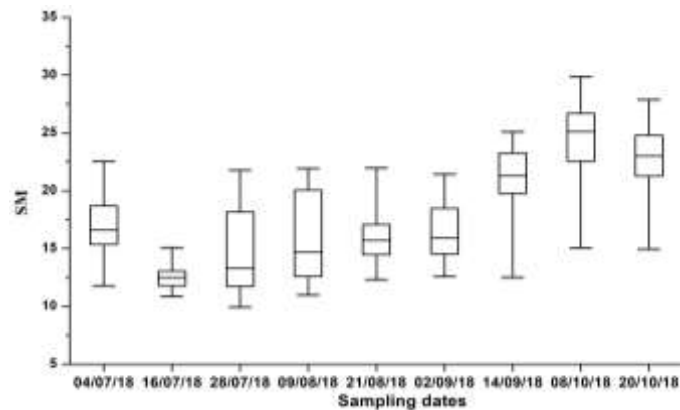


Figure 5.13 Spatio-temporal variation of soil moisture within tomato field during Sentinel-1a pass

5.6.5 Sugarcane field

Sugarcane is one of the main commercial crop which is narrow leaf structured crop selected to study effects of it on soil moisture retrieval. The crop period of sugarcane varies from 10 to 12 months in the present study it has been harvested in the 11th month. Data is collected over 36 sampling locations for the period of 05/05/2018 to 24/01/2019 in synchronization with sentinel-1a pass over the sugarcane field. The spatio-temporal variation of VV and VH backscattered energy is presented in Figure 5.14 & 5.15

respectively. The Spatio-temporal variation of soil (Figure 5.16) in the field remains almost uniform because of the controlled irrigation practices towards sugarcane.

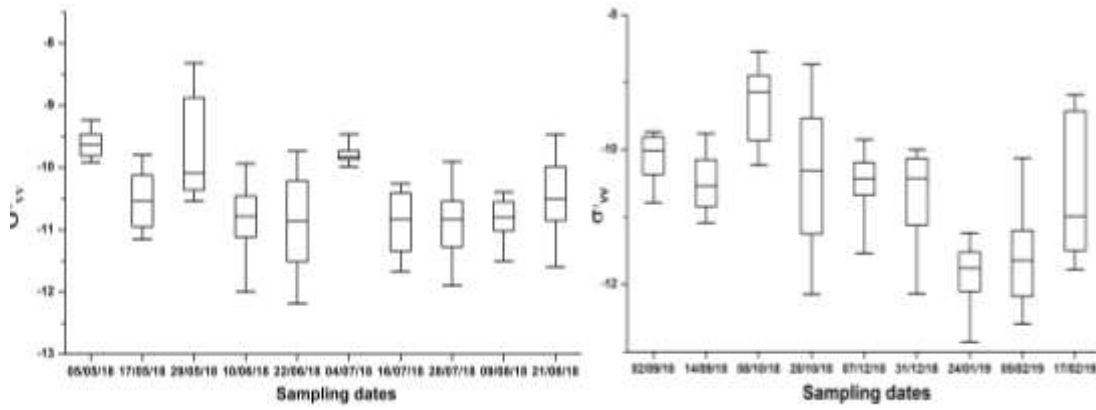


Figure 5.14 Spatio-temporal variation of VV backscattered energy within sugarcane field during Sentinel-1a pass

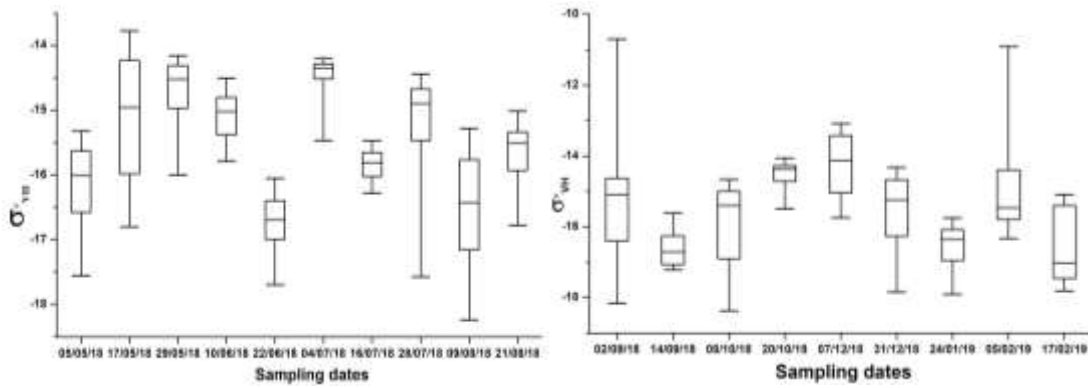


Figure 5.15 Spatio-temporal variation of VH backscattered energy within sugarcane field during Sentinel-1a pass

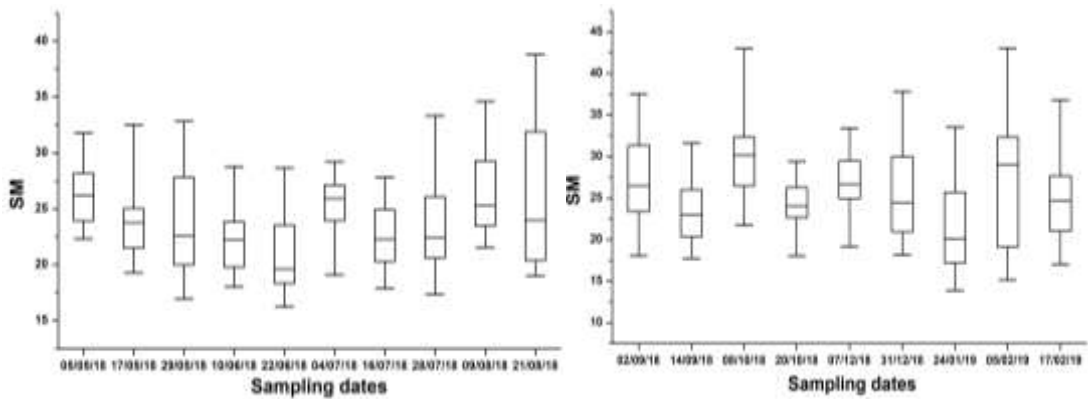


Figure 5.16 Spatio-temporal variation of soil moisture within sugarcane field

5.7 ALOS PALSAR-2 DATA ANALYSIS

The backscattered energy of quad polarized (VV, VH, HV & HH) ALOS PALSAR-2 images was extracted using R studio software for the given dates, 23/07/2018 and 01/10/2018. The spatio-temporal variation of polarized backscattered energy of barren fields and soil moisture is given in Figure 5.17 and Figure 5.18 respectively. From the Figure 5.17 and 5.18, it is noted there is not much variation with respect backscattered energy, soil moisture is observed, and both dates follow similar co polarization patterns.

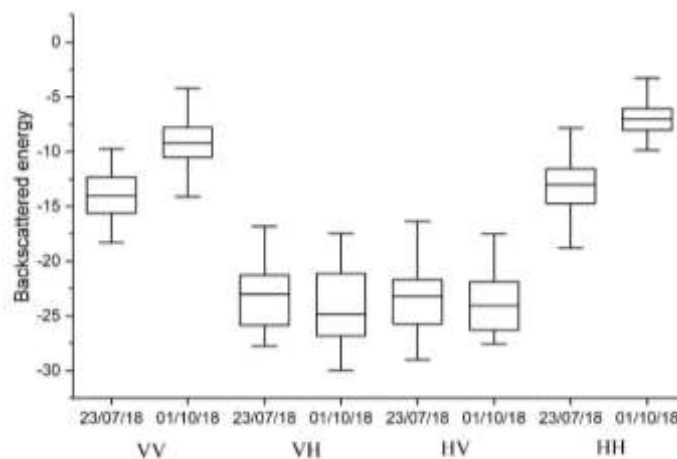


Figure 5.17 Spatio-temporal variation of backscattered energy within barren field during ALOS PALSAR-2 pass

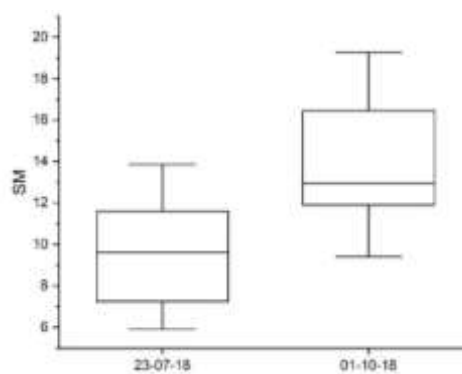


Figure 5.18 Spatio-temporal variation of soil moisture within barren field during ALOS PALSAR-2 pass

Paddy, sugarcane and tomato are in vegetative stage during first observation (23/07/2018) of ALOS PALSAR-2. Paddy, tomato, sugarcane and maize are in early

flowering, first harvesting and grand growing stage respectively during second observation (01/10/2018). The maize is a short term crop (90 days). So, during first observation it was in growing stage whereas during second observation it was harvested and not available. The spatio-temporal variation of backscattered energy and soil moisture of each field is given from Figure 5.19 to 5.26.

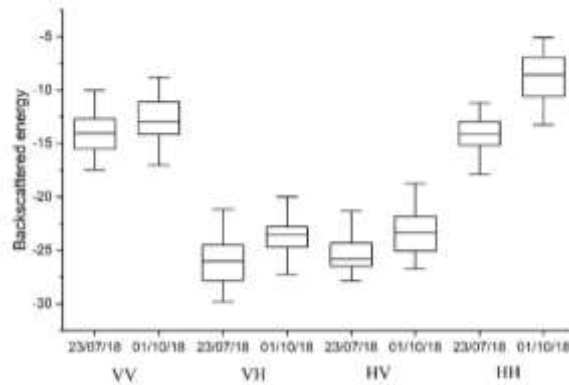


Figure 5.19 Spatio-temporal variation of backscattered energy within paddy field during ALOS PALSAR-2 pass

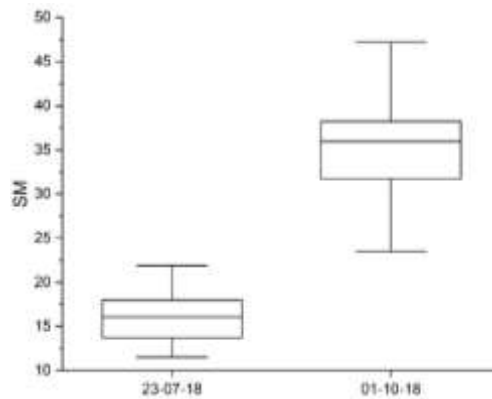


Figure 5.20 Spatio-temporal variation of soil moisture within paddy field during ALOS PALSAR-2 pass

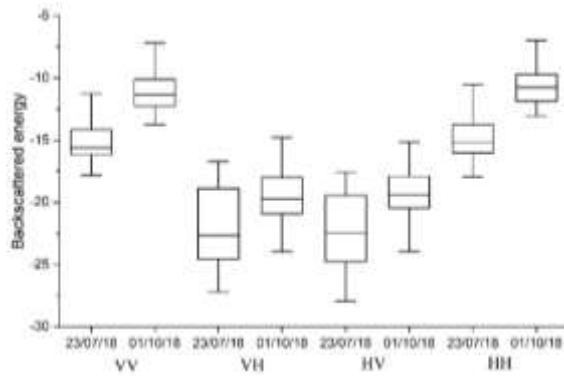


Figure 5.21 Spatio-temporal variation of backscattered energy within tomato field during ALOS PALSAR-2 pass

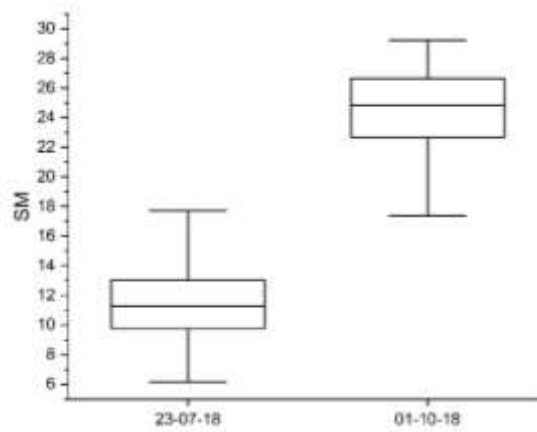


Figure 5.22 Spatio-temporal variation of soil moisture within tomato field during ALOS PALSAR-2 pass

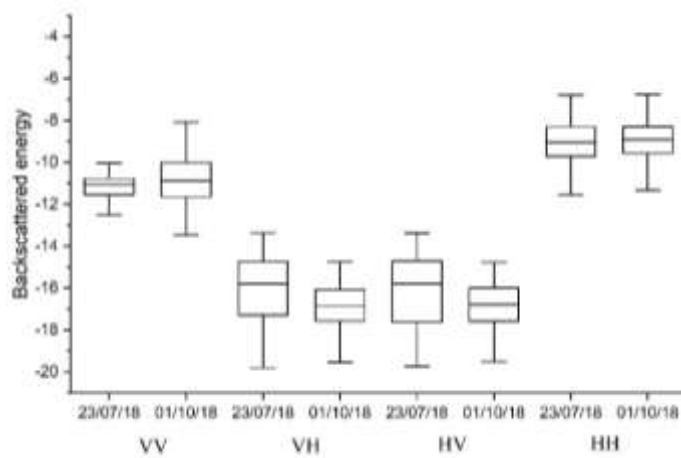


Figure 5.23 Spatio-temporal variation of backscattered energy within sugarcane field during ALOS PALSAR-2 pass

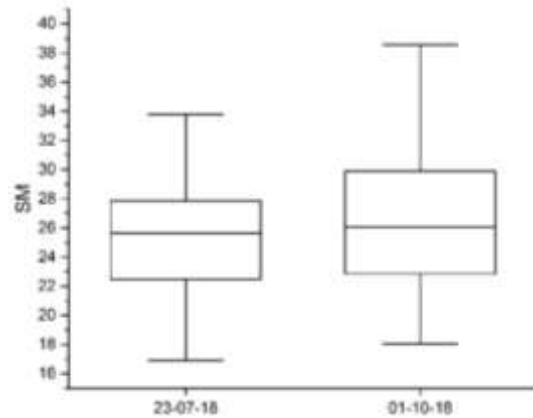


Figure 5.24 Spatio-temporal variation of soil moisture within sugarcane field during ALOS PALSAR-2 pass

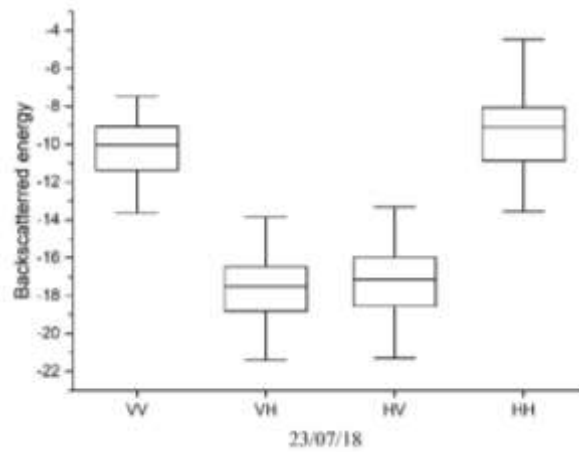


Figure 5.25 Spatio-temporal variation of backscattered energy within maize field during ALOS PALSAR-2 pass

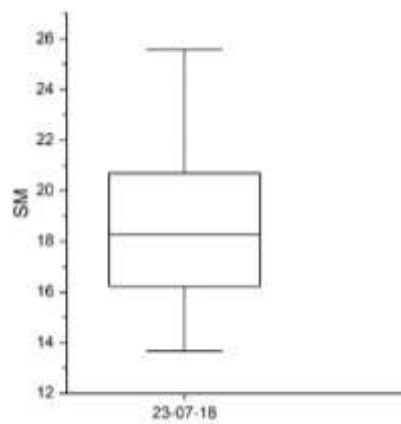


Figure 5.26 Spatio-temporal variation of soil moisture within maize field during ALOS PALSAR-2 pass

From the Figure 5.19 to 5.20, It is observed there is an increase in field soil moisture of 01/10/2018 compared with 23/07/2018 and corresponding to its backscatter energy. Soil moisture in sugarcane fields is almost same in both the observations. Also, observed a change in HV and VH backscattered energy according to vegetation growth in agricultural fields.

5.8 CROP HEIGHT

The crop height was measured using metal scale and a staff of 4m long. The ALOS PALSAR-2 observation crop height is given in Table 5.1. The variation of crop height during Sentinel-1a observation is shown in Figure 5.27. It observed from the figure 5.27 the height of paddy and tomato is more 1.2 and 1.3m but afterwards it reduced to 1 and 0.8 because of the fruit weight.

Table 5.1 Crop height during ALOS PALSAR-2 pass

Sl. No.	Crop	Height (m)	
		23/07/2018	01/10/2018
1	Paddy	0.2	0.8
2	Tomato	0.3	1.1
3	Sugarcane	1.2	2.6
4	Maize	0.9	----

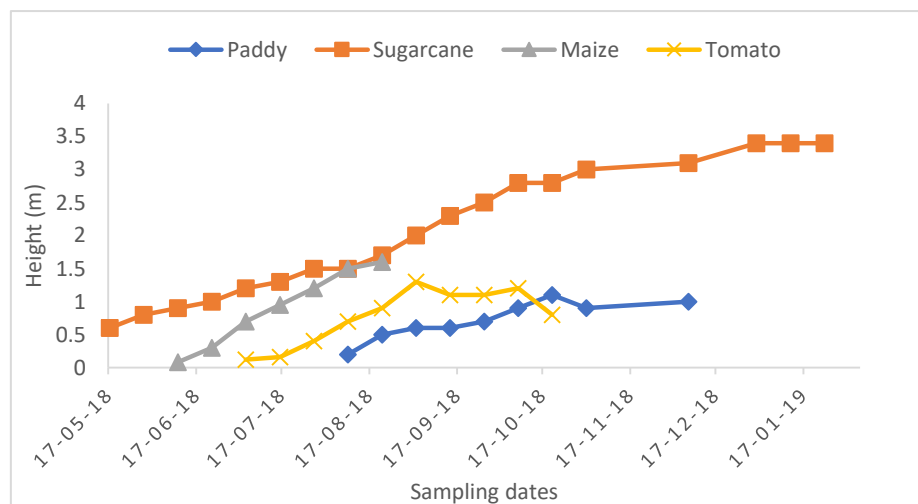


Figure 5.27 Crop height variation of paddy, sugarcane, tomato and maize crops during Sentinel-1a pass

5.9 VEGETATION WATER CONTENT (VWC)

VWC is measured to all crops till its flowering stage. Since it is destructive sampling method farmers does not allow to carry out after maturity of crops. From the collected data, the model will be developed to relate between vegetation indices and VWC and that will be further utilized. The observed values during PALSAR-2 pass are given in Table 5.2 and Sentinel-1a pass are given in Figure 5.28.

Table 5.2 VWC during ALOS PALSAR-2 pass

Sl. No.	Crop	VWC (kg/m ²)	
		23/07/2018	01/10/2018
1	Paddy	0.2	2.1
2	Tomato	0.8	2.9
3	Sugarcane	0.7	----
4	Maize	3.12	----

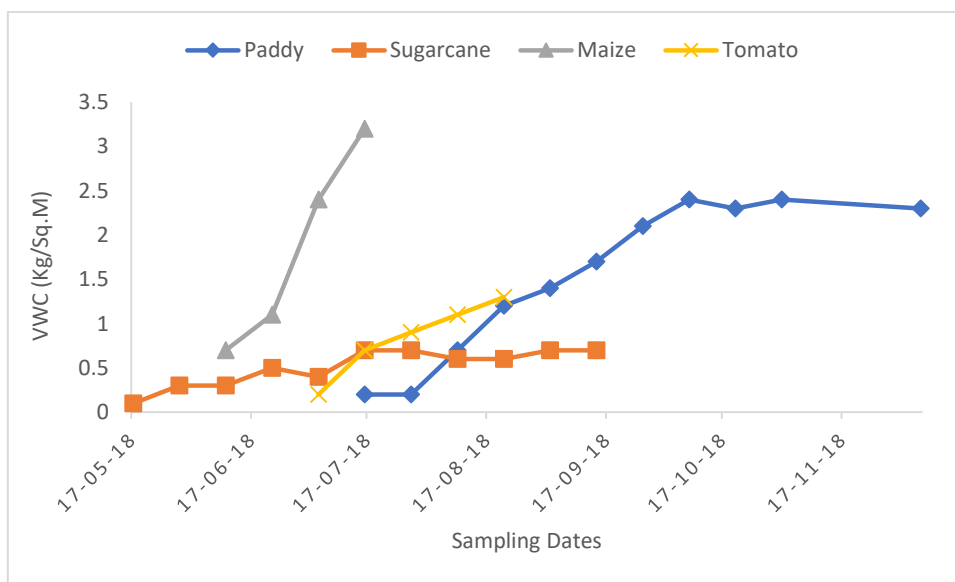


Figure 5.28 VWC variation of paddy, sugarcane, tomato and maize crop during Sentinel-1a pass

The upcoming chapter discusses about the surface soil moisture results obtained by C and L band SAR and discussion regarding it.

RESULTS AND DISCUSSION

6.1 INTRODUCTION

This chapter discuss about the surface soil moisture retrieved from various soil moisture models like Oh, WCM, and X-Bragg model. Later on, discusses about surface soil moisture model development using polarization decomposition technique and backscattered energy. Further, validation of existing and developed models using field collected data and accuracy assessment of these models was discussed. At the end, comparison between C and L-band soil moisture estimates is analysed. The results of this study is divided into three parts namely,

- i. Spatio-temporal variation of surface soil moisture.
- ii. Surface soil moisture retrieval using L and C-band SAR.
- iii. Comparison of quad and dual-pol surface soil moisture retrievals.

6.2 SPATIO-TEMPORAL VARIATION OF SURFACE SOIL MOISTURE

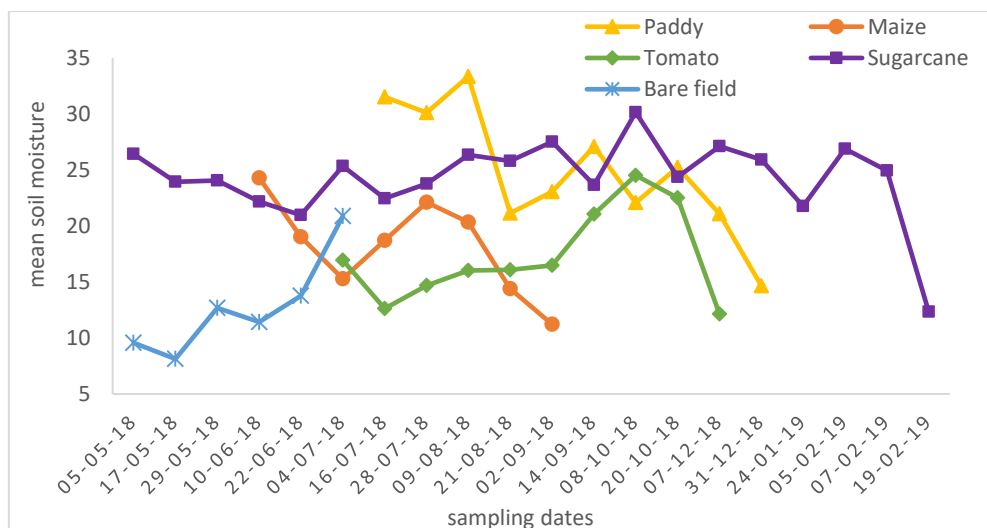


Figure 6.1 Mean surface soil moisture collected from time series in situ data for each agricultural plots.

Spatio-temporal variation of surface soil moisture of 5 different agricultural plots are studied using field/in-situ observations. We observed the surface soil moisture of sugarcane is almost uniform all over its crop cycle, no much change is observed (varied between 5%). In case of tomato plot, the soil moisture is considerably high during the planting and flowering stages. In rest of the crop cycle surface soil moisture is almost uniform (Figure 6.1). In case of paddy fields surface soil moisture varies in the range of 10% but higher soil moisture is observed during planting stage and decreased during harvesting stage. In case bare fields, no irrigation activity was seen though there was change in soil moisture at periphery of the field, this is due infiltration of water from neighbouring fields. In overall surface soil moisture of each field is less during the harvesting and more during planting/vegetative stage.

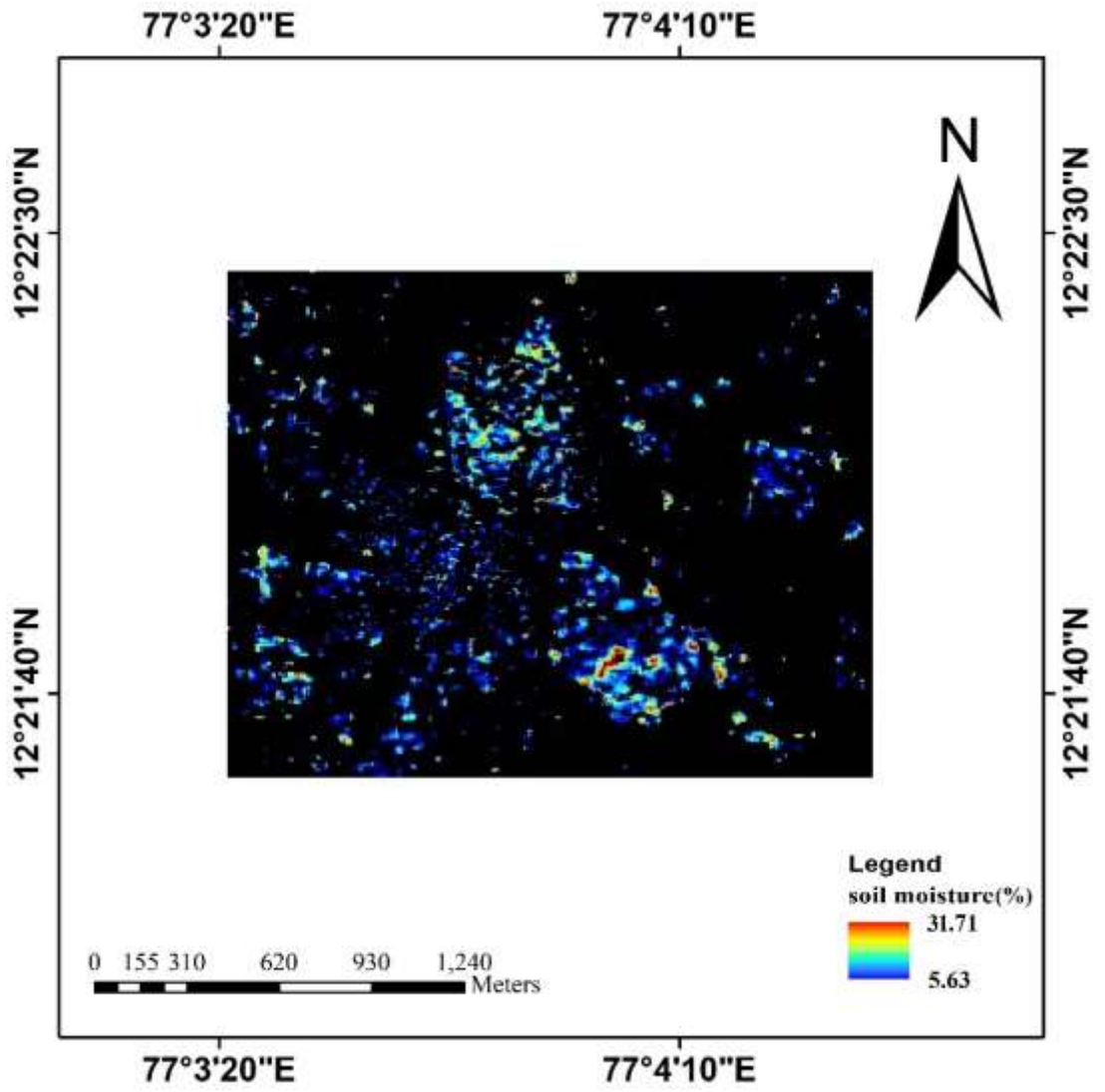
6.3 SURFACE SOIL MOISTURE RETRIEVAL USING SAR

The surface soil moisture retrieval over agriculture fields is discussed in 2 sections namely,

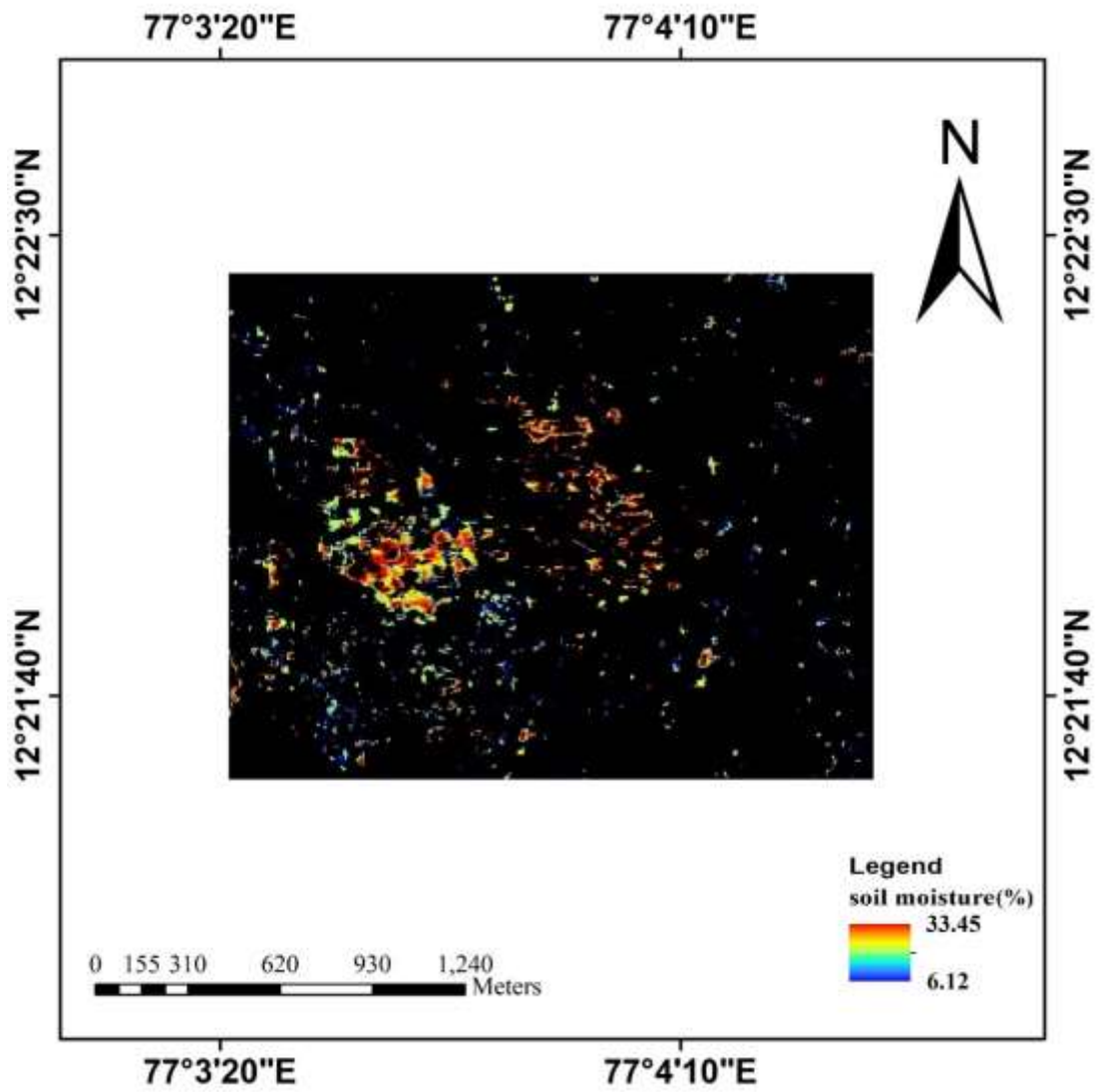
- Surface soil moisture retrieval using quad-pol, L-band SAR
- Surface soil moisture retrieval using dual-pol, C-band SAR

6.3.1 Surface soil moisture retrieval using quad-pol, L-band SAR

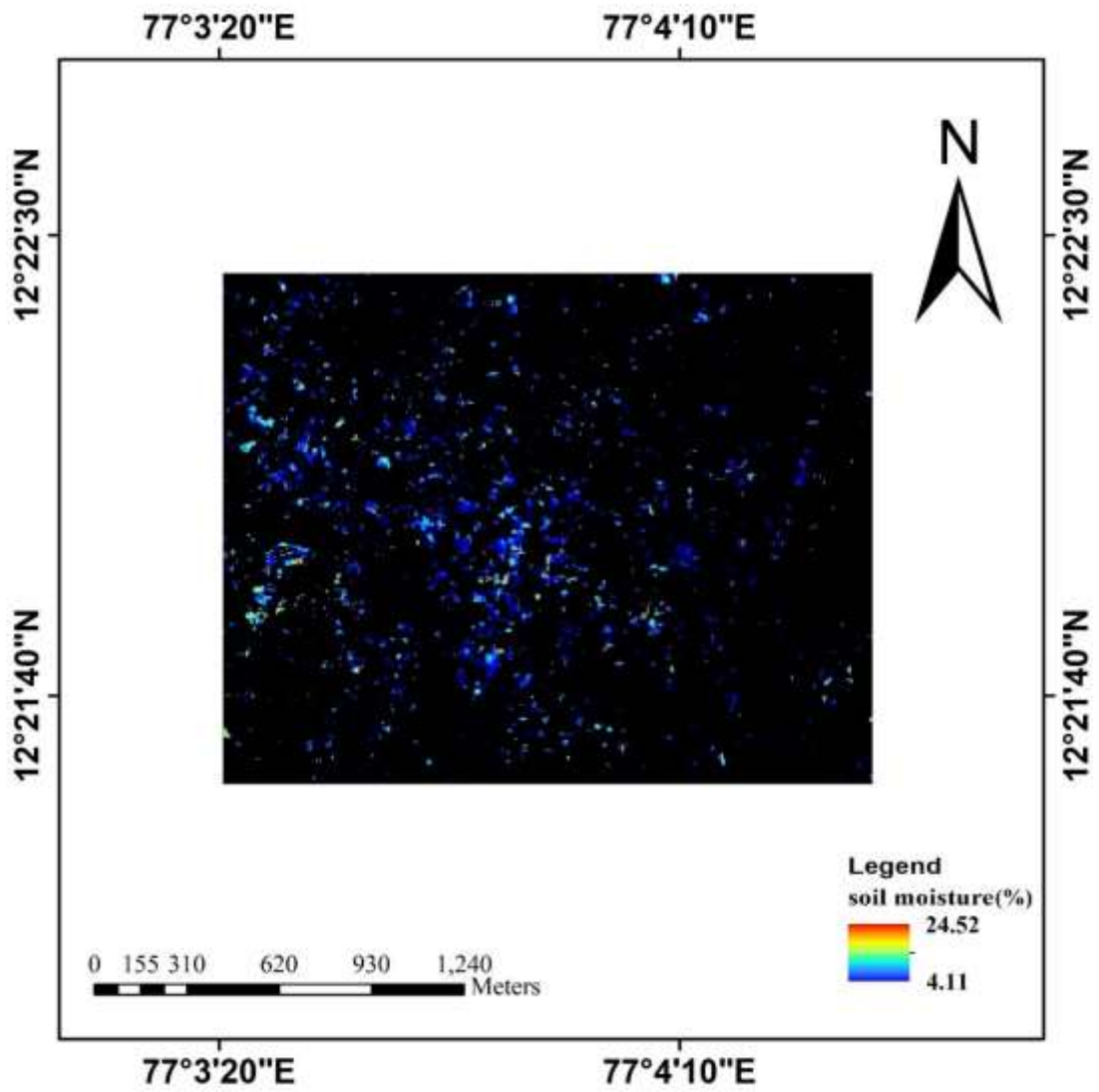
Processed ALOS-2 SAR data (dated 23/0/2018 & 01/10/2018) was used to estimate surface soil moisture. Evaluation of soil moisture models like Oh 1992, Oh 2004 and X-Bragg were carried out using PolSAR Pro 5.1.3 software. To run these models, incidence angle map was developed using a polynomial equation and metadata information provided along with the ALOS PALSAR-2 data (Ponnurangam and Rao, 2011). Soil moisture values of each sampled grid in the study site are extracted using R studio software version 1.1.423. These extracted soil moisture values of each model are assessed with field data for validation. The surface soil moisture maps of 23/07/2018 and 01/10/2018 derived using Oh 1992, Oh 2004 and X-Bragg models are shown in the Figure 6.2 and 6.3 respectively.



(a)

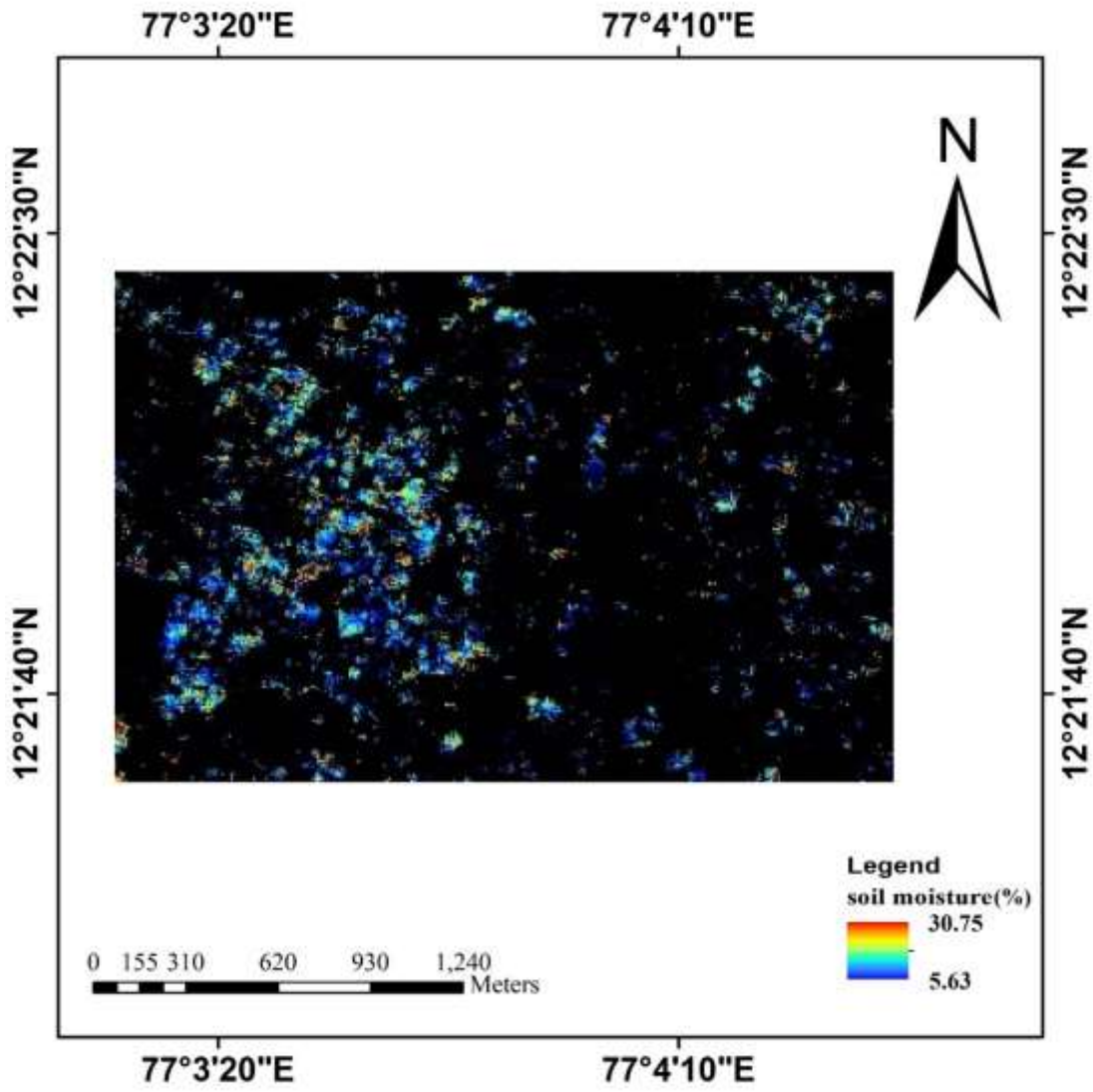


(b)

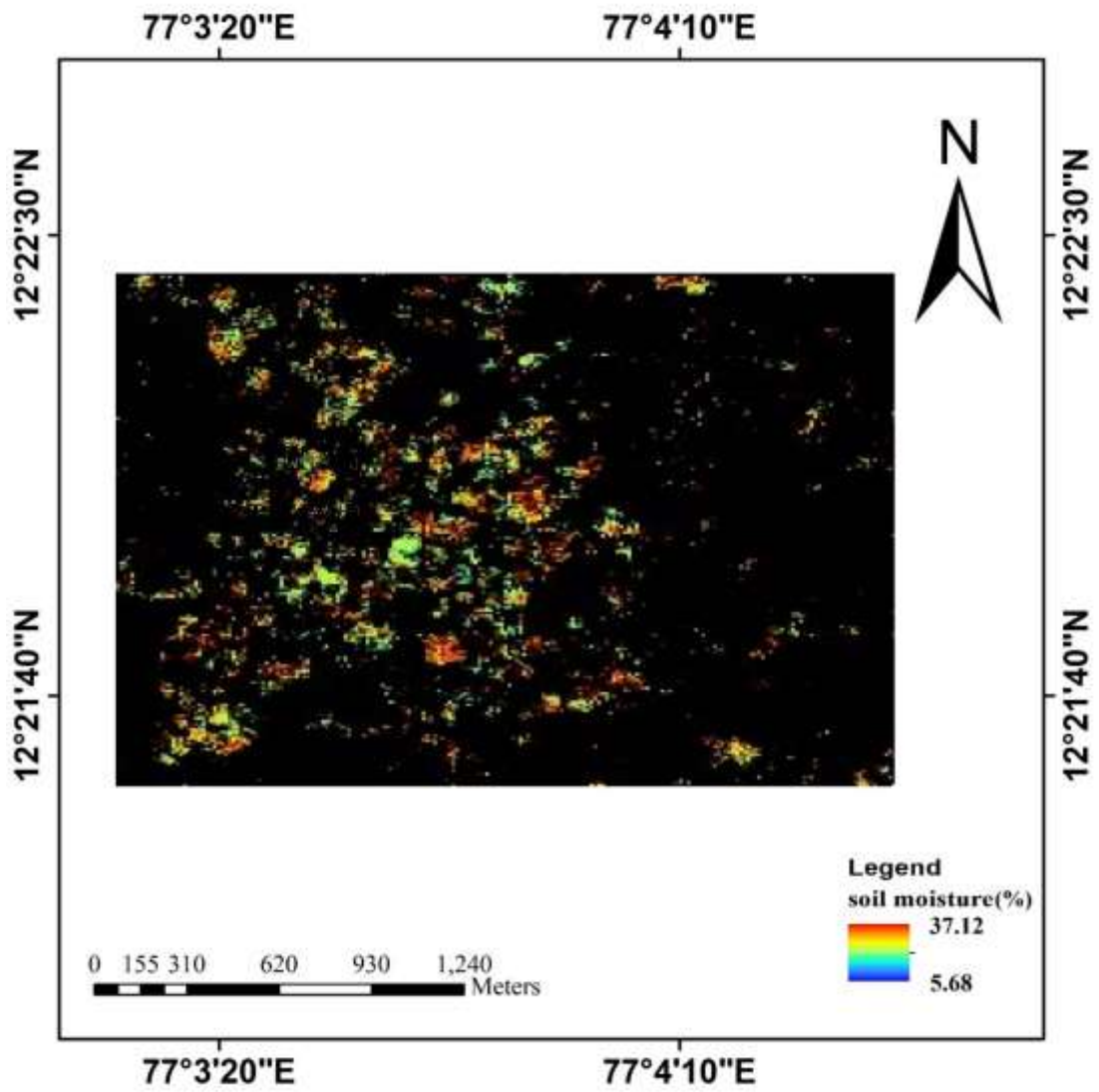


(c)

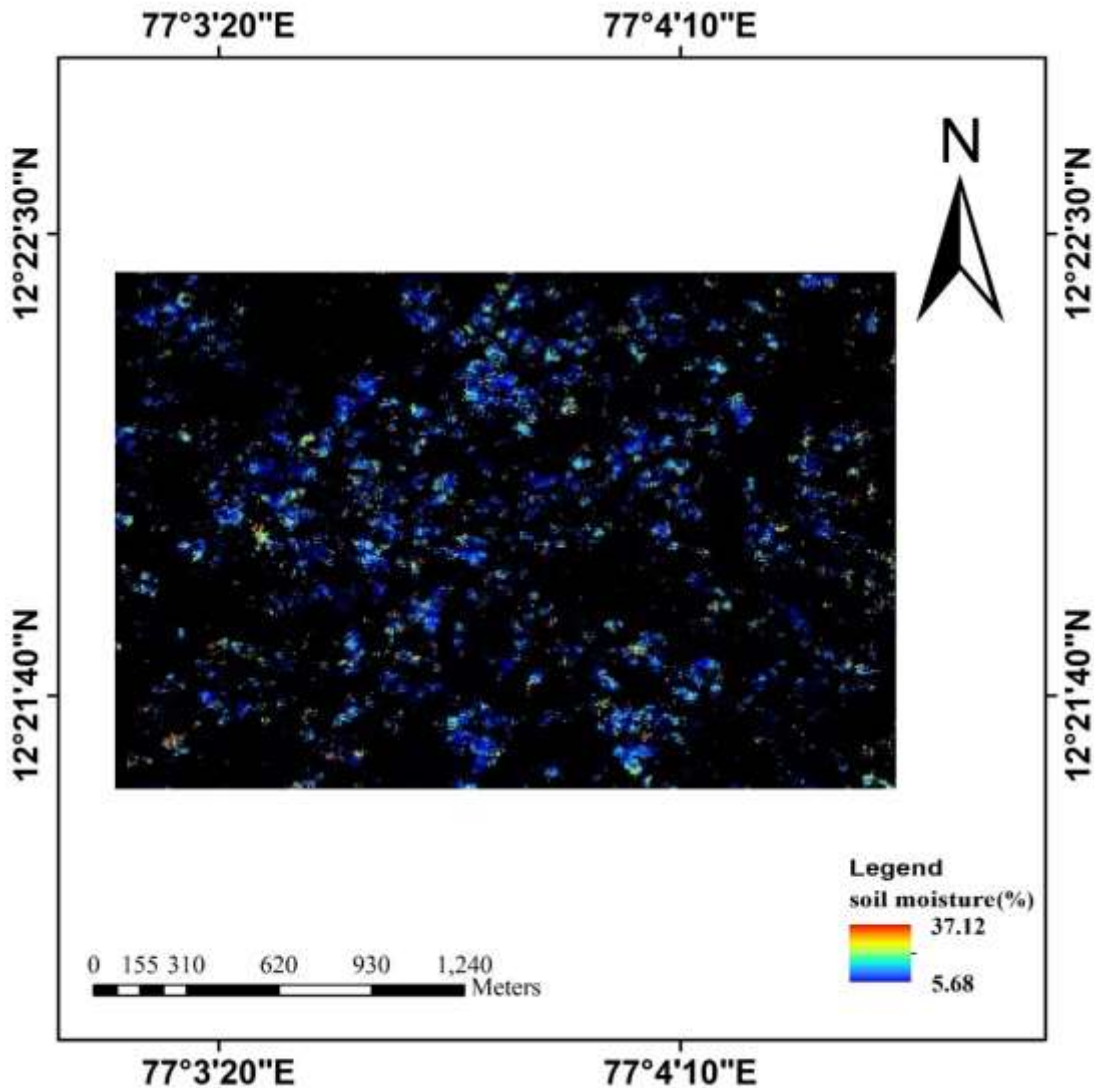
Figure 6.2 Surface soil moisture maps of 23/07/2018 derived using Oh 1992 (a), Oh 2004 (b) and X-Bragg (c) models



(a)



(b)



(c)

Figure 6.3 Surface soil moisture maps of 01/10/2018 derived using Oh 1992 (a), Oh 2004 (b) and X-Bragg (c) models

In case of WCM, 70% of soil moisture field grid sample data of each study site was used to derive model parameters and 30% were used for validation. RVI is used as vegetation descriptors and is calculated using Eq. 6.11. The model parameters were computed by using the genetic algorithm. This parameterization is performed using the Levenberg Marquardt Algorithm (LMA), which is a genetic algorithm and model parameters are formed by optimization of least squares with nonlinear regression technique and by minimizing the deviation between predicted data and SAR data

(Kumar et al, 2015). The model parameters are uniquely identifiable and computed non-linear regression model parameters are presented in Table 6.1.

$$RVI = \frac{8\sigma_{HV}}{\sigma_{HH} + \sigma_{VV} + 2\sigma_{HV}} \quad (6.11)$$

Table 6.1 WCM model parameter

Date	23/07/2018				01/10/2018			
Crop\parameters	A	B	C	D	A	B	C	D
Maize	0.092	1.088	0.024	0.00032	--	--	--	--
Paddy	0.288	1.131	0.017	0.00035	0.057	1.061	0.015	0.0004
Tomato	0.149	1.078	0.033	0.00061	0.063	0.956	0.047	0.00053
Sugarcane	0.354	3.11	0.06	0.00058	0.22	-1.215	0.052	0.00071
Bare field	0.066	1.556	0.018	0.0011	0.048	0.981	0.021	0.00092

A & B= model parameters; C & D= vegetation parameters

6.3.1.1 Model development

PolSARPro v5.1.3 an open-source software was used to decompose the quad polarized ALOS-2 data using 3 typical polarization decomposition techniques. The proportionality analysis (Fig. 6.4) found a difference in the decomposition of different scattering mechanisms. Surface scattering was the dominant scattering in Yamaguchi and Van Zyl techniques whereas in Freeman-Durden decomposition volume scattering was dominant. The proportion of dihedral scattering was least when compared to the proportion of surface and volume scattering. Dihedral scattering of Yamaguchi decomposition gave the lowest proportion of all. It is also observed that the proportion of volume scattering is near to the proportion of surface scattering this is because of the growing stage of maize which has more vegetation water content. This shows significant impact of vegetation on soil moisture. Therefore, to obtain actual soil moisture information about any field it is required to remove vegetation information. Van Zyl decomposition gave the highest surface scattering (43%) followed by Yamaguchi (41%). Van Zyl gave a lower proportion of volume scattering followed by Yamaguchi and Freeman-Durden decompositions. Finally, it was found that the surface

scattering component is increased and the volume scattering component is reduced in the Van Zyl method followed by Yamaguchi and Freeman-Durden decompositions.

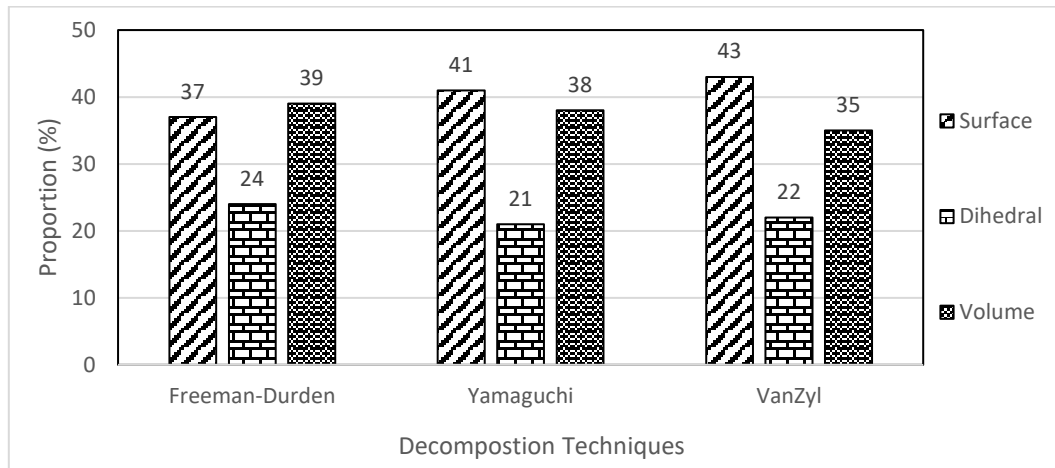


Figure 6.4 Proportion analysis of three polarization decomposition techniques of Maize

It was observed, surface scattering (<34%) is a significant component in all the three polarization decomposition techniques during the vegetative stage (23/07/2018) of paddy, tomato and sugarcane (Wang et al., 2017). In the case of a bare field, surface scattering is more prominent (<55%), showing less vegetation interaction with radar backscattering energy. As the crop grew (01/10/2018), an increase in the dihedral and volumetric scattering component of paddy and tomato was noticed. In case of sugarcane, dihedral scattering has reduced because of the spreading of leaves that act susceptible to waves. In case of bare field, not much change is observed since vegetation level remained more or less same. The proportionality of three scattering components of 23/07/2018 and 01/10/2018 are given in Figure 6.5 and Figure 6.6.

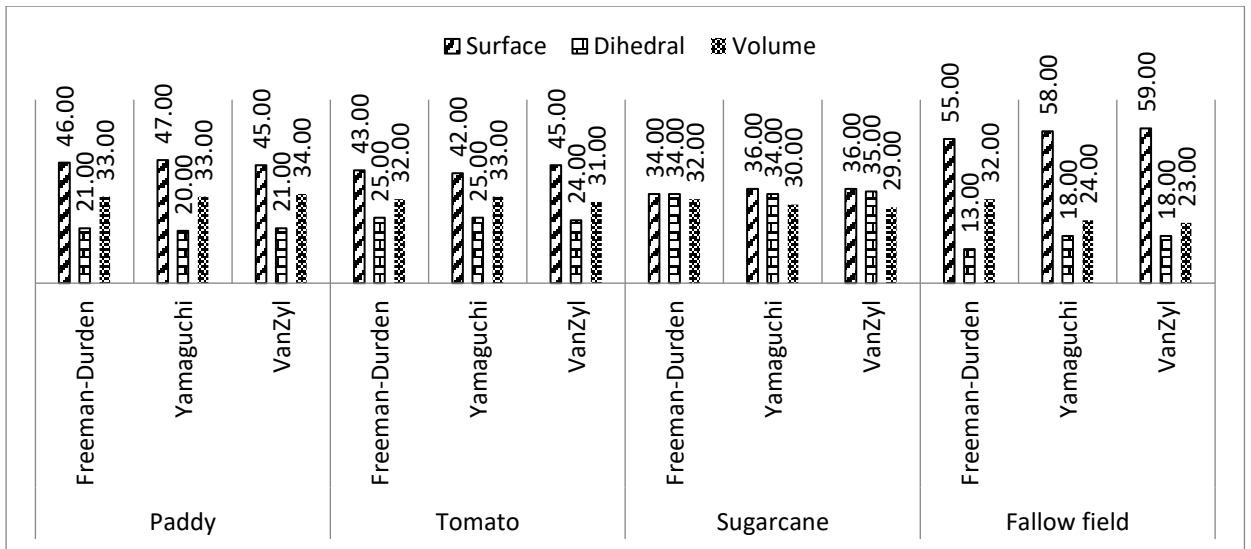


Figure 6.5 Proportionality of three scattering components on 23/07/2018 of paddy, Tomato, sugarcane and bare field

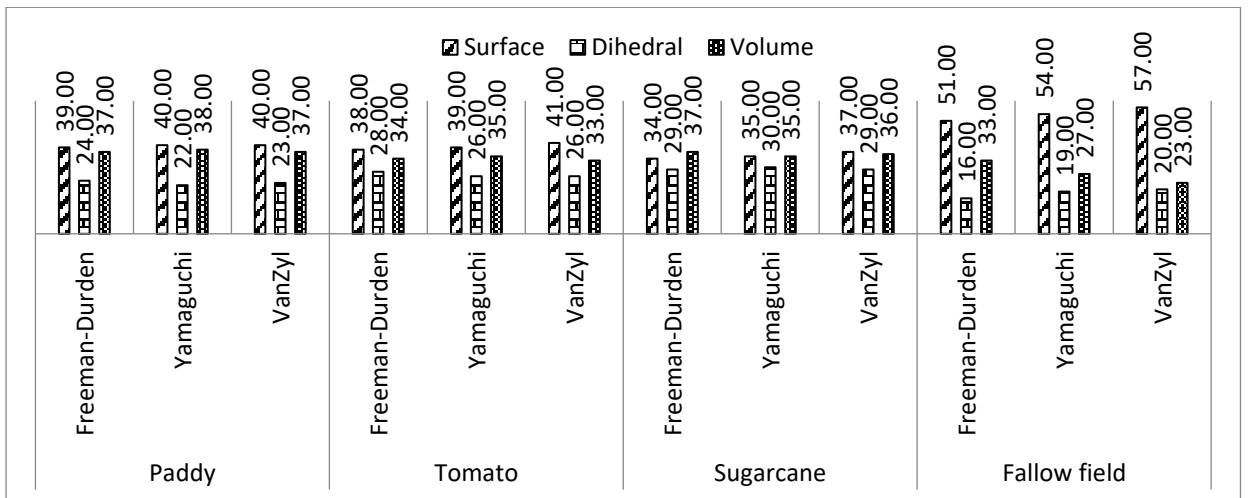


Figure 6.6 Proportionality of three scattering components on 01/10/2018 of paddy, Tomato, sugarcane and bare field

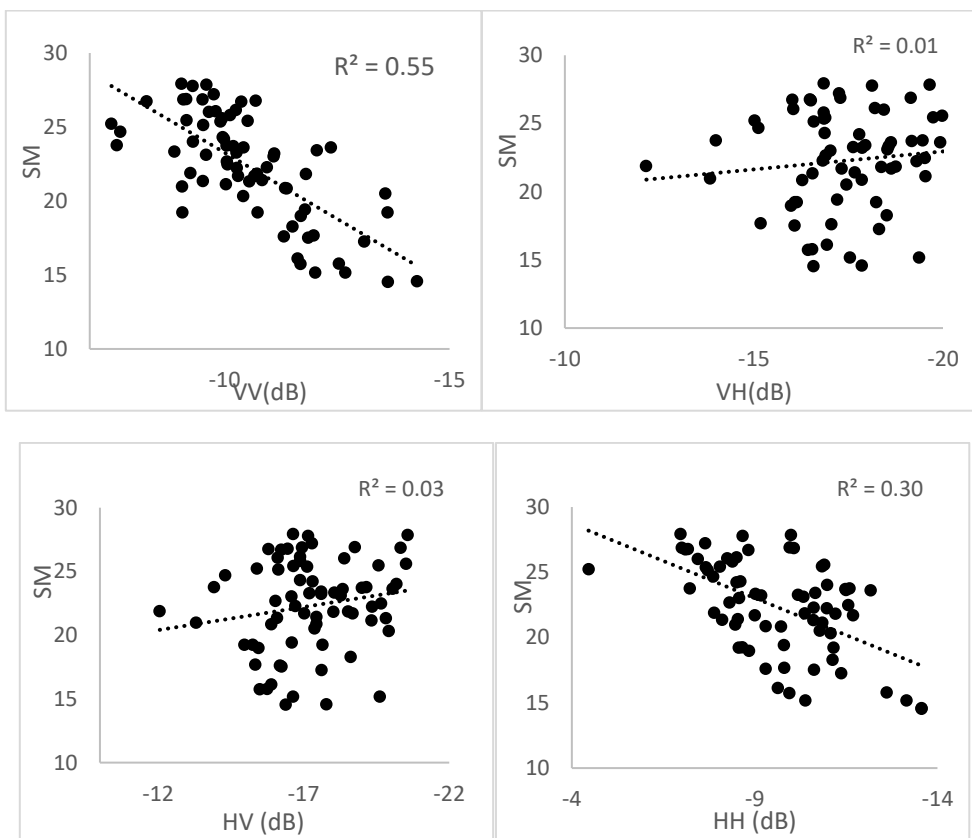
6.3.1.2 Regression analysis

Proportional analysis showed Freeman-Durden decomposition is over estimating the volume component, and Van Zyl decomposition over-estimating surface scattering component. From the analysis, surface scattering found to be dominant scattering component and can be used to retrieve surface soil moisture out of three scattering components. Regression analysis was carried out between soil moisture and surface, dihedral scattering components to analyse their dependence in the growing stage of

each crop. Linear regression models are used to examine the relationship between scattering components and soil moisture values whichever gave the best relationship that has been selected for modelling. ALOS PALSAR-2 quad polarized intensity data (HH, HV, VV and VH) and scattering components were examined individually to check the relationship with field measured surface soil moisture.

Maize field

The correlation between field measured soil moisture to backscattered energy of maize field is given in Figure 6.7.



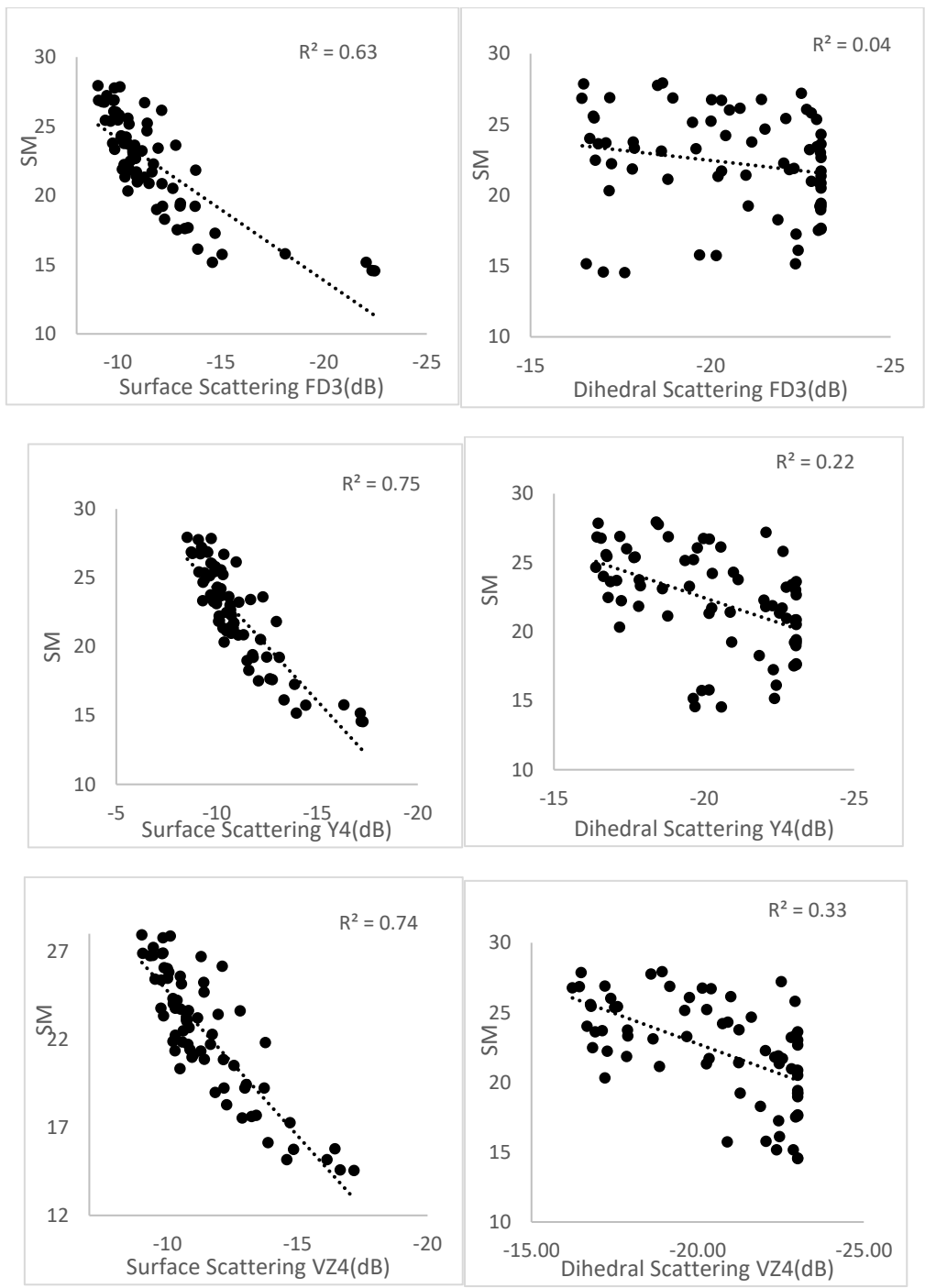
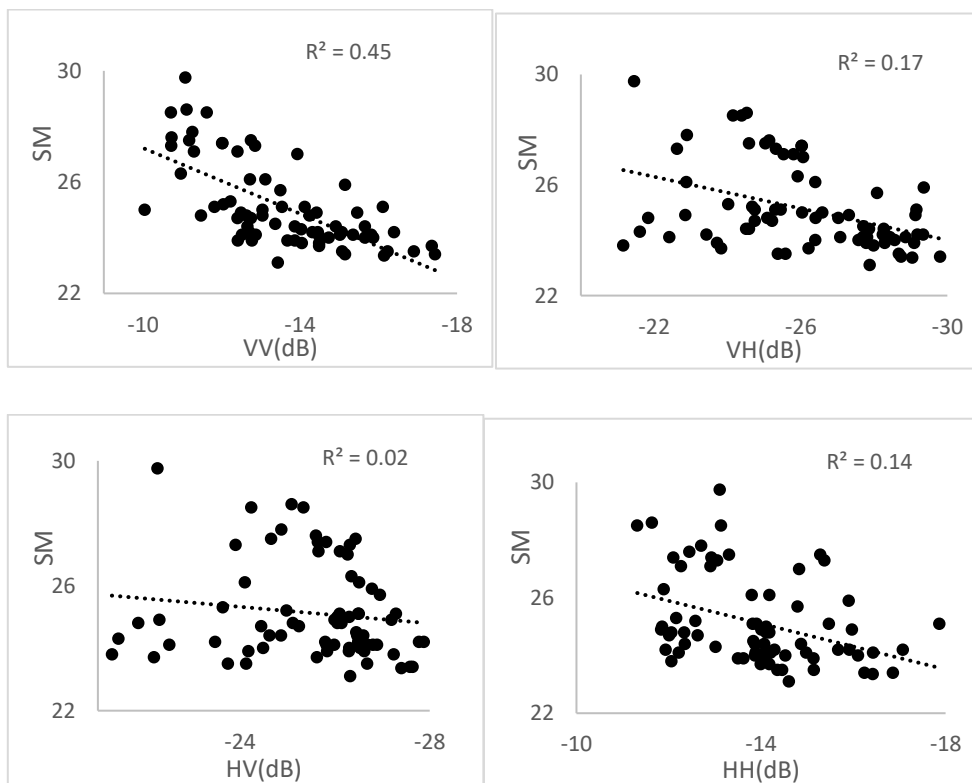


Figure 6.7 Relationship between polarization (HH, HV, VV & VH), surface scattering component, dihedral component and field-measured soil moisture at growing stage of maize (23/07/2018) (FD3- Freeman Durden; Y4- Yamaguchi and VZ4-Van Zyl polarimetric decomposition technique)

It was found that the decomposed surface scattering component shows good relation with surface soil moisture when compared with polarization data and dihedral scattering component. In case of polarization data VV ($R^2=0.55$) is having a good correlation with soil moisture. Dihedral scattering component of all three decomposition techniques has less than 0.5 correlation coefficient. From the study, Yamaguchi ($R^2 =0.75$) and Van Zyl ($R^2 =0.74$) surface scattering component is better than Freeman Durden ($R^2 =0.63$). From this, the Yamaguchi surface scattering component is considered the best decomposition technique to retrieve surface soil moisture from maize fields.

Paddy field

The relationship between field measured soil moisture to backscattered energy of paddy field at vegetative and flowering stage is given in Figure 6.8 and Figure 6.9 respectively. In the flowering stage of paddy field, along with surface scattering component, dihedral component showed good correlation with surface soil moisture. As the crop grows, vegetation's effect on backscattered energy increases and surface roughness is reduced.



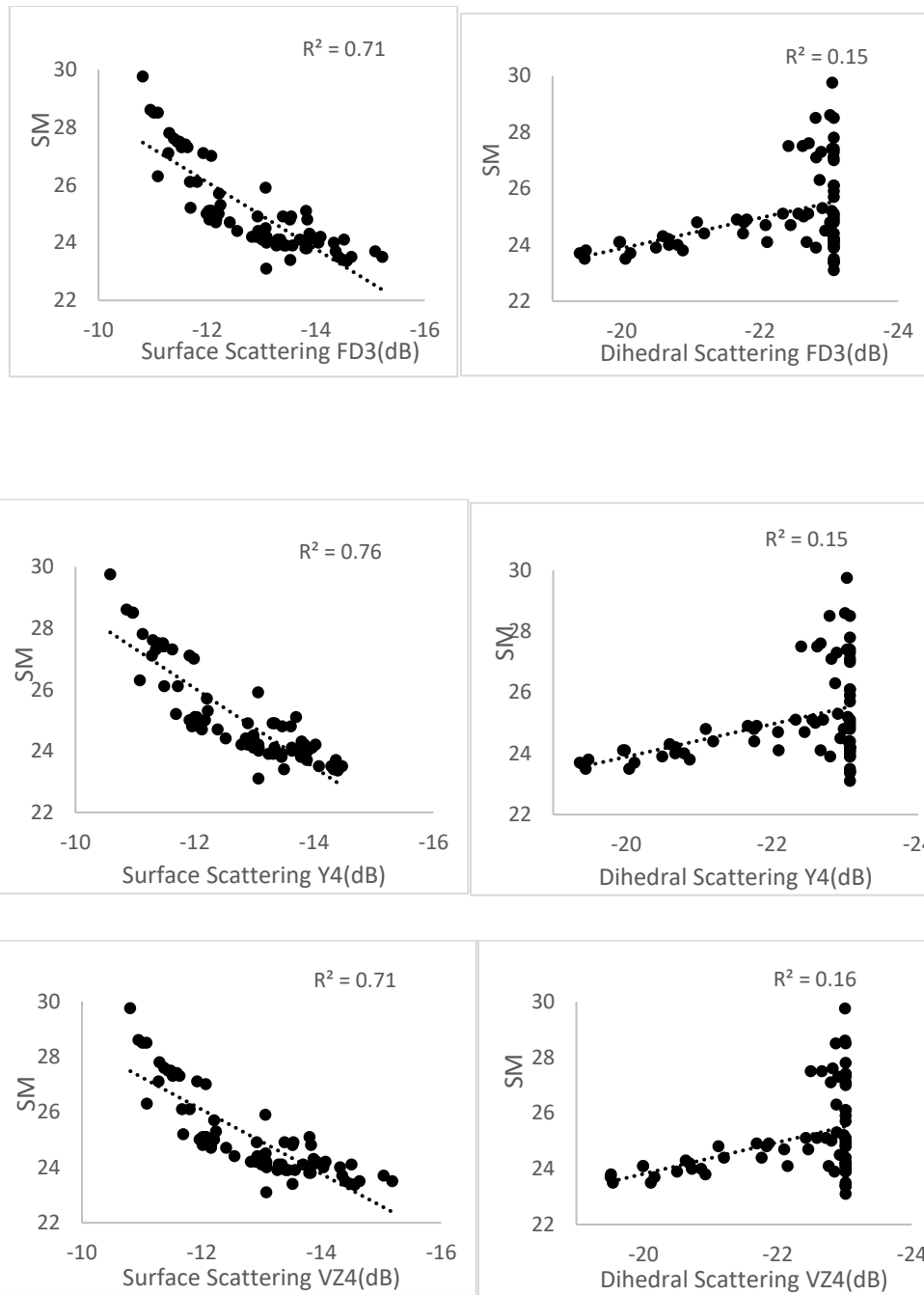
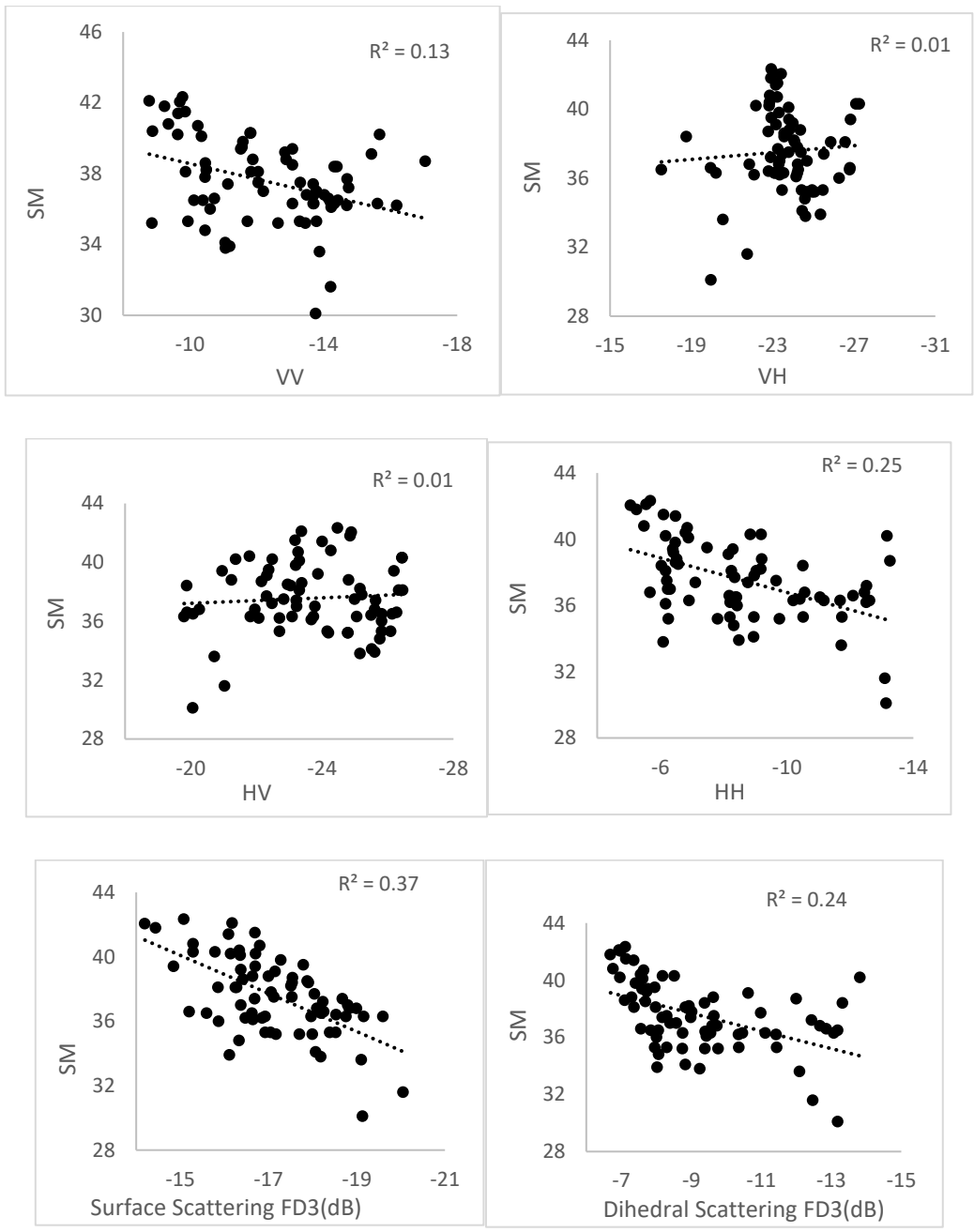


Figure 6.8 Relationship between polarization (HH, HV, VV & VH), surface scattering component, dihedral component and field-measured soil moisture at vegetative stage of paddy (23/07/2018) (FD3- Freeman Durden; Y4- Yamaguchi and VZ4-Van Zyl polarimetric decomposition)



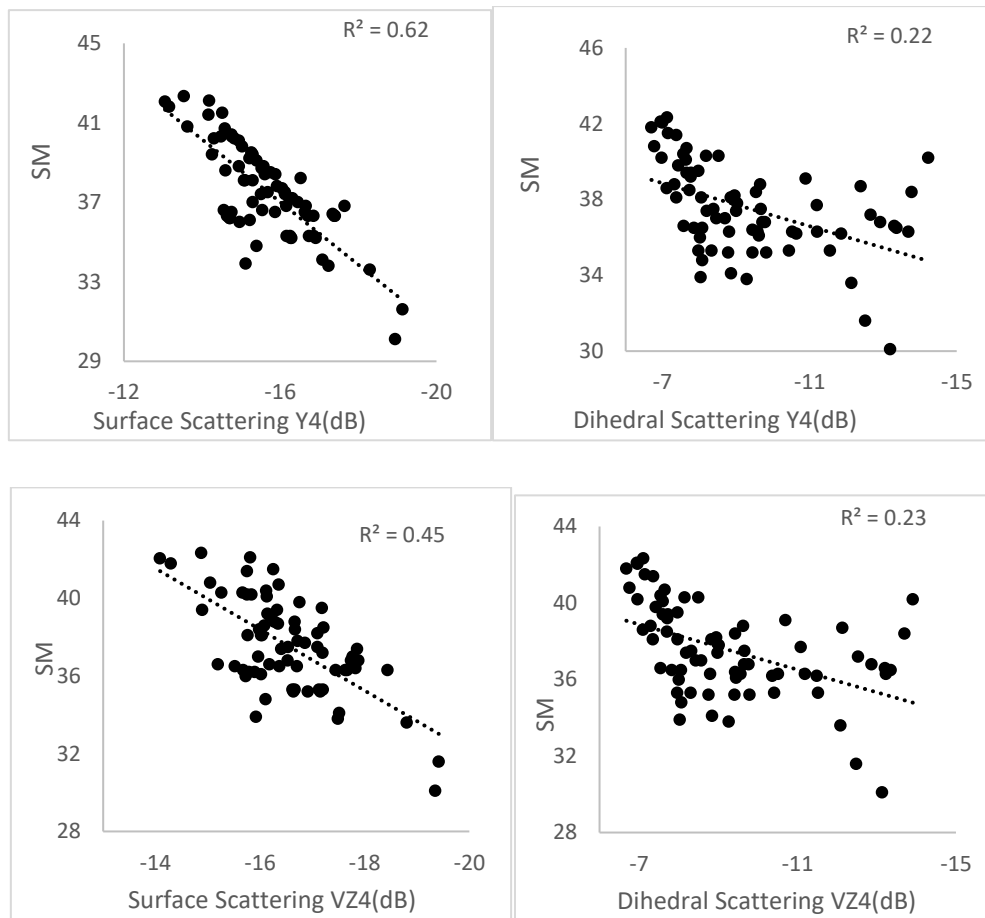
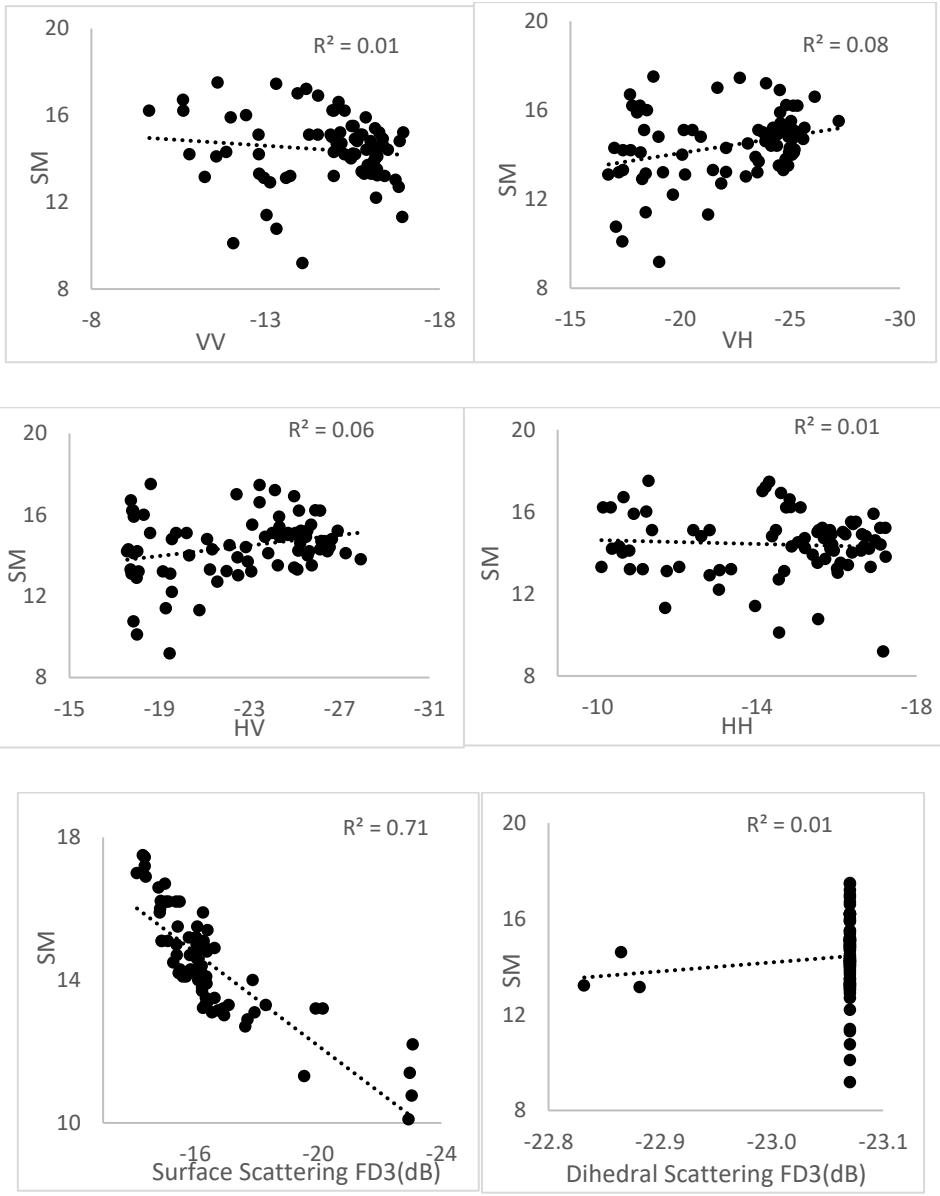


Figure 6.9 Relationship between polarization (HH, HV, VV & VH), surface scattering component, dihedral component and field-measured soil moisture at vegetative stage of paddy (01/10/2018) (FD3- Freeman Durden; Y4-Yamaguchi and VZ4-Van Zyl polarimetric decomposition)

Tomato field

The relationship between field measured soil moisture to backscattered energy of tomato field at vegetative and first harvesting stage is given in Figure 6.10 and 6.11 respectively.



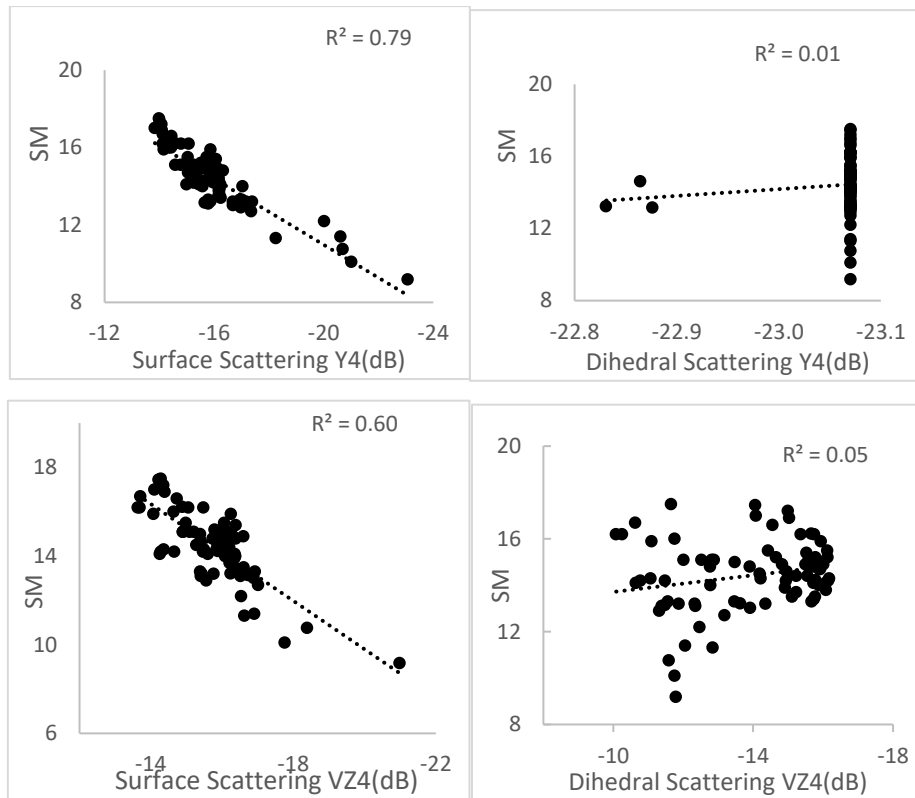
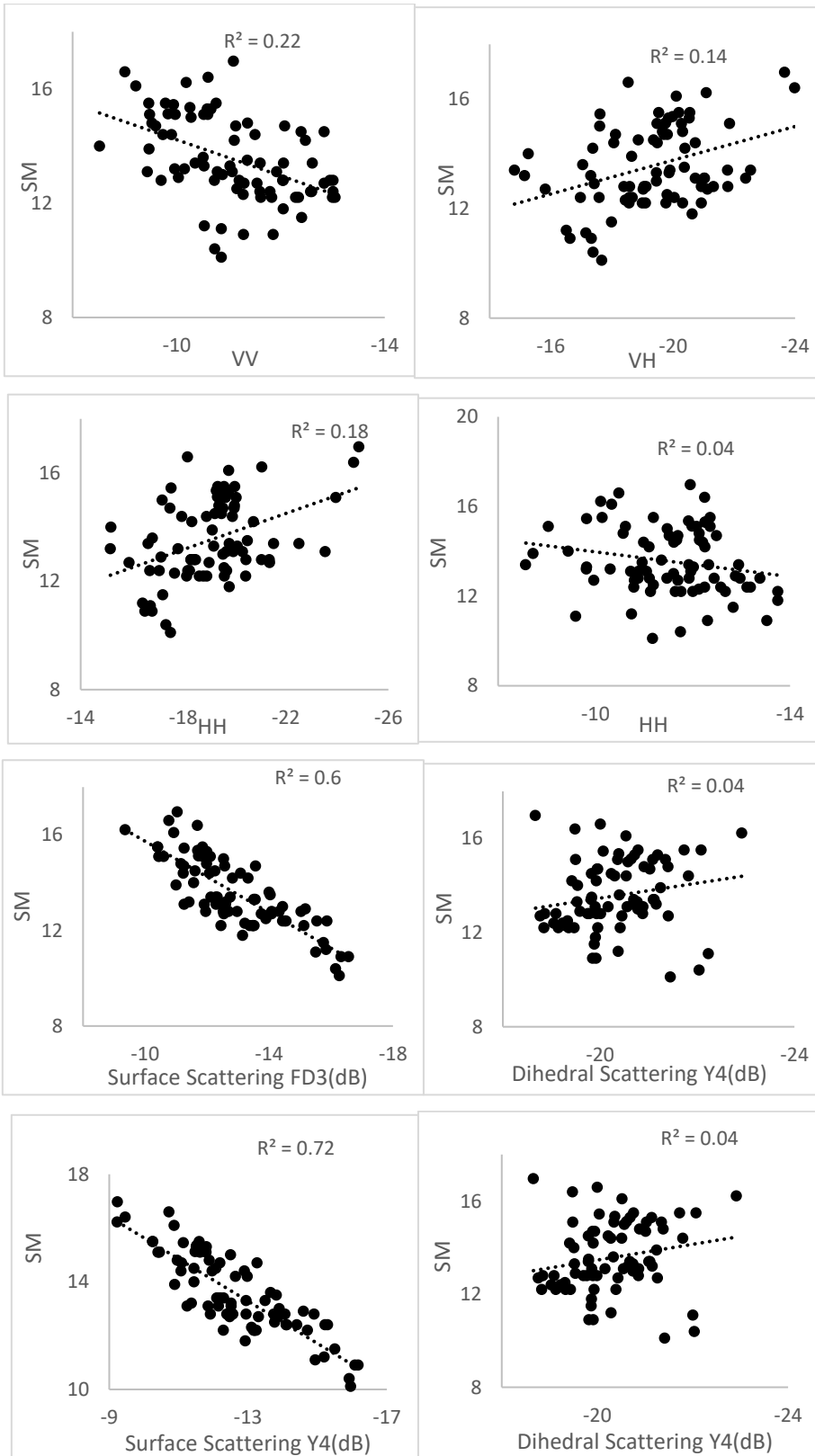


Figure 6.10 Relationship between polarization (HH, HV, VV & VH), surface scattering component, dihedral component and field-measured soil moisture at vegetative stage of Tomato field (23/07/2018) (FD3- Freeman Durden; Y4- Yamaguchi and VZ4-Van Zyl polarimetric decomposition)



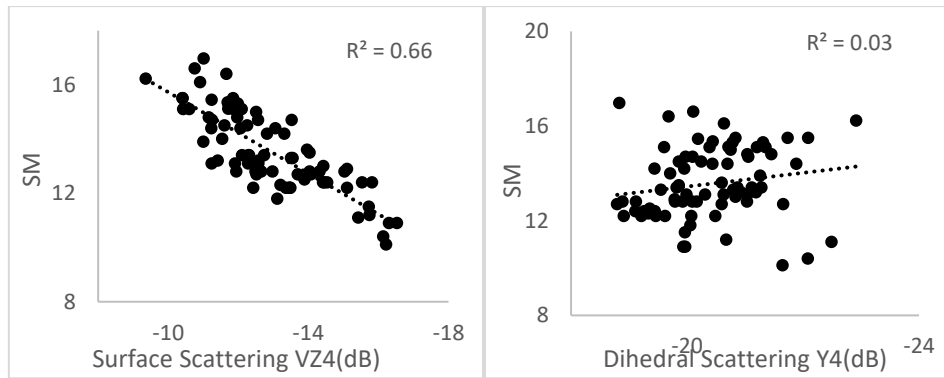
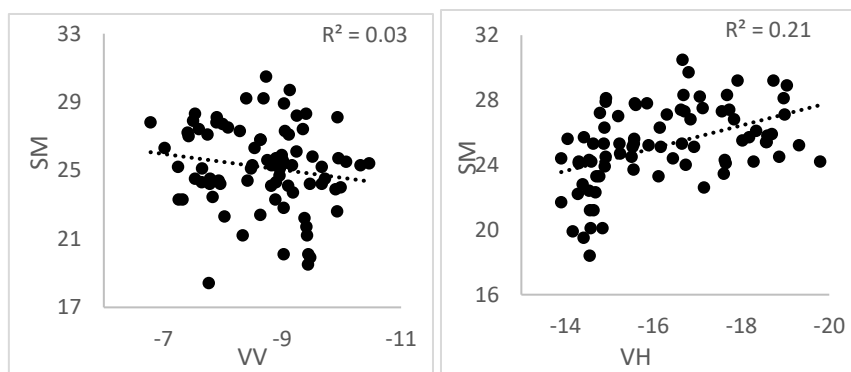


Figure 6.11 Relationship between polarization (HH, HV, VV & VH), surface scattering component, dihedral component and field-measured soil moisture at first harvest stage of Tomato field (01/10/2018) (FD3- Freeman Durden; Y4- Yamaguchi and VZ4-Van Zyl polarimetric decomposition)

From Figure 6.10 and 6.11 it is observed, that surface scattering component is having good relationship with surface soil moisture at vegetative stage. Whereas in first harvest stage dihedral scattering did not show any prominent relationship with surface soil moisture.

Sugarcane field

The relationship between field measured soil moisture to backscattered energy of sugarcane field at growing and grand growing stage is given in Figure 6.12 and 6.13 respectively.



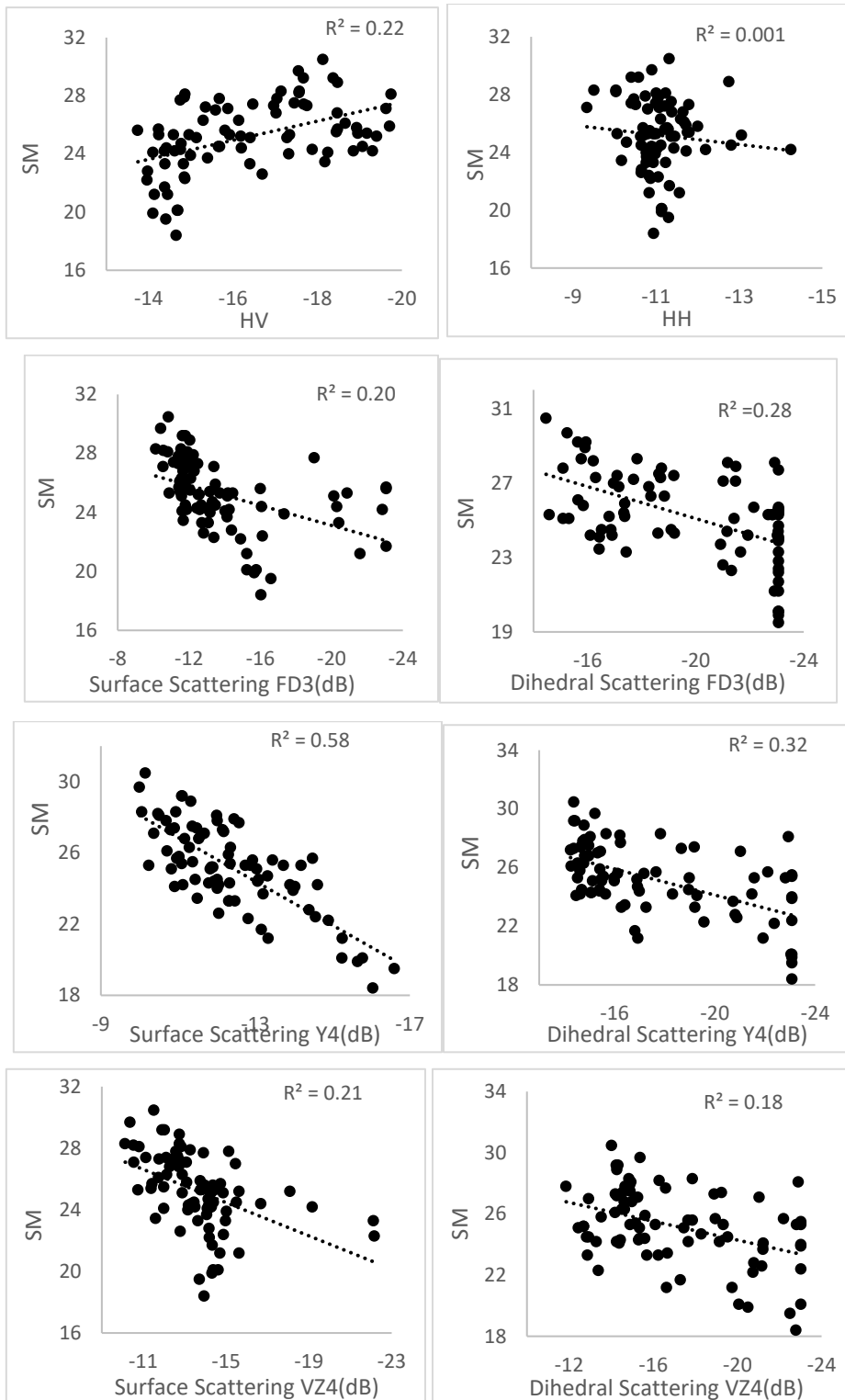
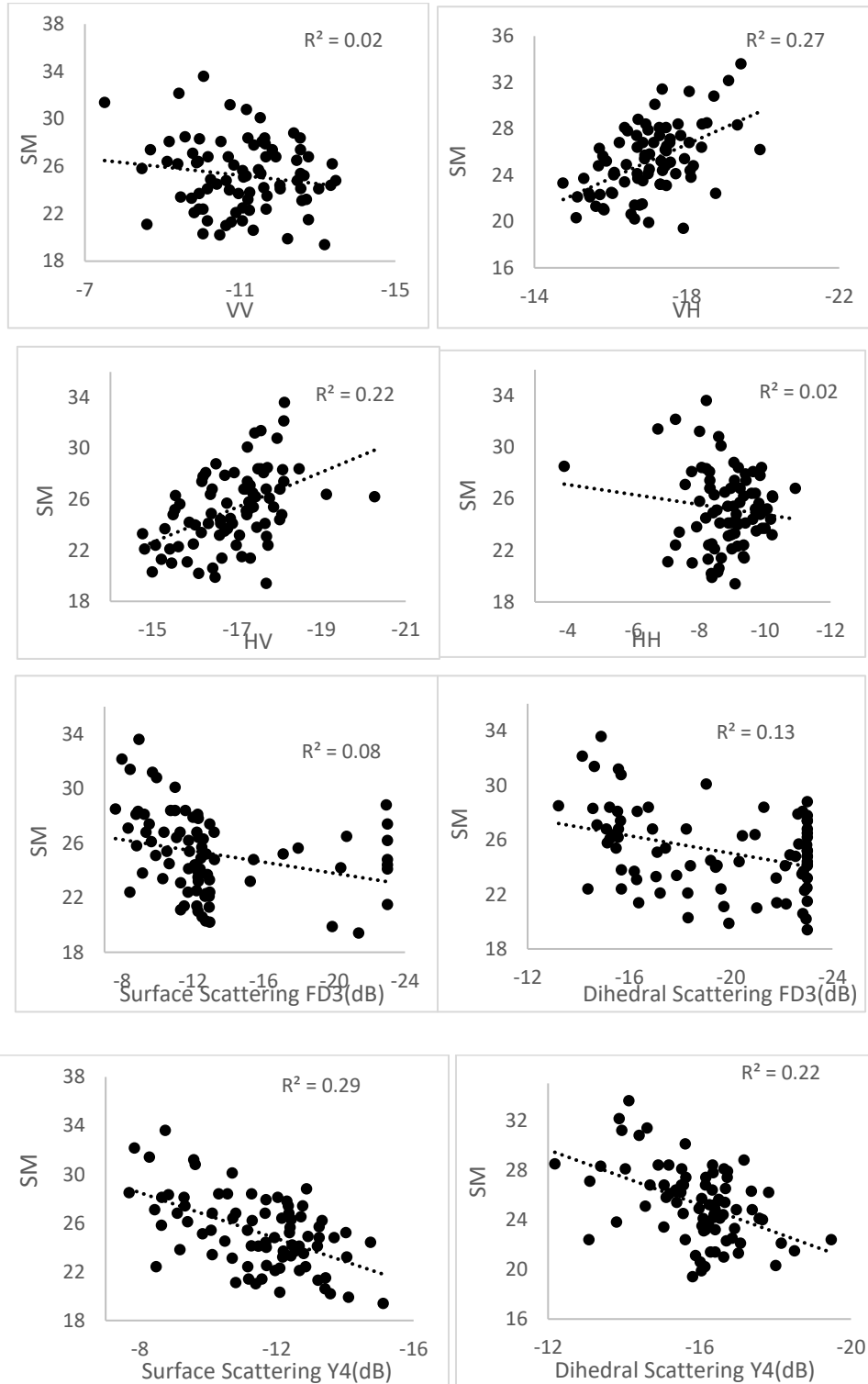


Figure 6.12 Relationship between polarization (HH, HV, VV & VH), surface scattering component, dihedral component and field-measured soil moisture at

vegetative stage of Sugarcane field (23/07/2018) (FD3- Freeman Durden; Y4- Yamaguchi and VZ4-Van Zyl polarimetric decomposition)



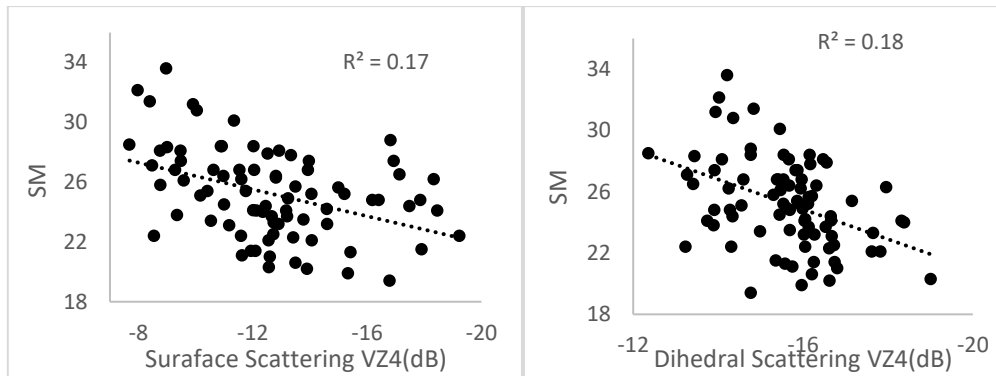
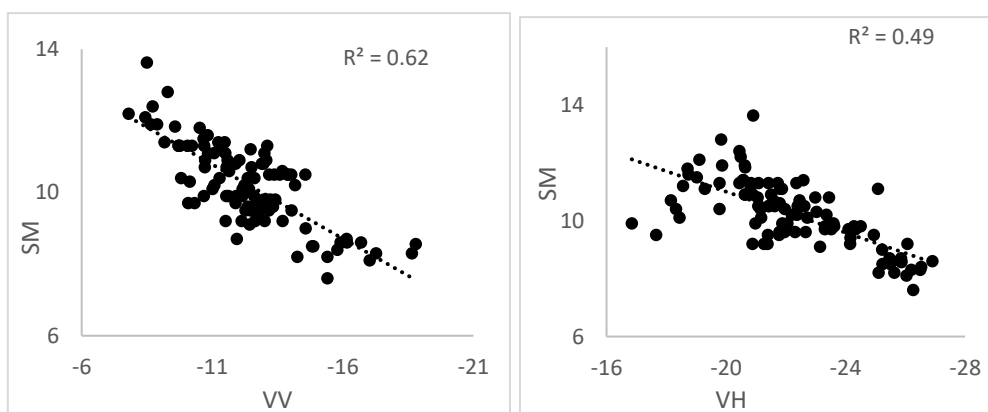


Figure 6.13 Relationship between polarization (HH, HV, VV & VH), surface scattering component, dihedral component and field-measured soil moisture at grand growing stage of Suagarcane field (01/10/2018) (FD3- Freeman Durden; Y4- Yamaguchi and VZ4-Van Zyl polarimetric decomposition)

Figure 6.12 and 6.13 show that surface soil moisture has a good relationship with surface and dihedral scattering. As vegetation biomass increased in grand growing stage of sugarcane we did not find much relation with surface or dihedral scattering component of sugarcane field with soil moisture.

Bare field

The relationship between field measured soil moisture to backscattered energy of bare field at two different scene is given in Figure 6.14 and 6.15 respectively.



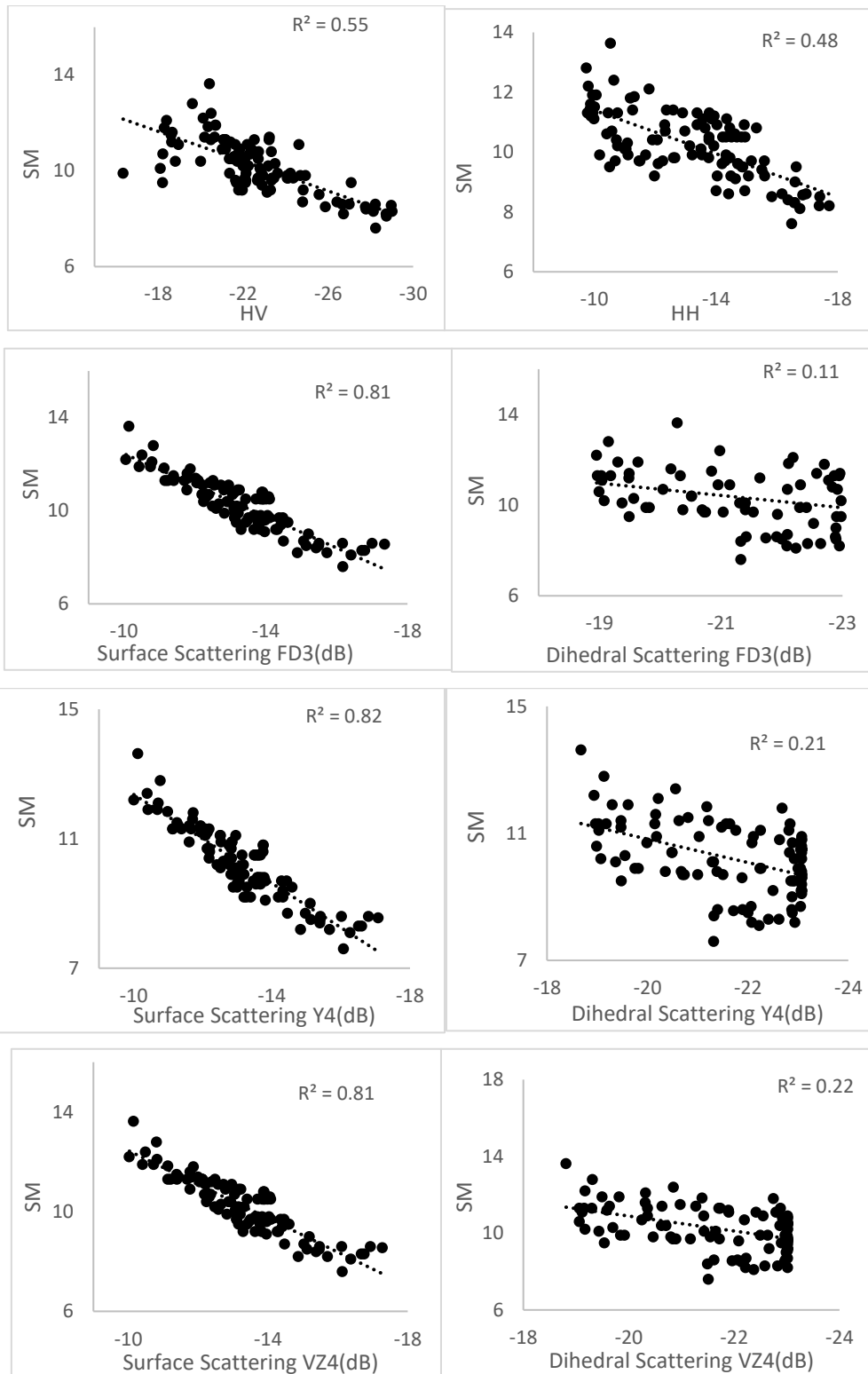
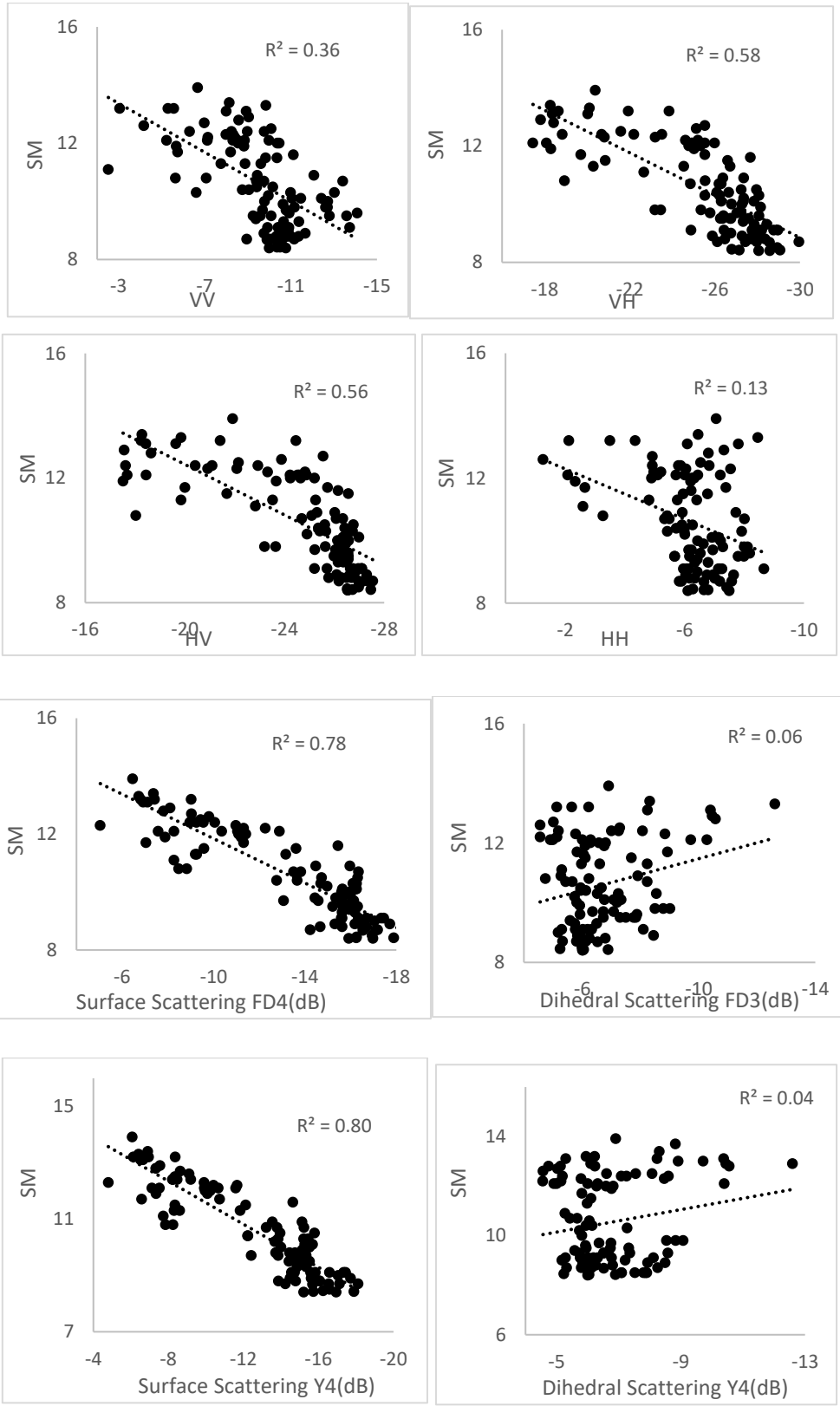


Figure 6.14 Relationship between polarization (HH, HV, VV & VH), surface scattering component, dihedral component and field-measured soil moisture of bare

field (23/07/2018) (FD3- Freeman Durden; Y4- Yamaguchi and VZ4-Van Zyl
 polarimetric decomposition)



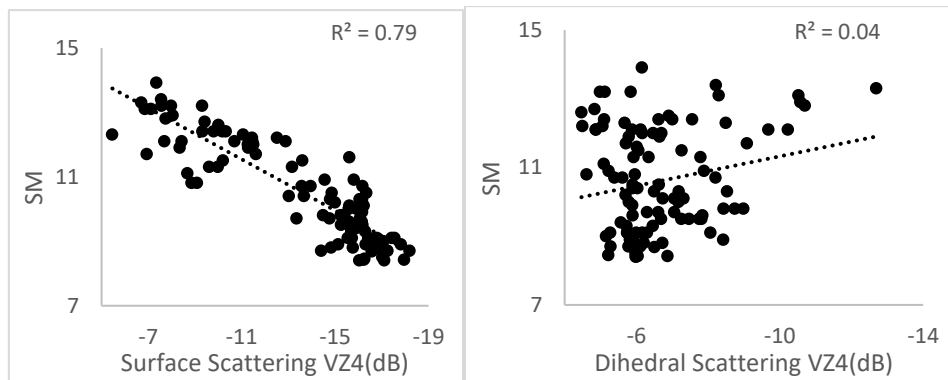


Figure 6.15 Relationship between polarization (HH, HV, VV & VH), surface scattering component, dihedral component and field-measured soil moisture of bare field (01/10/2018) (FD3- Freeman Durden; Y4- Yamaguchi and VZ4-Van Zyl polarimetric decomposition)

6.3.1.3 Semi empirical modelling

From the regression analysis, we came to know that Yamaguchi surface scattering component has a good relationship with surface soil moisture. The effect of surface roughness is not examined in the decomposed surface scattering component (Barrett et al., 2009; Ponnurangam and Rao, 2017). So, the depolarization ratio between VH and VV polarization is initially validated using field surface roughness samples (Srivastava et al. 2008). The correlation between field surface roughness and depolarization ratio of agricultural plot was found well from Figure 6.16 and 6.17 respectively. Hence effect of surface roughness is taken care by depolarization ratio and there was no tillage during the cycle. In case of sugarcane, depolarization ration did not give any relation so neglected for 23/07/2018. In case of 01/10/2018 acquisition only tomato and bare field gave relation between depolarization ratio and surface roughness. Which shows other surface roughness other crop are not affecting much due to vegetation cover. Yamaguchi polarization surface scattering component, depolarization ratio and dihedral scattering component were considered as effective parameters to develop the surface soil moisture model based on single L- band SAR imagery.

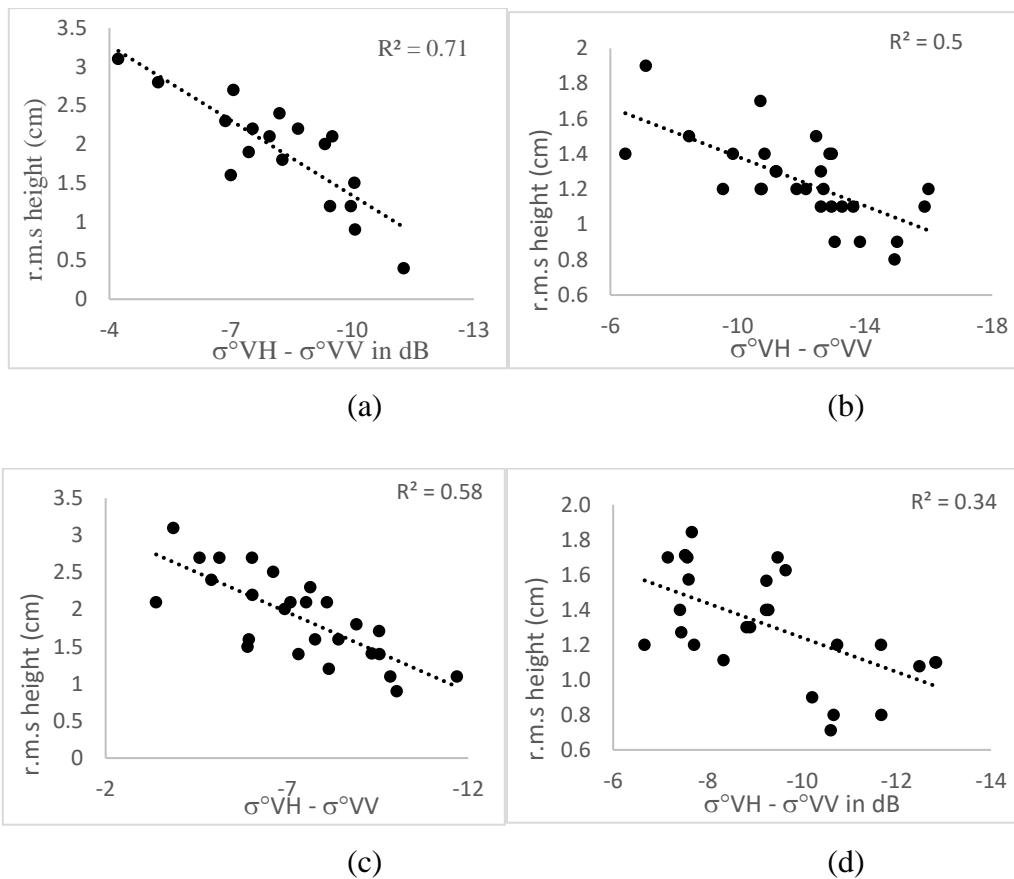


Figure 6.16 Relationship between depolarization ratio and surface roughness height of Maize (a), Paddy (b), Tomato (c) and bare field (d) of 23/07/2018

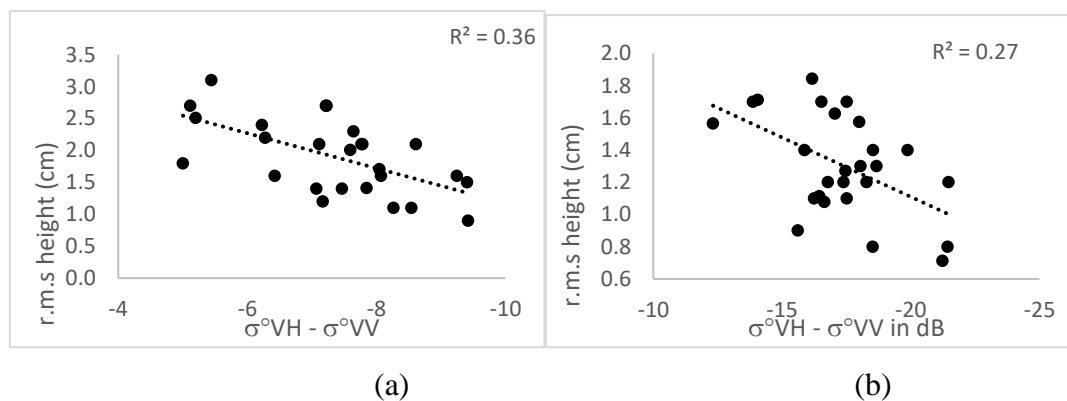


Figure 6.17 Relationship between depolarization ratio and surface roughness height of Tomato (a) and bare field (b) of 01/10/2018

Field collected soil moisture values correlate with Yamaguchi surface scattering component, Dihedral scattering component and depolarization ratio. Based on the

affecting parameters a Multi Linear Regression (MLR) analysis is carried out and a Semi-Empirical Model (SEM) is developed at a confidence interval 95% for each crops at two different crop stages is given in the Table 6.2 and 6.3 respectively.

Table 6.2 Details of developed Semi-Empirical Model (SEM) of 23/07/2018 for various crops

Sl. no.	Crops	Crop stage	SEM	Adj. R ²
1	Maize	Vegetative	$M_v = 38.04 + 1.52\sigma_{sur}^{\circ} + 0.15\sigma_{vh-vv}^{\circ}$	0.75
2	Paddy	Vegetative	$M_v = 42.6 + 1.32\sigma_{sur}^{\circ} + 0.06\sigma_{vh-vv}^{\circ}$	0.74
3	Tomato	Vegetative	$M_v = 28.86 + 0.81\sigma_{sur}^{\circ} + 0.63\sigma_{vh-vv}^{\circ}$	0.79
4	Sugarcane	Vegetative	$M_v = 40.84 + 1.1\sigma_{sur}^{\circ} + 0.15\sigma_{dihedral}^{\circ}$	0.59
5	Bare field	----	$M_v = 19.34 + 0.68\sigma_{sur}^{\circ} + 0.14\sigma_{vh-vv}^{\circ}$	0.84

Table 6.3 Details of developed Semi-Empirical Model (SEM) of 01/10/2018 for various crops

Sl. no.	Crops	Crop stage	SEM	Adj. R ²
1	Paddy	Flowering	$M_v = 61.8 + 1.5\sigma_{sur}^{\circ} + 0.2\sigma_{dihedral}^{\circ}$	0.61
2	Tomato	First harvest	$M_v = 25.6 + 0.88\sigma_{sur}^{\circ} + 0.12\sigma_{dihedral}^{\circ}$	0.7
3	Sugarcane	Grand growing	$M_v = 39.7 + 0.74\sigma_{sur}^{\circ} + 0.38\sigma_{dihedral}^{\circ}$	0.29
4	Bare field	----	$M_v = 15.27 + 0.39\sigma_{sur}^{\circ} + 0.12\sigma_{vh-vv}^{\circ}$	0.79

6.3.1.4 Validation

The Oh 1992, Oh 2004 and X-Bragg model estimated soil moisture is validated using grid sampled field soil moisture for both the acquisition (23/07/2018 & 01/10/2018). In the case of WCM and SEM, 70% of field data is already used in model parameterization, so 30% of data has been used to validate it. Root Mean Square Error (RMSE) and Absolute Error (AE) are used to check the accuracy of models. The results of the accuracy assessment of surface soil moisture models are shown in Table 6.4. In paddy plots' it can be noticed that, Oh model, 2004 is giving good results in both vegetative (RMSE=1.88; NSE=0.73) and flowering stage (RMSE=2.47; NSE=0.72) compared to X-Bragg and Oh 1992 models. The maximum absolute error is seen in the estimates of X-Bragg model ($AE_{max}=3.82$ & 3.22) which shows more deviation of

surface soil moisture estimates from observed one. In tomato plot also Oh 2004 model (RMSE=1.49 & RMSE=2.81) is performing marginally better than Oh 1992 model (RMSE=1.72 & RMSE=3.28) in both vegetative and first harvest stage. X-Bragg model shows more deviations from the observed ones in all agricultural crops. In case of sugarcane, during vegetative stage all three models performed more or less same. SEM (RMSE=2.48) and WCM (RMSE=2.43) model are performing marginally better than Oh 1992 (RMSE=2.52) and Oh 2004 models (RMSE=2.84) in sugarcane vegetative stage. In grand growing stage all models gave abrupt results with models AE_{max} ranging between 4.62-7.96. In fallow fields, all models are performing well with marginal error for both dates.

All in all, comparing existing soil moisture models, Oh 2004 model is performing better than Oh 1992 and X-Bragg model in paddy, tomato and bare filed plots. In case of sugarcane soil moisture estimates are good only in vegetative stage but in grand growing stage estimates are deviated much from the observed ones because of the high vegetation biomass. Developed SEM and WCM is performing better than Oh 2004 model because its model parameters were calibrated using actual field data and it is validated. The results of the accuracy assessment of surface soil moisture models are shown in Table 6.4.

Table 6.4 Accuracy assessment of surface soil moisture models of L-band SAR

Date		23/07/2018		01/10/2018	
Crop	Model\statistics	RMSE	AE_{max}	RMSE	AE_{max}
Maize	Oh model 1992	2.84	3.8	NA	
	Oh model 2004	2.23	3.17		
	X Bragg	2.78	4.21		
	WCM	1.98	3.1		
	SEM	1.81	2.88		
Paddy	Oh model 1992	2.1	2.49	2.88	3.1
	Oh model 2004	1.88	2.15	2.47	2.54
	X Bragg	2.26	3.82	2.80	3.22
	WCM	1.80	2.4	2.36	2.69

	SEM	1.68	2.1	2.45	2.7
Tomato	Oh model 1992	1.72	2.33	3.28	3.08
	Oh model 2004	1.49	2.11	2.81	2.77
	X Bragg	2.1	2.57	3.42	3.45
	WCM	1.53	1.92	3.12	2.93
	SEM	1.32	1.8	2.51	2.6
Sugarcane	Oh model 1992	2.84	3.37	4.7	6.84
	Oh model 2004	2.52	3.1	4.45	6.88
	X Bragg	2.63	4.21	4.23	7.96
	WCM	2.43	3.05	3.64	4.62
	SEM	2.48	3.08	4.1	5.22
Bare field	Oh model 1992	1.24	2.14	1.25	2.27
	Oh model 2004	0.85	1.76	0.84	1.9
	X Bragg	1.21	3.18	1.19	2.81
	WCM	0.8	2.03	0.83	1.88
	SEM	0.82	1.7	0.88	1.49

*RMSE=Root Mean Square error (% g/cm³/g/cm³); AE_{max}= Maximum Absolute Error (% g/cm³)

6.3.2 Surface soil moisture retrieval using dual-pol, C-band SAR

Processed Sentinel-1a data was used to estimate surface soil moisture for whole crop cycle of Paddy, Sugarcane, Tomato and Maize. Crop cycle of each crop is divided into stages namely, vegetative, maturity and yield stage according to FAO crop information (<https://www.fao.org/land-water/databases-and-software/cropinformation>). For each crop stage surface soil moisture is evaluated using soil moisture models like Oh 2004 and WCM (discussed in section 6.3.1.1) to understand the capability of a model to retrieve surface soil moisture at various vegetation spread levels. In case of Oh model 2004 the surface roughness parameter is replaced using depolarization ratio. In case of WCM, RVI is calculated using modified dual polarized RVI (Haldar et al., 2018; Liao et al., 2018) given in Eq. 6.12. The soil moisture estimates are validated using field data.

$$RVI = \frac{4\sigma_{VH}}{\sigma_{VV} + \sigma_{VH}} \quad (6.12)$$

6.3.2.1 Model development

To develop the model, the effect soil moisture, roughness and vegetation on radar backscattered energy was analysed and affective parameters are selected to develop the surface soil moisture models at three different crop stages of selected agricultural test plots.

Maize field

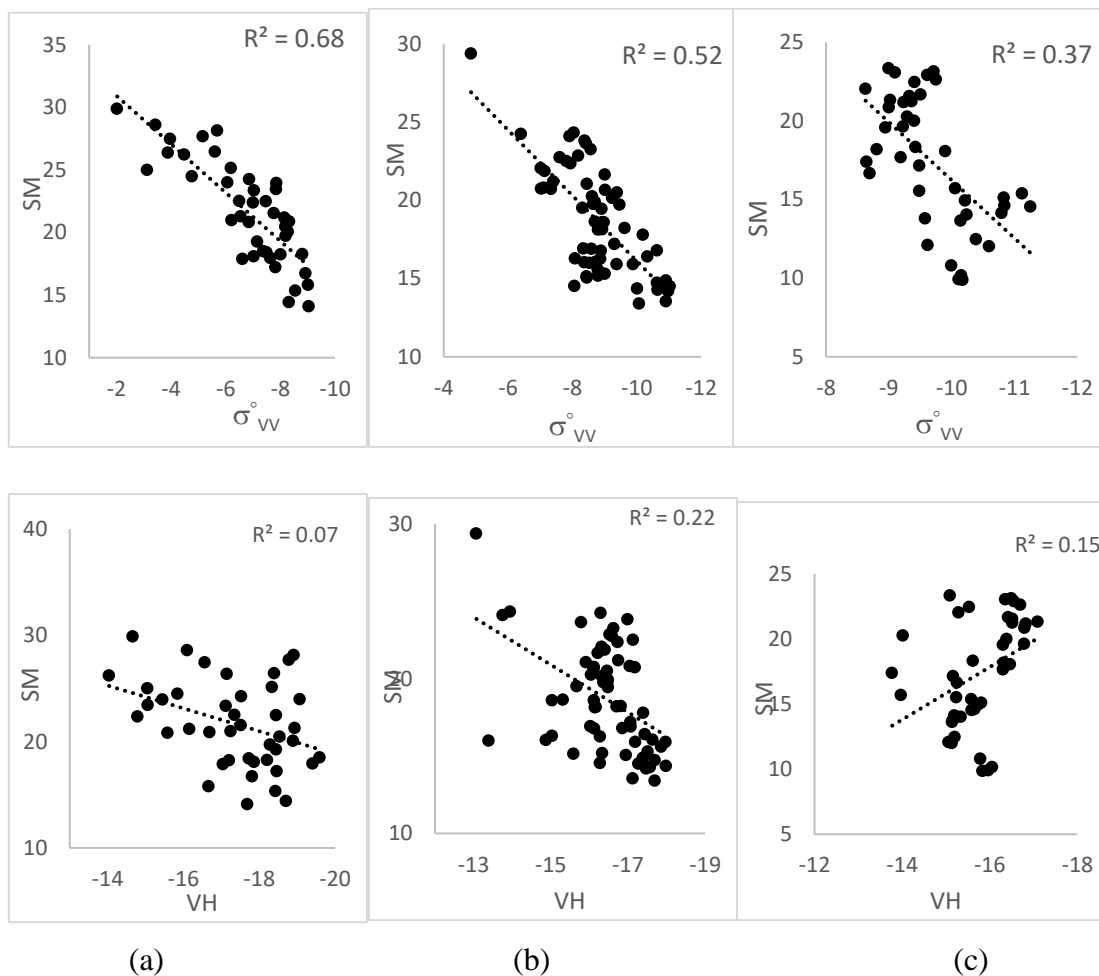


Figure 6.18 Relationship between soil moisture and radar signal VV and VH polarization at seedling (a), vegetative (b) and yield stage (c) of Maize field

The Maize crop cycle is divided into three crop stages namely, seedling, vegetative and yield stage. The relationship between field measured surface soil moisture and backscattered energy (VV & VH) at each crop stage of maize is analysed and presented in Figure 6.18. It can be seen that the backscattered radar signals have a clear

dependence on soil moisture with VV polarization than VH polarization. This is because cross polarization has a poorer penetrability than co-polarization and is more susceptible to vegetation blocking.

RVI is considered a vegetation parameter, to analyse the vegetation intervention on SAR backscattered energy. RVI values of each sampling grid were calculated using amplitude data (power units) of Sentinel-1a data. Figure 6.19 shows that RVI has a positive relationship with σ° (VH) of vegetative and yield stage of maize crop with $R^2=0.33$ and $R^2 = 0.42$ respectively. The RVI values finds good relationship with VH backscattered energy then VV. The values of RVI are within the range at seedling stage in which a radar signal is not much affected (Sikdar and Cumming 2004), implying that there is no need to minimize the effect of vegetation at seedling stage.

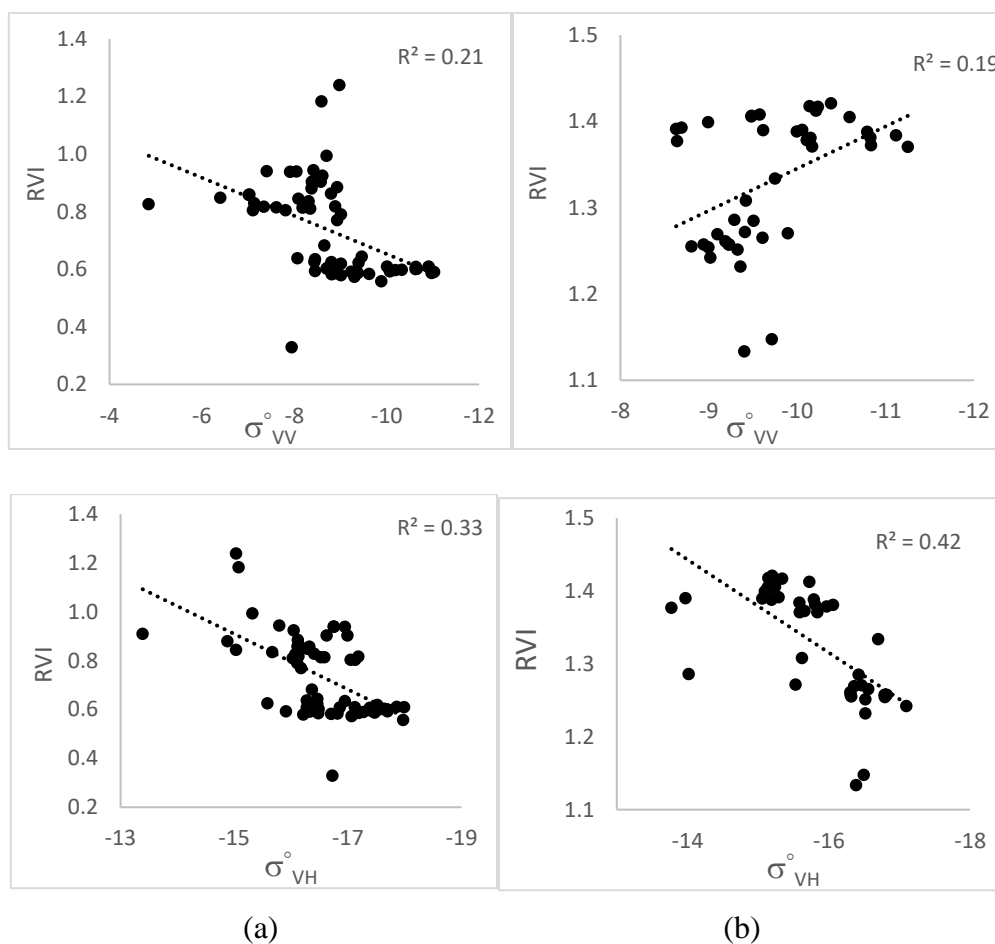


Figure 6.19 Relationship between radar signal (VV and VH polarization) and RVI at vegetative (a) and yield (b) stage of Maize field

Paddy field

The paddy crop cycle is divided into three crop stages namely, vegetative, maturity and yield stage. The relationship between field measured surface soil moisture and backscattered energy (VV) and (VH) at each crop stage of paddy is analysed and presented in Figure 6.20. From Fig. 6.21, it is observed that backscattered radar signals have a clear dependence on soil moisture with VV polarization than VH polarization. But as the crop grows the dependence of backscattered energy on soil moisture is reduced. The effect of crop growth on backscattered energy is analysed using RVI. The relationship between RVI and backscattered energy is presented in Figure 6.21.

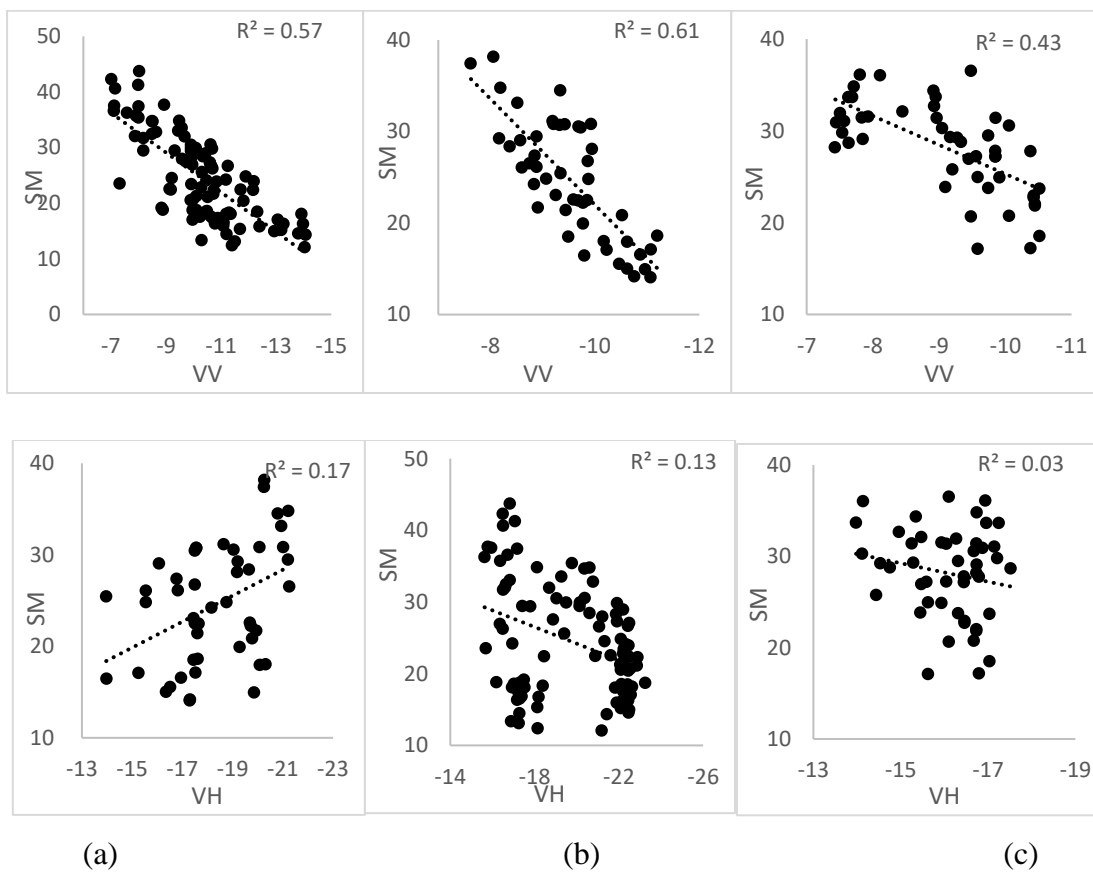


Figure 6.20 Relationship between soil moisture and radar signal VV and VH polarization at vegetative (a), maturity (b) and yield stage (c) of paddy field

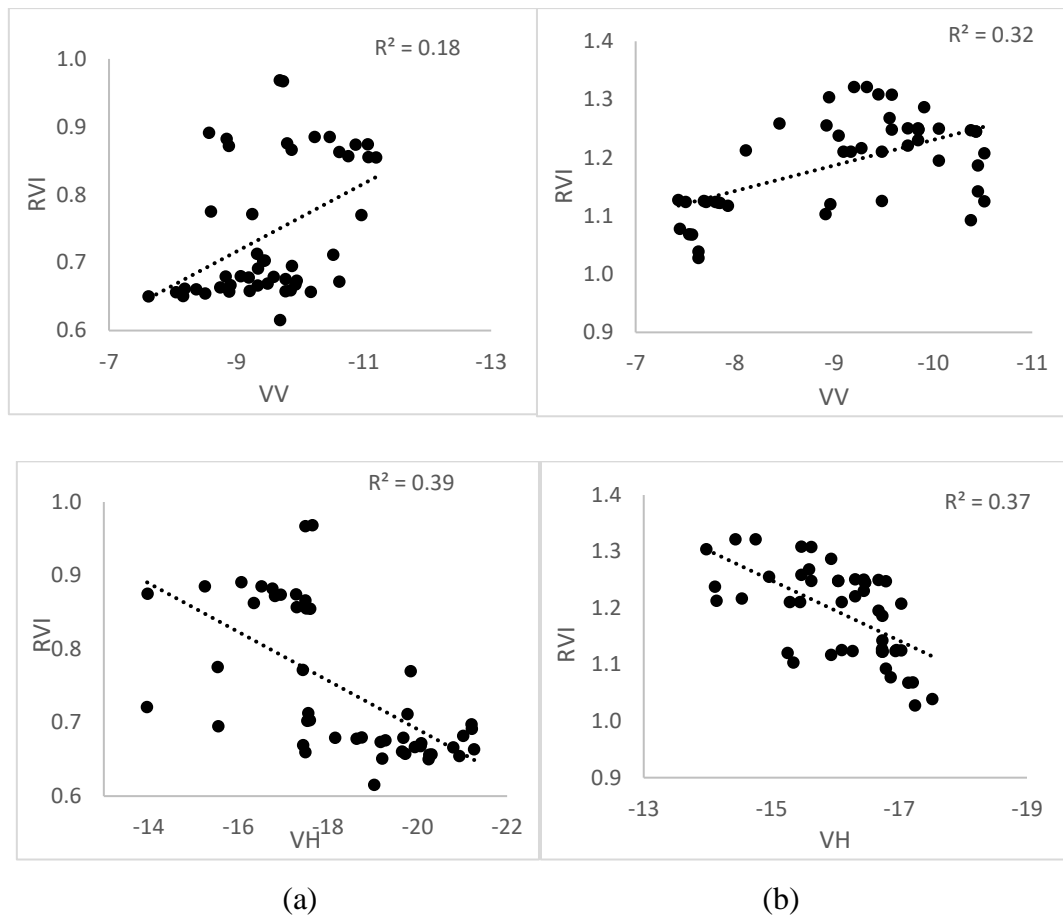


Figure 6.21 Relationship between radar signal (VV and VH polarization) and RVI at maturity (a) and yield (b) stage of paddy field

Tomato field

The Tomato crop cycle is divided into three crop stages namely, vegetative, maturity and yield stage. The relationship between field measured surface soil moisture and backscattered energy (VV) and (VH) at each crop stage of paddy is analysed and presented in Figure 6.22. The effect of vegetation (RVI) is shown in Figure 6.23. Tomato crop showed VV backscattered energy having almost same dependence on surface soil moisture at different tomato crop stages. The effect vegetation on backscattered energy (VH) at two different stages of crop gives almost same relationship ($\sim R^2=0.35$)

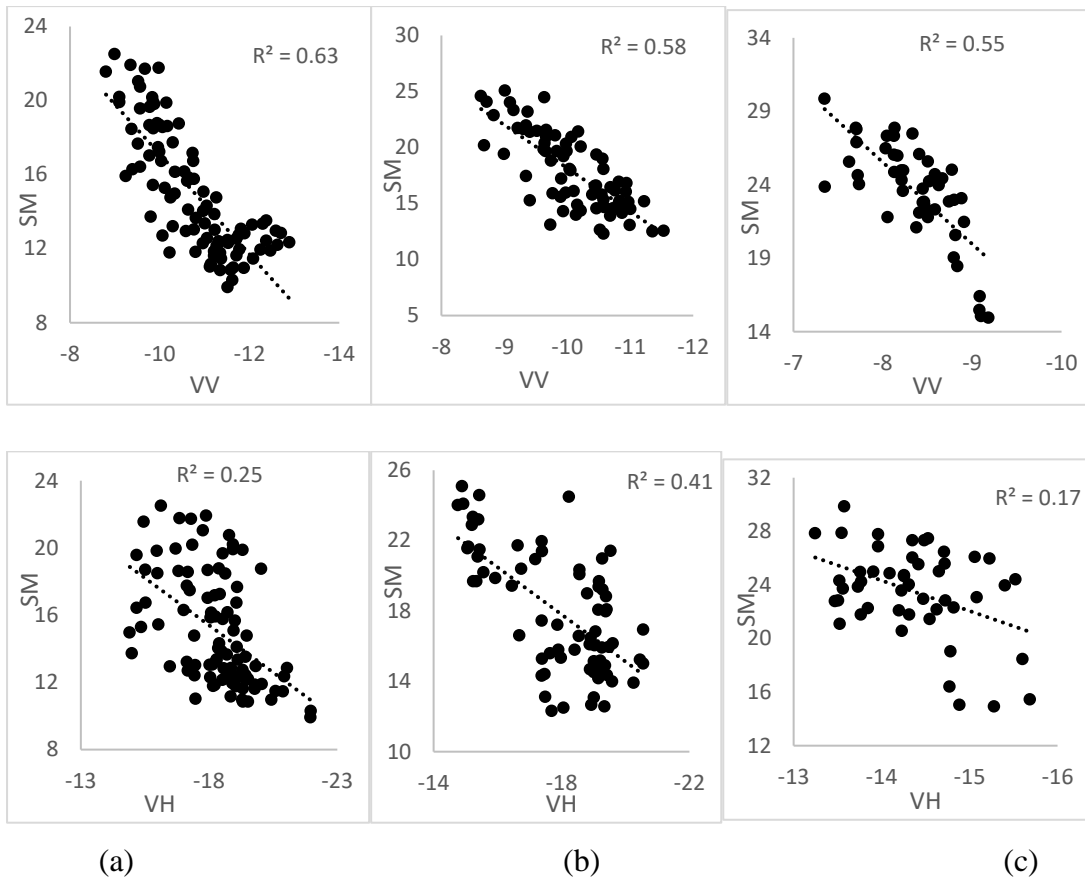
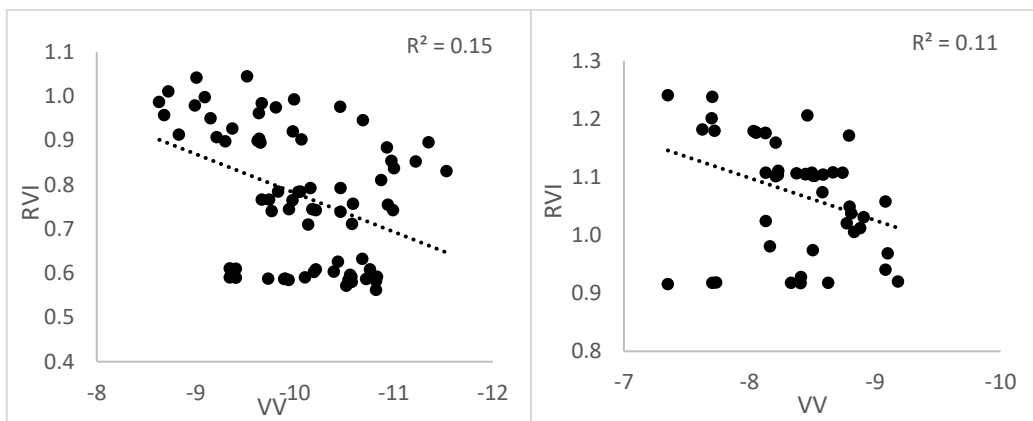


Figure 6.22 Relationship between soil moisture and radar signal VV and VH polarization at vegetative (a), maturity (b) and yield stage (c) of Tomato field



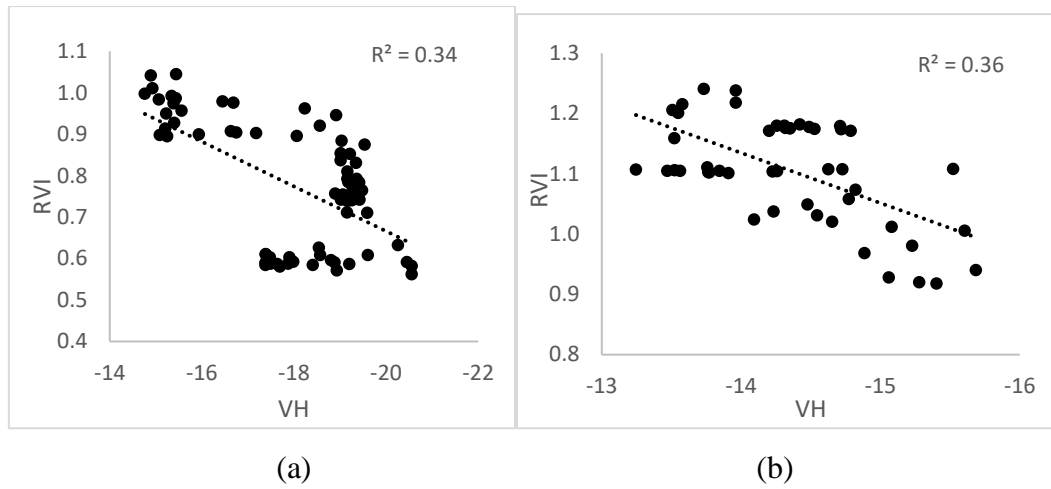
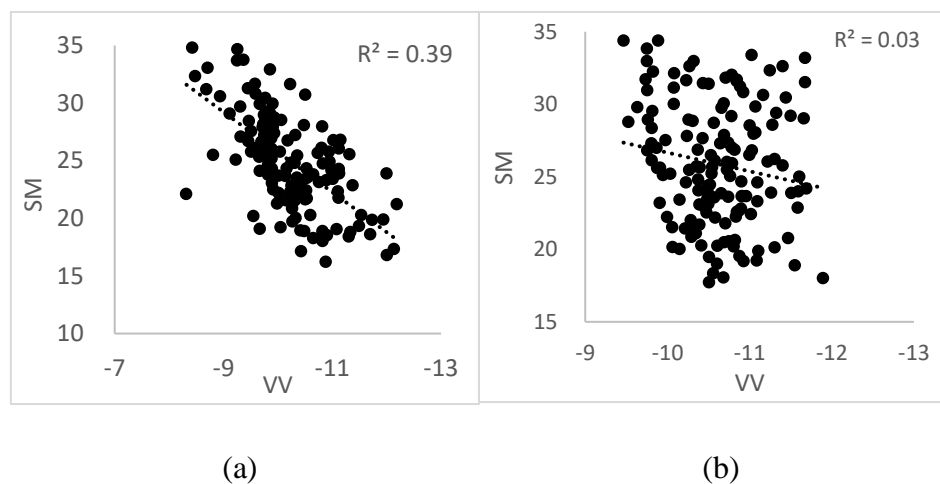


Figure 6.23 Relationship between radar signal (VV and VH polarization) and RVI at maturity (a) and yield (b) stage of tomato field

Sugarcane field

Sugarcane crop cycle is divided into four crop stages namely, vegetative, growing, grand growing and yield stage. The relationship between field measured surface soil moisture and backscattered energy (VV) and (VH) at each crop stage of paddy is analysed and presented in Figure 6.24 and Figure 6.25. Sugarcane fields showed backscattered energy dependence on surface soil moisture dependence is reduced as the crop passes to growing stages.



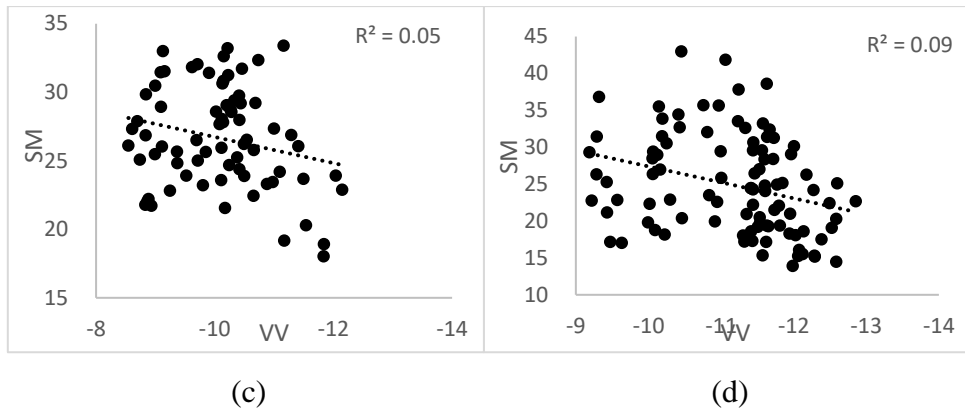


Figure 6.24 Relationship between soil moisture and radar signal VV polarization at early growth (a) vegetative (b) grand growing (c) and yield stage (d) of sugarcane field

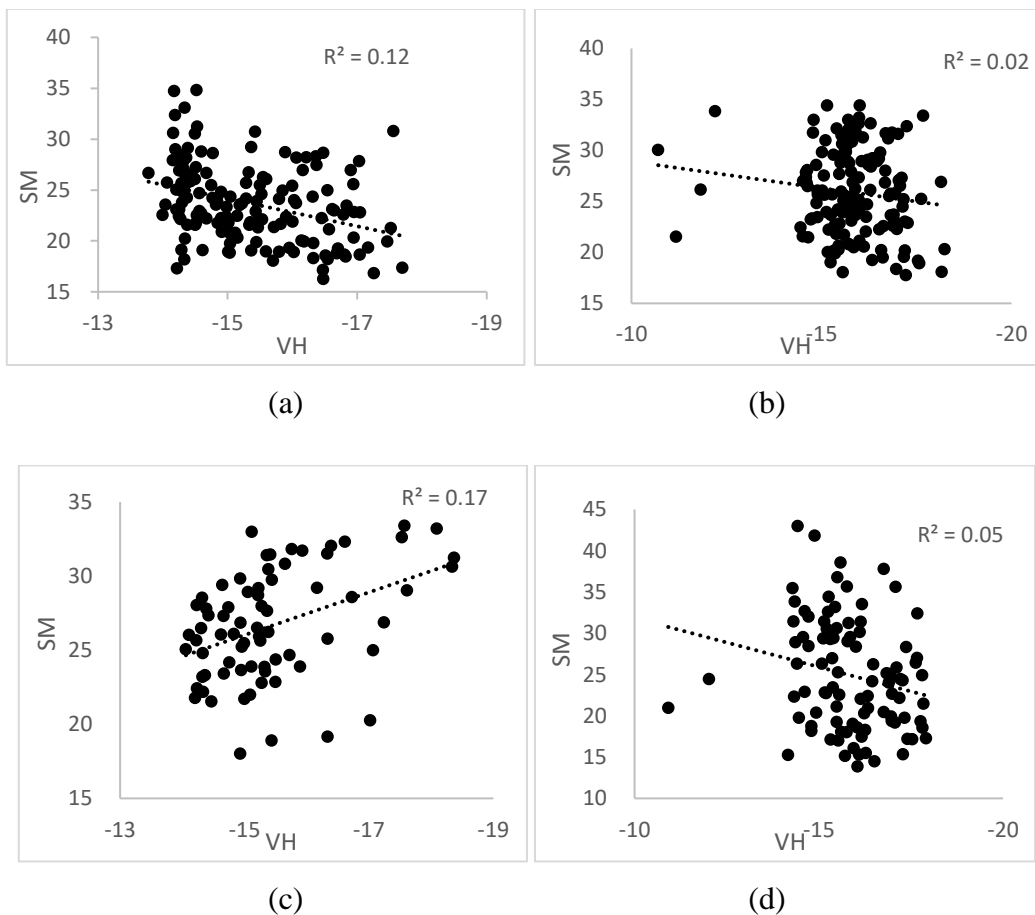


Figure 6.25 Relationship between soil moisture and radar signal VH polarization at early growth (a) vegetative (b) grand growing (c) and yield stage (d) of sugarcane field

The relationship between surface soil moisture and backscattered energy is found only in early growth stage of sugarcane. In case of vegetative, grand growing and maturity stage, it found to be no relationship between C-band SAR backscattered energy and soil moisture. It is because of the C-band SAR has lesser penetration power compared at biomass level or vegetation spread of sugarcane. Figure 6.26 illustrates the relationship between RVI and backscattered energy of VV and VH polarization at early growth stage. Which shows no much dependence between RVI and backscattered energy. Since no relationship found between backscattered energy and soil moisture at vegetative, grand growing and yield stage. The effect of RVI on VV and VH polarization at vegetative, grand growing and yield stage was not considered.

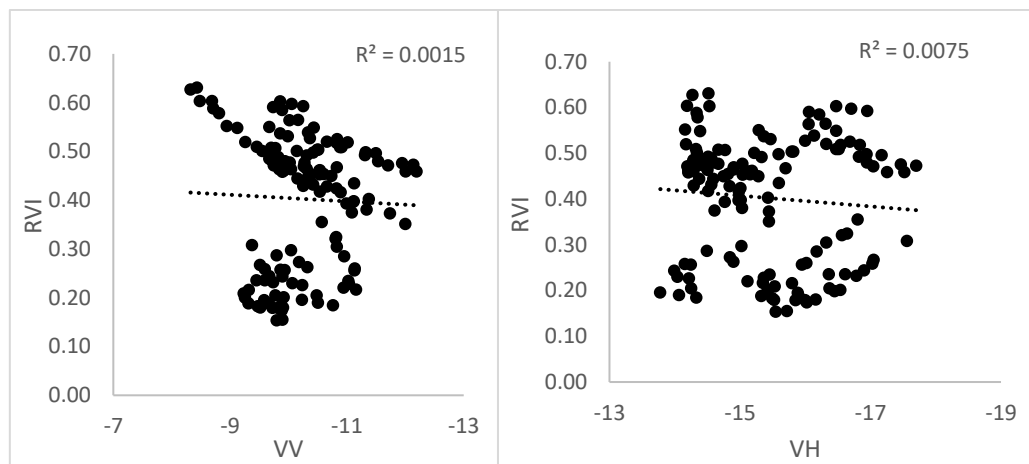


Figure 6.26 Relationship between radar signal (VV and VH polarization) and RVI at Early growth stage of sugarcane.

Bare field

Figure 6.27 illustrates the relationship between surface soil moisture and backscattered energy VV and VH polarization backscattered energy for data acquired from 05/05/2018 to 04/07/2018 at 12-day intervals. It can be seen that the backscattered energy has a clear dependence on soil moisture. The results show that VV polarization soil backscattering coefficient has the highest correlation with the field measured soil moisture. The effect of vegetation on VV and VH polarization is shown in Figure 6.28. Vegetation in bare field corresponds to weeds, and the effect of this vegetation is negligible on polarization channels (Ulaby et al. 1982; Sikdar and Cumming 2004).

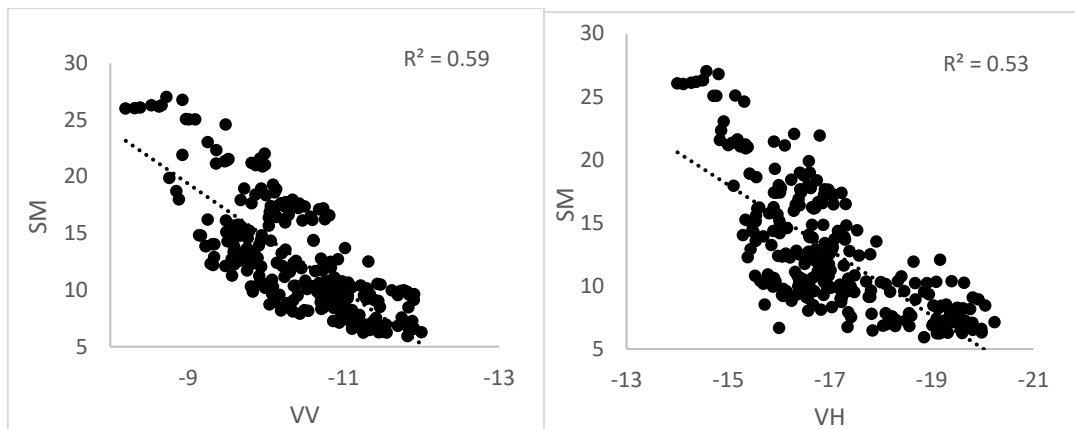


Figure 6.27 Relationship between soil moisture and radar signal VV and VH polarizations of bare field

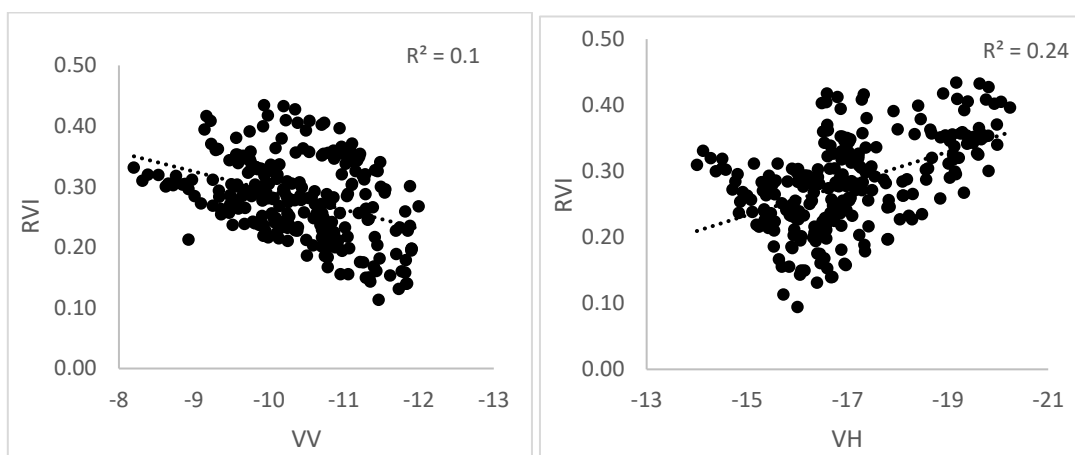


Figure 6.28 Relationship between RVI and radar signal VV and VH polarizations of bare field

6.3.2.2 Semi-empirical modelling

From the regression analysis, we came to know that VV backscattered energy has a good relationship with surface soil moisture. VH backscattered energy showing the effect of vegetation cover on surface soil moisture. The effect of surface roughness is not examined, in the case depolarization ratio is used surface roughness parameter and relation between surface roughness and depolarization ratio is presented in Figure 6.29A to 6.29C. Figure 6.29 shows that only during initial crop stages of Maize and Sugarcane surface roughness affects backscattered energy. Once the crop is grown, the effect of surface roughness is gradually decreased. Major parameters affecting the

sensitivity of backscattered energy are considered to model the surface soil moisture. To model surface soil moisture, multilinear regression analysis is carried out in which soil moisture (M_v) is a dependent variable and σ°_{VV} , $\sigma^{\circ}_{VH} - \sigma^{\circ}_{VV}$ and RVI are considered independent variables. Where σ°_{VV} is function of soil moisture, $\sigma^{\circ}_{VH} - \sigma^{\circ}_{VV}$ is function of surface roughness and RVI is the function of vegetation water content. The developed semi-empirical model of each crop at different crop stages is given in Table 6.5 with adjusted R^2 and confidence interval of 95%.

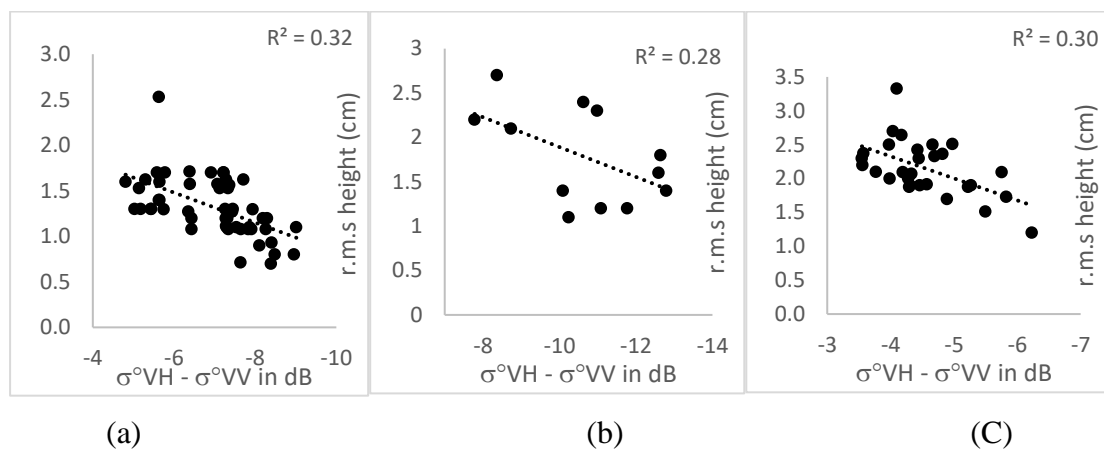


Figure 6.29A Relationship between depolarization ratio and surface roughness height of bare (a), Maize (b) and Sugarcane (c) at vegetative stage.

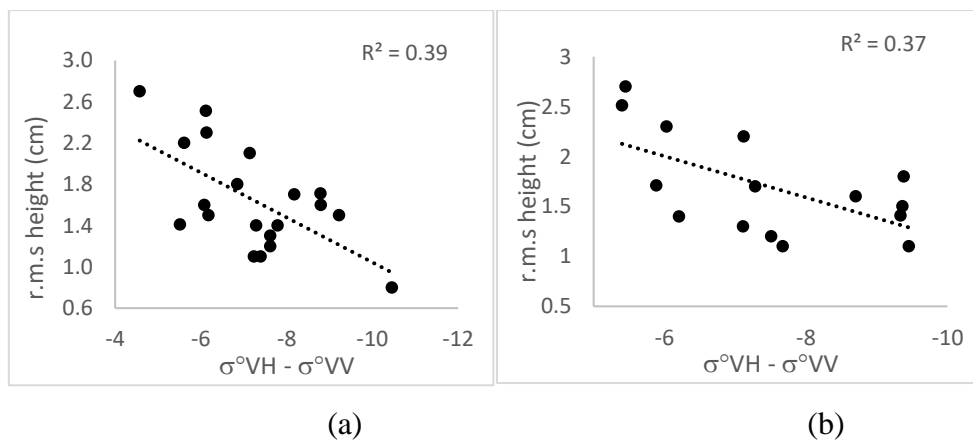


Figure 6.29B Relationship between depolarization ratio and surface roughness height of Tomato at vegetative (a) and maturity stage (b)

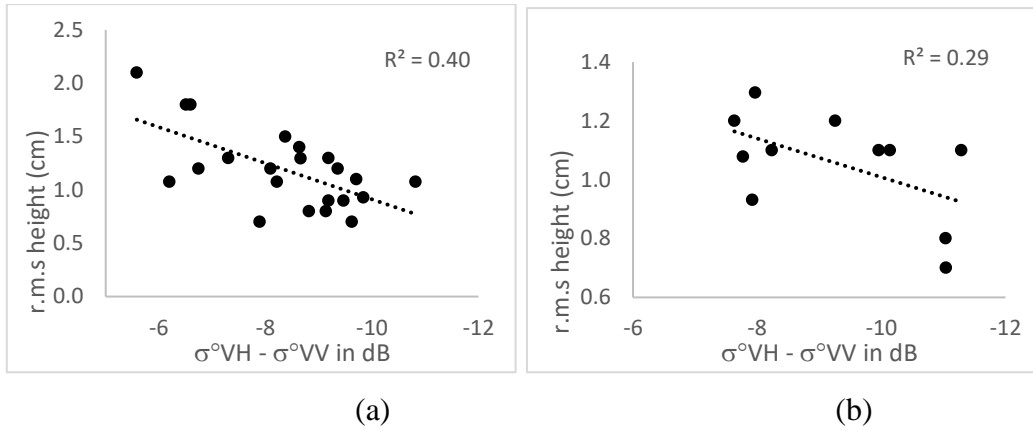


Figure 6.29C Relationship between depolarization ratio and surface roughness height of Paddy at vegetative (a) and maturity stage (b)

Table 6.5 Details of developed Semi-Empirical Model (SEM) at crop stages

Sl. No.	Crop	Crop stage	SEM	Adj. R ²
1	Maize	Seedling	$M_v = 37.06 + 2.04\sigma_{VV}^\circ + 0.15\sigma_{VH-VV}^\circ$	0.66
		Vegetative	$M_v = 27.74 + 1.71\sigma_{VV}^\circ - 0.46\sigma_{VH-VV}^\circ + 5.7RVI$	0.5
		Yield	$M_v = 63.2 + 3.72\sigma_{VV}^\circ - 28.24RVI$	0.35
2	Paddy	Vegetative	$M_v = 59.7 + 3.54\sigma_{VV}^\circ - 0.13\sigma_{VH-VV}^\circ$	0.57
		Maturity	$M_v = 51.1 + 4.48\sigma_{VV}^\circ - 0.83\sigma_{VH-VV}^\circ + 24.3RVI$	0.62
		Yield	$M_v = 49.43 + 3.12\sigma_{VV}^\circ + 12.83RVI$	0.4
3	Tomato	Vegetative	$M_v = 44.66 + 2.04\sigma_{VV}^\circ + 0.15\sigma_{VH-VV}^\circ$	0.63
		Maturity	$M_v = 39.02 + 3.1\sigma_{VV}^\circ - 0.12\sigma_{VH-VV}^\circ + 25.38RVI$	0.62
		Yield	$M_v = 71.1 + 5.7\sigma_{VV}^\circ - 11.07RVI$	0.54
4	Sugarcane	Early growth	$M_v = 61.63 + 3.6\sigma_{VV}^\circ - 0.33\sigma_{VH-VV}^\circ$	0.45
5	Bare field	----	$M_v = 39.8 + 1.8\sigma_{VV}^\circ - 0.17\sigma_{VH-VV}^\circ$	0.8

The relationship between surface soil moisture and backscattered energy is very poor for sugarcane at growing, grand growing and yield formation stage. So, semi-empirical model is not developed. This is because vegetation density affects the penetration capability of dual-polarized C-band SAR data.

6.3.2.3 Validation

The developed model is validated and compared with existing model soil moisture estimates. From the study, SEM is observed performing well compared to the other two models in vegetative and maturity crop stages. In case yield formation stage WCM is performing well. None of the models performing well in yield stage of sugarcane. The validation results of surface soil models is given in Table 6.6.

Table 6.6 Validation results of surface soil moisture models of C-band SAR

Crop	Crop stage	Vegetative		Maturity		Yield	
		Model\statistics	RMSE	AE _{max}	RMSE	AE _{max}	RMSE
Maize	Oh model 2004	2.6	2.71	3.42	5.91	4.6	7.17
	WCM	2.37	2.68	3.35	5.7	4.11	6.6
	SEM	2.24	2.63	3.06	5.18	4.24	6.84
Paddy	Oh model 2004	2.6	3.31	4.7	6.04	4.2	5.1
	WCM	2.23	3.02	4.37	5.56	3.92	4.15
	SEM	2.1	2.71	4.25	5.4	3.66	4.44
Tomato	Oh model 2004	2.24	2.96	3.2	4.31	3.39	4.96
	WCM	2.07	2.57	2.92	4.18	3.34	4.8
	SEM	1.8	2.42	2.89	4.12	3.12	4.73
Sugarcane	Oh model 2004	3.65	5.81	NA			
	WCM	3.22	5.31				
	SEM	3.17	5.4				
Bare field	Oh model 2004	2.14	3.42	NA			
	WCM	2.1	3.18				
	SEM	1.93	3.2				

*RMSE=Root Mean Square error (% g/cm³/g/cm³); AE_{max}= Maximum Absolute Error (% g/cm³)

6.4 COMPARISON OF QUAD AND DUAL-POL SURFACE SOIL MOISTURE

The soil moisture estimates of C-band dual-pol SAR are compared with L-band quad-pol SAR at two crop stages. It is observed that soil moisture errors are similar for both C-band dual pol and L- band quad-pol SAR at the vegetative stage of paddy, tomato and maize crop. Hence, dual-pol SAR can be used to retrieve soil moisture in vegetative stage of these crops. Whereas in case of maturity and yield stage, L-band quad-pol SAR soil moisture estimates are better than C-band dual-pol SAR moisture estimates. Both C and L-band showed poor efficiency in retrieving surface soil moisture at vegetative, grand growth and yield stage of Sugarcane.

The upcoming chapter presents the summary, major conclusions, limitations and future scope of the work.

SUMMARY AND CONCLUSIONS

7.1 SUMMARY

The primary objective of the study is to retrieve surface soil moisture over agricultural plots at different crop stages using active microwave remote sensing. To accomplish this, an extensive literature review was conducted, focusing on popular soil moisture retrieval models for both bare and vegetated fields. The work is demonstrated utilizing quad-pol ALOS PALSAR-2 and dual-pol Sentinel-1a to retrieve surface soil moisture from various agricultural plots at different crop stages. The research work was carried out in Malavalli, Mandya region of Karnataka, India. Firstly four different crops (Paddy, Sugarcane, Maize and Tomato) which are pre-dominantly grown in this region were selected along with a bare field. Systematic gridded soil sampling was carried out for entire crop cycle in synchronized with satellite pass over study area. These samples were transported into labs and conducted experiment (according IS 1605) to calculate soil moisture, bulk density and vegetation water content. The crop cycle of each crop was divided into seedling/vegetative, maturity and harvesting stage to retrieve surface soil moisture using L and C band SAR data at different crop stages. ALOS PALSAR-2 and Sentinel-1a SAR data was pre-processed, speckles were removed using suitable filter and geocoded.

SAR based surface soil moisture models like Oh-1992, Oh-2004, X-Bragg and Water Cloud Model (WCM) were used to retrieve surface soil moisture of each crop at different crop stages. A Semi Empirical Model (SEM) was also developed based on parameters affecting backscattered energy using Multi Linear Regression (MLR) analysis for each crop stage. Comparison between existing and developed SEM is carried using field data. In the meantime, study also concentrated on the C and L-band SAR capability in retrieving surface soil moisture beneath different crop cover and crop stage.

Various factors, including small agricultural land (less than two acres), inability to manage advanced technological equipment due to financial constraints, and a lack of technical knowledge among farmers, are driving a decline in awareness of sustainable utilization of irrigation water and precision agriculture in many underdeveloped and developing countries, including India. Under such a condition, this study is helpful in understanding the spatio-temporal soil moisture variation within the field derived from space-borne sensors to marginal farmers and policy makers for better supply of irrigation water.

7.2 CONCLUSIONS

Objective 1: To investigate the surface soil moisture variation across crop stages and crops in semi-arid tropical region.

- Temporal surface soil moisture of sugarcane is almost uniform all over its crop cycle, no much change is observed (~5%). Overall, temporal variation of surface soil moisture in each field is high during the initial cropping stage and comparatively less during the yield/harvesting stage.
- It is observed higher surface soil moisture content in side walls of agricultural plots compared with central part of agricultural land spatially. Whereas in case of paddy fields soil moisture is almost uniform spatially apart from few random dry patches and water stagnation near field inlet and outlets

Objective 2: To develop surface soil moisture model and comparison of its performance with existing models.

- It is found that the correlation between the surface scattering component of the Yamaguchi technique ($R^2=0.82\sim 0.5$) is more than other surface scattering component (Freeman-Durden and Van Zyl) and individual polarized data of Maize, Paddy, Sugarcane, Tomato and Bare fields.
- Developed semi empirical model based on polarization decomposition and backscattered energy is performing better than all other models. Quad-pol, X-Bragg model is underestimating surface soil moisture of paddy, maize, tomato and sugarcane field plots.

- Dual-pol surface soil moisture models are performing well in initial crop stages like vegetative and maturity stage. Whereas, in yield formation stage of maize and paddy error is comparatively high.

Objective 3: To study the potential of dual and quad-pol SAR data in surface soil moisture retrieval over heterogeneous agricultural plots.

- In comparison between C-band dual-pol data and L-band quad-pol data, dual-pol data can be used to estimate moisture at initial crop stages but as vegetation density increases quad-pol L band SAR is more suitable.
- None of the soil moisture models, SAR band and polarizations (dual and quad) performed well in case of sugarcane field in the grand growing and yield stage ($R^2=0.1$). Since vegetation attenuation is more and SAR penetration is limited. In case of bare fields, soil moisture estimates are within acceptable limits irrespective of polarization and SAR band.

7.3 LIMITATIONS OF THE WORK

The surface soil moisture range obtained is adequate information for future soil moisture estimates. However, the study has been limited by small sample size. For adequate information on the spatial variability in the small-size farm, a design to increase the number of the sample grids and crops must be carried out. The developed regression models are limited well within the range of field values collected, this can be further explained by optimization techniques as well as more field values.

7.4 SCOPE FOR THE FUTURE WORK

- In future, this developed models can be refined into single model irrespective of crop type and its stages by developing look up tables for each crop. Hence this model can be scalable to wide region.
- Future research may also concentrate on effect of SAR incidence angle on developed surface soil moisture models.

- This study is narrowed down to one agricultural site of each crop this can be verified with some other test sites where surface soil moisture variation is different.
- In this research, RMSE and AE_{\max} are used for the evaluation of model performance; other statistical parameters can be considered. The uncertainty analysis involved due to the choice of calibration set, georeferencing errors, and laboratory reference values could also be studied

REFERENCES

- Al-Bakri, J., Suleiman, A., and Berg, A. (2014). "A comparison of two models to predict soil moisture from remote sensing data of RADARSAT II". *Arab. J. Geosci.*, 7(11), 4851-4860.
- Altese, E., Bolognani, O., Mancini, M., and Troch, P. A. (1996), "Retrieving soil moisture over bare soil from ERS 1 Synthetic Aperture Radar data: Sensitivity analysis based on a theoretical surface scattering model and field data", *Water Resour. Res.*, 32(3), 653– 661.
- Attema, E. P. W., and Ulaby, F. T. (1978). "Vegetation modeled as a water cloud". *Radio sci.*, 13(2), 357-364.
- Bach, H., and Mauser, W. (2003). "Methods and examples for remote sensing data assimilation in land surface process modeling". *IEEE Trans. Geosci. Remote Sens.*, 41(7), 1629-1637.
- Baghdadi, N., and Zribi, M. (2006). "Evaluation of radar backscatter models IEM, OH and Dubois using experimental observations". *Int. J. Remote Sens.*, 27(18), 3831-3852.
- Baghdadi, N., Cerdan, O., Zribi, M., Auzet, V., Darboux, F., El Hajj, M., and Kheir, R. B. (2008). "Operational performance of current synthetic aperture radar sensors in mapping soil surface characteristics in agricultural environments: application to hydrological and erosion modelling". *Hydrol. Process.*, 22(1), 9-20.
- Baghdadi, N., El Hajj, M., Zribi, M., and Bousbih, S. (2017). "Calibration of the water cloud model at C-band for winter crop fields and grasslands". *Remote Sens.*, 9(9), 969.
- Baghdadi, N., Gherboudj, I., Zribi, M., Sahebi, M., King, C., and Bonn, F. (2004). "Semi-empirical calibration of the IEM backscattering model using radar images and moisture and roughness field measurements". *Int. J. Remote Sens.*, 25(18), 3593-3623.

Baghdadi, N., King, C., Chanzy, A., and Wigneron, J. P. (2002). “An empirical calibration of the integral equation model based on SAR data, soil moisture and surface roughness measurement over bare soils”. *Int. J. Remote Sens.*, 23(20), 4325-4340.

Baghdadi, N., Saba, E., Aubert, M., Zribi, M. and Baup, F. (2011). “Evaluation of Radar Backscattering Models IEM, Oh, and Dubois for SAR Data in X-Band Over Bare Soils”. *IEEE Geosci. Remote Sens. Lett.*, 8(6), 1160–1164.

Baghdadi, N., Saba, E., Aubert, M., Zribi, M., and Baup, F. (2011). “Comparison between backscattered TerraSAR signals and simulations from the radar backscattering models IEM, Oh, and Dubois”. *IEEE Geosci. Remote Sens. Lett.*, 6(8), 1160.

Bai, X., He, B., and Li, X. (2015). “Optimum surface roughness to parameterize advanced integral equation model for soil moisture retrieval in prairie area using Radarsat-2 data”. *IEEE Trans. Geosci. Remote Sens.*, 54(4), 2437-2449.

Bai, X., He, B., Xing, M., and Li, X. (2015). “Method for soil moisture retrieval in arid prairie using TerraSAR-X data”. *J. Appl. Remote Sens.*, 9(1), 096062.

Balenzano, A., Satalino, G., Lovergine, F., Rinaldi, M., Iacobellis, V., Mastronardi, N., and Mattia, F. (2013). “On the use of temporal series of L-and X-band SAR data for soil moisture retrieval. Capitanata plain case study”. *Eur. J. Remote Sens.*, 46(1), 721-737.

Barrett, B. W., Dwyer, E., and Whelan, P. (2009). “Soil moisture retrieval from active spaceborne microwave observations: An evaluation of current techniques”. *Remote Sens.*, 1(3), 210-242.

Barrett, B., Whelan, P., and Dwyer, E. (2013). “Detecting changes in surface soil moisture content using differential SAR interferometry”. *Int. J. Remote Sens.*, 34(20), 7091-7112.

Baup, F., Mougin, E., de Rosnay, P., Timouk, F., and Chênerie, I. (2007). “Surface soil moisture estimation over the AMMA Sahelian site in Mali using ENVISAT/ASAR data”. *Remote Sens. Environ.*, 109(4), 473-481.

- Bertoldi, G., Della Chiesa, S., Notarnicola, C., Pasolli, L., Niedrist, G., and Tappeiner, U. (2014). "Estimation of soil moisture patterns in mountain grasslands by means of SAR RADARSAT2 images and hydrological modeling". *J. Hydrol.*, 516, 245-257.
- Bhogapurapu, N., Dey, S., Mandal, D., Bhattacharya, A., Karthikeyan, L., McNairn, H., and Rao, Y. S. (2022). "Soil moisture retrieval over croplands using dual-pol L-band GRD SAR data". *Remote Sens. Environ.*, 271, 112900.
- Bindlish, R., and Barros, A. P. (2000). "Multifrequency soil moisture inversion from SAR measurements with the use of IEM". *Remote Sens. Environ.*, 71(1), 67-88.
- Bindlish, R., and Barros, A. P. (2001). "Parameterization of vegetation backscatter in radar-based, soil moisture estimation". *Remote Sens. Environ.*, 76(1), 130-137.
- Boisvert, J. B., Gwyn, Q. H. J., Chanzy, A., Major, D. J., Brisco, B., and Brown, R. J. (1997). "Effect of surface soil moisture gradients on modelling radar backscattering from bare fields". *Int. J. Remote Sens.*, 18(1), 153-170.
- Borgeaud, M., and Noll, J. (1994). "Analysis of theoretical surface scattering models for polarimetric microwave remote sensing of bare soils". *Int. J. Remote Sens.*, 15(14), 2931-2942.
- Bourgeau-Chavez, L. L., Kasischke, E. S., Riordan, K., Brunzell, S., Nolan, M., Hyer, E., and Ames, S. (2007). "Remote monitoring of spatial and temporal surface soil moisture in fire disturbed boreal forest ecosystems with ERS SAR imagery". *Int. J. Remote Sens.*, 28(10), 2133-2162.
- Bousbih, S., Zribi, M., Mougenot, B., Fanise, P., Lili-Chabaane, Z., and Baghdadi, N. (2018). "Monitoring of surface soil moisture based on optical and radar data over agricultural fields". In *4th International Conference on Advanced Technologies for Signal and Image Processing, IEEE (ATSIP)*, 1-5.
- Carlson, T. N., Gillies, R. R., and Schmugge, T. J. (1995). "An interpretation of methodologies for indirect measurement of soil water content". *Agric. For. Meteorol.*, 77(3-4), 191-205.

Champion, I., (1996). "Simple modelling of radar backscattering coefficient over a bare soil: Variation with incidence angle, frequency and polarization". *Int. J. Remote Sens.* 17, 783:800.

Chen, L., Xing, M., He, B., Wang, J., Xu, M., Song, Y., and Huang, X. (2022). "Estimating soil moisture over winter wheat fields during growing season using RADARSAT-2 data". *Remote Sens.*, 14(9), 2232.

Choker, M., Baghdadi, N., Zribi, M., El Hajj, M., Paloscia, S., Verhoest, N. E., and Mattia, F. (2017). "Evaluation of the Oh, Dubois and IEM backscatter models using a large dataset of SAR data and experimental soil measurements". *Water*, 9(1), 38.

Choudhury, B. J., Schmugge, T. J., Chang, A., and Newton, R. W. (1979). "Effect of surface roughness on the microwave emission from soils". *J. Geophys. Res. Oceans*, 84(C9), 5699-5706.

Das, K., and Paul, P. K. (2015). "Soil moisture retrieval model by using RISAT-1, C-band data in tropical dry and sub-humid zone of Bankura district of India". *Egypt. J. Remote Sens. Space Sci.*, 18(2), 297-310.

Dash, S., and Prusty, G. (2007). "Simulation of radar backscattering coefficients using IEM-A tool for surface soil moisture retrieval". In *3rd International Conference on Recent Advances in Space Technologies*, IEEE, 383-388.

Dave, R., Kumar, G., Kr. Pandey, D., Khan, A. and Bhattacharya, B. (2019). "Evaluation of modified Dubois model for estimating surface soil moisture using dual polarization RISAT-1 C-band SAR data". *Geocarto Int.*, 1–11.

De Jeu, R. A. (2003). "Retrieval of land surface parameters using passive microwave remote sensing". PhD dissertation, *Vrije Universiteit*, Amsterdam.

De Roo, R. D., Du, Y., Ulaby, F. T., and Dobson, M. C. (2001). "A semi-empirical backscattering model at L-band and C-band for a soybean canopy with soil moisture inversion". *IEEE Trans. Geosci. Remote Sens.*, 39(4), 864-872.

- Della Vecchia, A., Ferrazzoli, P., Wigneron, J. P., and Grant, J. P. (2007). "Modeling forest emissivity at L-band and a comparison with multitemporal measurements". *IEEE Geosci. Remote Sens. Lett.*, 4(4), 508-512.
- Dobson, M. C., Ulaby, F. T., Hallikainen, M. T., & El-Rayes, M. A. (1985). "Microwave dielectric behavior of wet soil-Part II: Dielectric mixing models". *IEEE Trans. Geosci. Remote Sens.*, (1), 35-46.
- Dubois, P. C., Van Zyl, J., and Engman, T. (1995). "Measuring soil moisture with imaging radars". *IEEE Trans. Geosci. Remote Sens.*, 33(4), 915-926.
- El Hajj, M., Baghdadi, N., and Zribi, M. (2019). "Comparative analysis of the accuracy of surface soil moisture estimation from the C-and L-bands". *Int. J. Appl. Earth Obs. Geoinf.*, 82, 101888.
- El Hajj, M., Baghdadi, N., Zribi, M., and Bazzi, H. (2017). "Synergic use of Sentinel-1 and Sentinel-2 images for operational soil moisture mapping at high spatial resolution over agricultural areas". *Remote Sens.*, 9(12), 1292.
- El Hajj, M., Baghdadi, N., Zribi, M., Belaud, G., Cheviron, B., Courault, D., and Charron, F. (2016). "Soil moisture retrieval over irrigated grassland using X-band SAR data". *Remote Sens. Environ.*, 176, 202–218.
- Engman, E. T. (1992). "Soil moisture needs in Earth sciences". In Proceedings of *IEEE Int. Geosci. Remote Sens. Symposium (IGARSS)*, 27–47.
- Engman, E. T. and Wang, J.R. (1987). "Evaluating Roughness Models of Radar Backscatter". *IEEE Trans. Geosci. Remote Sens.*, GE-25(6), 709–713.
- Engman, E. T., and Chauhan, N. (1995). "Status of microwave soil moisture measurements with remote sensing". *Remote Sens. Environ.*, 51(1), 189-198.
- Ezzahar, J., Ouaadi, N., Zribi, M., Elfarkh, J., Aouade, G., Khabba, S., ... and Jarlan, L. (2019). "Evaluation of backscattering models and support vector machine for the retrieval of bare soil moisture from Sentinel-1 data". *Remote Sens.*, 12(1), 72.

Fan, D., Zhao, T., Jiang, X., Xue, H., Moukomla, S., Kuntiyawichai, K., and Shi, J. (2021). “Soil moisture retrieval from Sentinel-1 time-series data over croplands of northeastern Thailand”. *IEEE Geosci. Remote. Sens. Lett.*, 19, 1-5.

Fieuzal, R. and Baup, F. (2016) “Improvement of Bare Soil Semi-Empirical Radar Backscattering Models (Oh and Dubois) with SAR Multi-Spectral Satellite Data (X-, C- and L-Bands)”. *Adv. Remote Sens.*, 5, 296-314.

Fung, A. K., Li, Z., and Chen, K. S. (1992). “Backscattering from a randomly rough dielectric surface”. *IEEE Trans. Geosci. Remote Sens.*, 30(2), 356-369.

Garg, A., Munoth, P., and Goyal, R. (2016). “Application of soil moisture sensors in agriculture: A review. Calibration of VH400 soil moisture sensors view project”. *Water Resour. Coast Eng.*, 21, 1662–1672.

Ghafouri, A., Amini, J., Dehmollaian, M., and Kavooosi, M. A. (2017). “Better estimated IEM input parameters using random fractal geometry applied on multi-frequency SAR data”. *Remote Sens.*, 9(5), 445.

Gharechelou, S., Tateishi, R., Sri Sumantyo, J. T., and Johnson, B. A. (2021). “Soil Moisture Retrieval Using Polarimetric SAR Data and Experimental Observations in an Arid Environment”. *ISPRS Int. J. Geoinf.*, 10(10), 711.

Guo, P., Shi, J., Liu, Q., and Du, J. (2013). “A new algorithm for soil moisture retrieval with L-band radiometer”. *IEEE J. Sel. Top. Appl. Earth Obs. Remote Sens.*, 6(3), 1147-1155.

Gupta, M., Srivastava, P. K., and Islam, T. (2016). “Integrative use of near-surface satellite soil moisture and precipitation for estimation of improved irrigation scheduling parameters”. In *Satellite Soil Moisture Retrieval*, Elsevier, 271-288.

Hajnsek, I., Cloude, S. R., Lee, J. S., and Pottier, E. (2000). “Inversion of surface parameters from polarimetric SAR data”. In *IGARSS 2000. IEEE 2000 International Geoscience and Remote Sensing Symposium. Taking the Pulse of the Planet: The Role of Remote Sensing in Managing the Environment. Proceedings (Cat. No. 00CH37120)*, 3, 1095-1097

- Hajnsek, I., Jagdhuber, T., Schon, H., Papathanassiou, K.P. (2009). "Potential of estimating soil moisture under vegetation cover by means of PolSAR". *IEEE Trans Geosci Remote Sens.* 47(2), 442–454.
- Hajnsek, I., Pottier, E., and Cloude, S. R. (2003). "Inversion of surface parameters from polarimetric SAR". *IEEE Trans. Geosci. Remote Sens.*, 41(4), 727-744.
- Haldar, D., Dave, R., and Dave, V. A. (2018). "Evaluation of full-polarimetric parameters for vegetation monitoring in rabi (winter) season". *Egyptian J. Remote Sens. Space Sci*, 21, S67-S73.
- Hallikainen, M. (2014). "Microwave Dielectric Properties of Materials". In: Njoku, E.G. (eds) *Encyclopedia of Remote Sensing*. Encyclopedia of Earth Sciences Series. Springer, New York, NY. https://doi.org/10.1007/978-0-387-36699-9_100.
- Hallikainen, M. T., Ulaby, F. T., Dobson, M. C., El-Rayes, M. A., and Wu, L. K. (1985). "Microwave dielectric behavior of wet soil-part 1: Empirical models and experimental observations". *IEEE Trans. Geosci. Remote Sens.*, (1), 25-34.
- Han, D., Vahedifard, F. and Aanstoos, J. V. (2017). "Investigating the correlation between radar backscatter and in situ soil property measurements". *Int. J. Appl. Earth Obs. Geoinf.*, 57,136- 144.
- Hassan, Q. K., Bourque, C. P. A., Meng, F. R., and Cox, R. M. (2007). "A wetness index using terrain-corrected surface temperature and normalized difference vegetation index derived from standard MODIS products: an evaluation of its use in a humid forest-dominated region of eastern Canada". *Sensors*, 7(10), 2028-2048.
- Holah, N., Baghdadi, N., Zribi, M., Bruand, A., and King, C. (2005). "Potential of ASAR/ENVISAT for the characterization of soil surface parameters over bare agricultural fields". *Remote Sens Environ.*, 96(1), 78-86.
- Hosseini, M., and McNairn, H. (2017). "Using multi-polarization C-and L-band synthetic aperture radar to estimate biomass and soil moisture of wheat fields". *Int. J. Appl. Earth Obs. Geoinf.*, 58, 50-64.

Houser, P. R., Shuttleworth, W. J., Famiglietti, J. S., Gupta, H. V., Syed, K. H., and Goodrich, D. C. (1998). "Integration of soil moisture remote sensing and hydrologic modeling using data assimilation". *Water Resour.*, 34(12), 3405-3420.

Huang, S., Ding, J., Zou, J., Liu, B., Zhang, J., and Chen, W. (2019). "Soil moisture retrieval based on sentinel-1 imagery under sparse vegetation coverage". *Sensors*, 19(3), 589.

Ji, J., Skriver, H. and Gudmandsen, P., (1995). "Estimation of soil moisture from the MAESTRO-1 SAR data of Flevoland". *Proceedings of Sensor and Environmental Applications of Remote Sensing*, 103–110.

Joseph, A. T., van der Velde, R., O'Neill, P. E., Lang, R., and Gish, T. (2010). "Effects of corn on C-and L-band radar backscatter: A correction method for soil moisture retrieval". *Remote Sens. Environ.*, 114(11), 2417-2430.

Kerr, Y. H., Wigneron, J. P., Al Bitar, A., Mialon, A., and Srivastava, P. K. (2016). "Soil moisture from space: Techniques and limitations". In *Satellite Soil Moisture Retrieval Elsevier*, 3-27.

Khabazan, S., Motagh, M. and Hosseini, M. (2013). "Evaluation of Radar Backscattering Models IEM, OH, and Dubois using L and C-Bands SAR Data over different vegetation canopy covers and soil depths". *Int. Arch. Photogramm. Remote Sens. Spat. Inf. Sci.*, XL-1/W3, 225-230.

Kim, S. B., Van Zyl, J. J., Johnson, J. T., Moghaddam, M., Tsang, L., Colliander, A. ... and Yueh, S. H. (2017). "Surface soil moisture retrieval using the L-band synthetic aperture radar onboard the soil moisture active-passive satellite and evaluation at core validation sites". *IEEE Trans. Geosci. Remote Sens.*, 55(4), 1897-1914.

Kim, S., Liu, Y. Y., Johnson, F. M., Parinussa, R. M., and Sharma, A. (2015). "A global comparison of alternate AMSR2 soil moisture products: Why do they differ?". *Remote Sens. Environ.*, 161, 43-62.

Kornelsen, K. C., and Coulibaly, P. (2013). "Advances in soil moisture retrieval from synthetic aperture radar and hydrological applications". *J. Hydrol.*, 476, 460-489.

- Koyama, C. N., Korres, W., Fiener, P., and Schneider, K. (2010). “Variability of surface soil moisture observed from multitemporal C-band synthetic aperture radar and field data”. *Vadose Zone J.*, 9(4), 1014-1024.
- Kumar, K., Suryanarayana Rao, H. P., and Arora, M. K. (2015). “Study of water cloud model vegetation descriptors in estimating soil moisture in Solani catchment”. *Hydrol. Process.*, 29(9), 2137-2148.
- Kumar, P., Prasad, R., Choudhary, A., Gupta, D. K., Mishra, V. N., Vishwakarma, A. K., ... and Srivastava, P. K. (2019). “Comprehensive evaluation of soil moisture retrieval models under different crop cover types using C-band synthetic aperture radar data”. *Geocarto Int.*, 34(9), 1022-1041.
- Li, J., and Wang, S. (2018). “Using SAR-derived vegetation descriptors in a water cloud model to improve soil moisture retrieval”. *Remote Sens.*, 10(9), 1370.
- Liao, C., Wang, J., Shang, J., Huang, X., Liu, J., and Huffman, T. (2018). “Sensitivity study of Radarsat-2 polarimetric SAR to crop height and fractional vegetation cover of corn and wheat”. *Int. J. Remote Sens.*, 39(5), 1475-1490.
- Lievens, H., Verhoest, N. E. C., De Keyser, E., Vernieuwe, H., Matgen, P., Álvarez-Mozos, J., and De Baets, B. (2011). “Effective roughness modelling as a tool for soil moisture retrieval from C- and L-band SAR”. *Hydrol. Earth Syst. Sci.*, 15, 151–162.
- MacDonald, J. M., Korb, P., and Hoppe, R. A. (2013). “Farm size and the organization of U.S. crop farming,” *Tech. Rep. ERR-152*, US Department of Agriculture, Economic Research Service, Washington, DC, USA.
- McLaughlin, D. (1995). “Recent developments in hydrologic data assimilation”. *Rev. Geophys.*, 33(S2), 977-984.
- Meyer, T., Weihermüller, L., Vereecken, H., and Jonard, F. (2018). “Vegetation optical depth and soil moisture retrieved from L-band radiometry over the growth cycle of a winter wheat”. *Remote sens.*, 10(10), 1637.

- MirMazloumi, S. M., and Sahebi, M. R. (2016). "Assessment of different backscattering models for bare soil surface parameters estimation from SAR data in band C, L and P". *Eur. J. Remote Sens.*, 49(1), 261-278.
- Mo, T., Choudhury, B. J., Schmugge, T. J., Wang, J. R., and Jackson, T. J. (1982). "A model for microwave emission from vegetation-covered fields". *J. Geophys. Res. Oceans*, 87(C13), 11229-11237.
- Narayanan, R. M., and Hegde, M. S. (2000). "Soil moisture estimation using combined multifrequency SAR data: A comparison between two inversion models using simulation". *Geocarto Int.*, 15(3), 65-76.
- Narayanan, R. M., and Hirsave, P. P. (2001). "Soil moisture estimation models using SIR-C SAR data: a case study in New Hampshire, USA". *Remote Sens. Environ.*, 75(3), 385-396.
- Narvekar, P. S., Entekhabi, D., Kim, S. B., and Njoku, E. G. (2015). "Soil moisture retrieval using L-band radar observations". *IEEE Trans. Geosci. Remote Sens.*, 53(6), 3492-3506.
- Neusch, T., and Sties, M. (1999). "Application of the Dubois-model using experimental synthetic aperture radar data for the determination of soil moisture and surface roughness". *ISPRS J. Photogramm. Remote Sens.*, 54(4), 273-278.
- Njoku, E. G., and Entekhabi, D. (1996). "Passive microwave remote sensing of soil moisture". *J. Hydrol*, 184(1-2), 101-129.
- Njoku, E. G., Wilson, W. J., Yueh, S. H., and Rahmat-Samii, Y. (2000). "A large-antenna microwave radiometer-scatterometer concept for ocean salinity and soil moisture sensing". *IEEE Trans. Geosci. Remote Sens.*, 38(6), 2645-2655.
- Notarnicola, C., Angiulli, M., and Posa, F. (2006). "Use of radar and optical remotely sensed data for soil moisture retrieval over vegetated areas. *IEEE Trans. Geosci. Remote Sens.*, 44(4), 925-935.

- Oh, Y. (2004). "Quantitative retrieval of soil moisture content and surface roughness from multipolarized radar observations of bare soil surfaces". *IEEE Trans. Geosci. Remote Sens.*, 42(3), 596-601.
- Oh, Y., Sarabandi, K., and Ulaby, F. T. (1992). "An empirical model and an inversion technique for radar scattering from bare soil surfaces". *IEEE Trans. Geosci. Remote Sens.*, 30(2), 370-381.
- Ouellette, J. D., Johnson, J. T., Balenzano, A., Mattia, F., Satalino, G., Kim, S. B., ... and Berg, A. A. (2017). "A time-series approach to estimating soil moisture from vegetated surfaces using L-band radar backscatter". *IEEE Trans. Geosci. Remote Sens.*, 55(6), 3186-3193.
- Owe, M., de Jeu, R., and Walker, J. (2001). "A Methodology for surface soil moisture and vegetation optical depth retrieval using the microwave polarization difference index". *IEEE Trans. Geosci. Remote Sens.*, 39(8), 1643-1654.
- Paloscia, S., Pettinato, S., Santi, E., Notarnicola, C., Pasolli, L., and Reppucci, A. J. R. S. O. E. (2013). "Soil moisture mapping using Sentinel-1 images: Algorithm and preliminary validation". *Remote Sens. Environ.*, 134, 234-248.
- Panciera, R., Tanase, M. A., Lowell, K., and Walker, J. P. (2013). "Evaluation of IEM, Dubois, and Oh radar backscatter models using airborne L-band SAR". *IEEE Trans. Geosci. Remote Sens.*, 52(8), 4966-4979.
- Peng, J., and Loew, A. (2017). "Recent advances in soil moisture estimation from remote sensing". *Water*, 9(7), 530.
- Petropoulos, G. P., Ireland, G. and Barrett, B. (2015). "Surface soil moisture retrievals from remote sensing: status, products and future trends". *Phys. Chem. Earth.*, 83(84), 36– 56.
- Ponnurangam, G. G., & Rao, Y. S. (2017). "Evaluation of different orientation angle distributions within the X-Bragg scattering model for bare soil moisture estimation". *Int. J. Remote Sens.*, 38(15), 4379-4395.

Ponnurangam, G. G., Jagdhuber, T., Hajnsek, I., and Rao, Y. S. (2015). "Soil moisture estimation using hybrid polarimetric SAR data of RISAT-1". *IEEE Trans. Geosci. Remote Sens.*, 54(4), 2033-2049.

Ponnurangam, G.G. and Rao, Y.S. (2011) "Soil moisture mapping using ALOS PALSAR and ENVISAT ASAR data over India," In 3rd *International Asia-Pacific Conference on Synthetic Aperture Radar (AP SAR)*, 1-4

Prakash, R., Singh, D., and Pathak, N. P. (2011). "A fusion approach to retrieve soil moisture with SAR and optical data". *IEEE J. Sel. Top Appl. Earth Obs. Remote Sens.*, 5(1), 196-206.

Pulvirenti, L., Squicciarino, G., Cenci, L., Boni, G., Pierdicca, N., Chini, M., and Campanella, P. (2018). "A surface soil moisture mapping service at national (Italian) scale based on Sentinel-1 data". *Environ. Model. Softw.*, 102, 13-28.

Rawat, K. S., Sehgal, V. K., Pradhan, S., and Ray, S. S. (2018). "Semi-empirical model for retrieval of soil moisture using RISAT-1 C-Band SAR data over a sub-tropical semi-arid area of Rewari district, Haryana (India)". *J. Earth Syst. Sci.*, 127(2), 1-11.

Romshoo, S. A., Taikan, O., and Katumi, M. (2002). "C-band radar for soil moisture estimation under agricultural conditions". In *IGARSS IEEE Trans. Geosci. Remote Sens.*, 4, 2217-2219.

Sahebi, M. R., Bonn, F., and Gwyn, Q. H. J. (2003). "Estimation of the moisture content of bare soil from RADARSAT-1 SAR using simple empirical models". *Int. J. Remote Sens.*, 24(12), 2575-2582.

Saleh, A. (1993). "Soil roughness measurement: chain method". *J Soil Water Conserv.*, 48(6), 527–529

Saux-Picart, S., Ottlé, C., Decharme, B., André, C., Zribi, M., Perrier, A., Coudert, B., Boulain, N., Cappelaere, B., Descroix, L., and Ramier, D. (2009). "Water and energy budgets simulation over the AMMA-Niger super-site spatially constrained with remote sensing data". *J. Hydrol.*, 375(1-2), 287-295.

Schmugge, T. J., Jackson, T. J., and McKim, H. L. (1980). "Survey of methods for soil moisture determination". *Water Resour.*, 16(6), 961-979.

Schmugge, T.J. (1984). "Microwave remote sensing of soil moisture". Recent Advances in Civil Space Remote Sensing, *SPIE*, 481, 249–256.

Sekertekin, A., Marangoz, A. M., and Abdikan, S. (2020). "ALOS-2 and Sentinel-1 SAR data sensitivity analysis to surface soil moisture over bare and vegetated agricultural fields". *Comput. Electron. Agric.*, 171, 105303.

Shi, J., Chen, K. S., Li, Q., Jackson, T. J., O'Neill, P. E., and Tsang, L. (2002). "A parameterized surface reflectivity model and estimation of bare-surface soil moisture with L-band radiometer". *IEEE Trans. Geosci. Remote Sens.*, 40(12), 2674-2686.

Shi, J., Wang, J., Hsu, A. Y., O'Neill, P. E., and Engman, E. T. (1997). "Estimation of bare surface soil moisture and surface roughness parameter using L-band SAR image data". *IEEE Trans. Geosci. Remote Sens.*, 35(5), 1254-1266.

Sikdar, M., and Cumming, I. (2004). "A modified empirical model for soil moisture estimation in vegetated areas using SAR data". In *IGARSS 2004, IEEE International Geoscience and Remote Sensing Symposium*, 2, 803-806.

Singh, R. P., Mishra, D. R., Sahoo, A. K., and Dey, S. (2005). "Spatial and temporal variability of soil moisture over India using IRS P4 MSMR data". *Int. J. Remote Sens.*, 26(10), 2241-2247.

Song, K., Zhou, X., and Fan, Y. (2009). "Empirically adopted IEM for retrieval of soil moisture from radar backscattering coefficients". *IEEE Trans. Geosci. Remote Sens.*, 47(6), 1662-1672.

Song, K., Zhou, X., and Fan, Y. (2010). "Retrieval of soil moisture content from microwave backscattering using a modified IEM model". In *Electromagnetics Research B*, 26, 383-399.

Srivastava, H. S., Patel, P., Manchanda, M. L., and Adiga, S. (2003). "Use of multiincidence angle RADARSAT-1 SAR data to incorporate the effect of surface

roughness in soil moisture estimation”. *IEEE Trans. Geosci. Remote Sens.*, 41(7), 1638-1640.

Srivastava, H. S., Patel, P., Navalgund, R. R., and Sharma, Y. (2008). “Retrieval of surface roughness using multi-polarized Envisat-1 ASAR data”. *Geocarto Int.*, 23(1), 67-77.

Tao, L., Li, J., Chen, X, Cai, Q., and Zhang, Y. (2017). “An effective model to retrieve soil moisture from L- and C-band SAR data”. *J. Indian Soc. Remote Sens.*, 45, 621–629.

Thoma, D. P., Moran, M. S., Bryant, R., Rahman, M., Holifield-Collins, C. D., Skirvin, S., Sano, E. E., and Slocum, K. (2006). “Comparison of four models to determine surface soil moisture from C-band radar imagery in a sparsely vegetated semiarid landscape”, *Water Resour.*, 42, W01418.

Thoma, D., Moran, M., Bryant, R., Collins, C. H., Rahman, M., and Skirvin, S. (2004). “Comparison of two methods for extracting surface soil moisture from C-band radar imagery”. In *IGARSS IEEE Trans. Geosci. Remote Sens.*, 2, 827-830.

Topp, G. C., Davis, J. L., and Annan, A. P. (1980). “Electromagnetic determination of soil water content: Measurements in coaxial transmission lines”. *Water Resour.*, 16(3), 574-582.

Tripathi, A., and Tiwari, R. K. (2020). “Synergetic utilization of sentinel-1 SAR and sentinel-2 optical remote sensing data for surface soil moisture estimation for Rupnagar, Punjab, India”. *Geocarto Int.*, 1-22.

Ulaby, F. T., and Batlivala, P. P. (1976). “Optimum radar parameters for mapping soil moisture”. *IEEE Trans. Geosci. Remote Sens.*, GE-14(2):81-93.

Ulaby, F. T., Aslam, A., and Dobson, M. C. (1982). “Effects of vegetation cover on the radar sensitivity to soil moisture”. *IEEE Trans. Geosci. Remote Sens.*, (4), 476-481.

Ulaby, F. T., Dubois, P. C., and Van Zyl, J. (1996). “Radar mapping of surface soil moisture”. *J. Hydrol.*, 184(1-2), 57-84.

Ulaby, F. T., Moore, R. K., and Fung, A. K. (1981). "Microwave Remote Sensing: Fundamentals and Radiometry" (Reading, Massachusetts: Addison–Wesley).

Ulaby, F. T., Moore, R. K., and Fung, A. K. (1986). "Microwave Remote Sensing, Active and Passive". 3, *Artech House*, Norwood, MA.

Uppender, P. (2015). "Soil moisture estimation with PALSAR data near Roorkee region". In *National Conference on Recent Advances in Electronics & Computer Engineering* (RAECE, IEEE), 52-58.

Van Oevelen, P. J., and Hoekman, D. H. (1999). "Radar backscatter inversion techniques for estimation of surface soil moisture: EFEDA-Spain and HAPEX-Sahel case studies". *IEEE Trans. Geosci. Remote Sens.*, 37(1), 113-123.

Venturini, V., Bisht, G., Islam, S., and Jiang, L. (2004). "Comparison of evaporative fractions estimated from AVHRR and MODIS sensors over South Florida". *Remote Sens. Environ.*, 93(1-2), 77-86.

Walker, J. P., and Houser, P. R. (2004). "Requirements of a global near-surface soil moisture satellite mission: accuracy, repeat time, and spatial resolution". *Adv. Water Resour.*, 27(8), 785-801.

Wang, H., Magagi, R., and Goita, K. (2017). "Comparison of different polarimetric decompositions for soil moisture retrieval over vegetation covered agricultural area". *Remote Sens. Environ.*, 199, 120-136.

Wang, J. R., and Choudhury, B. J. (1981). "Remote sensing of soil moisture content, over bare field at 1.4 GHz frequency". *J. Geophys. Res. Oceans*, 86(C6), 5277-5282.

Wang, J. R., Hsu, A., Shi, J. C., O'Neill, P. E., and Engman, E. T. (1997). "A comparison of soil moisture retrieval models using SIR-C measurements over the Little Washita River watershed". *Remote Sens. Environ.*, 59(2), 308-320.

Wang, S. G., Li, X., Han, X. J., and Jin, R. (2011). "Estimation of surface soil moisture and roughness from multi-angular ASAR imagery in the Watershed Allied Telemetry Experimental Research (WATER)". *Hydrol. Earth Sys. Sci.*, 15(5), 1415-1426.

Wigneron, J. P., Calvet, J. C., Pellarin, T., Van de Griend, A. A., Berger, M., and Ferrazzoli, P. (2003). “Retrieving near-surface soil moisture from microwave radiometric observations: Current status and future plans”. *Remote Sens. Environ.*, 85(4), 489-506.

Woodhouse, I. H. (2009). “Introduction to microwave remote sensing” (Special Indian edition), CRC press.

Xing, M., He, B., Ni, X., Wang, J., An, G., Shang, J., and Huang, X. (2019). “Retrieving surface soil moisture over wheat and soybean fields during growing season using modified water cloud model from Radarsat-2 SAR data”. *Remote Sens.*, 11(16), 1956.

Yang, L., Feng, X., Liu, F., Liu, J., and Sun, X. (2019). “Potential of soil moisture estimation using C-band polarimetric SAR data in arid regions”. *Int. J. Remote Sens.*, 40(5-6), 2138-2150.

Yang, L., Li, Y., Li, Q., Sun, X., Kong, J., and Wang, L. (2017). “Implementation of a multiangle soil moisture retrieval model using RADARSAT-2 imagery over arid Juyanze, northwest China”. *J. Appl. Remote Sens.*, 11(3), 036029.

Zhan, X., Houser, P. R., Walker, J. P., and Crow, W. T. (2006). “A method for retrieving high-resolution surface soil moisture from hydros L-band radiometer and radar observations”. *IEEE Trans. Geosci. Remote Sens.*, 44(6), 1534-1544.

Zhang, D., Li, Z. L., Tang, R., Tang, B. H., Wu, H., Lu, J., and Shao, K. (2015). “Validation of a practical normalized soil moisture model with in situ measurements in humid and semi-arid regions”. *Int. J. Remote Sens.*, 36(19-20), 5015-5030.

Zhang, L., Li, H., and Xue, Z. (2020). “Calibrated integral equation model for bare soil moisture retrieval of synthetic aperture radar: A case study in Linze County”. *Appl. Sci.*, 10(21), 7921.

Zhang, L., Lv, X., Chen, Q., Sun, G., and Yao, J. (2020). “Estimation of surface soil moisture during corn growth stage from SAR and optical data using a combined scattering model”. *Remote Sens.*, 12(11), 1844.

Zhang, M., Lang, F., and Zheng, N. (2021). "Soil moisture retrieval during the wheat growth cycle using SAR and optical satellite data". *Water*, 13(2), 135.

Zhang, X., Chen, B., Zhao, H., Li, T., and Chen, Q. (2018). "Physical-based soil moisture retrieval method over bare agricultural areas by means of multi-sensor SAR data". *Int. J. Remote Sens.*, 39(12), 3870-3890.

Zribi, M., and Dechambre, M. (2003). "A new empirical model to retrieve soil moisture and roughness from C-band radar data". *Remote Sens Environ.*, 84(1), 42-52.

Zribi, M., Muddu, S., Bousbih, S., Al Bitar, A., Tomer, S. K., Baghdadi, N., and Bandyopadhyay, S. (2019)." Analysis of L-band SAR data for soil moisture estimations over agricultural areas in the tropics". *Remote Sens.*, 11(9), 1122.

LIST OF PUBLICATIONS

International Journals

- 1 Gururaj, P., Umesh, P. & Shetty, A. (2021), “Modeling of surface soil moisture using C-band SAR data over bare fields in the tropical semi-arid region of India”. *Appl Geomat.* 13, 555–564. <https://doi.org/10.1007/s12518-021-00370-7>.
- 2 Gururaj, P., Umesh, P. & Shetty, A. (2021), “Assessment of surface soil moisture from ALOS PALSAR-2 in small-scale maize fields using polarimetric decomposition technique”. *Acta. Geophys.* 69, 579–588. <https://doi.org/10.1007/s11600-021-00557-x>.
- 3 Gururaj, P., Umesh, P. & Shetty, A. (2022), “Evaluation of surface soil moisture models over heterogeneous agricultural plots using L-band SAR observations”. *Geocarto Int.* <https://doi.org/10.1080/10106049.2022.2032398>.
- 4 Gururaj, P., Umesh, P. & Shetty, A. “Surface soil moisture model development based on different crop stages using C-band SAR observations”. (*Accepted, Modelling of Earth Systems and Environment*)

Conference Papers

- 1 Punithraj G., Pruthviraj U., Shetty A. (2020), “Surface Soil Moisture Retrieval Using C-Band Synthetic Aperture Radar (SAR) over Yanco Study Site, Australia—A Preliminary Study”. In: Ghosh J., da Silva I. (eds) *Applications of Geomatics in Civil Engineering. Lecture Notes in Civil Engineering*, vol 33, 107-121, Springer, Singapore. https://doi.org/10.1007/978-981-13-7067-0_8.
- 2 Punithraj Gururaj, Pruthviraj Umesh, and Amba Shetty (2019), "Assessment of spatial variation of soil moisture during maize growth cycle using SAR observations", Proc. SPIE 11149, Remote Sensing for Agriculture, Ecosystems, and Hydrology XXI, 1114916 (21 October 2019). <https://doi.org/10.1117/12.2532953>.
- 3 Gururaj, P., Umesh, P., and Shetty, A. (2020), “Assessment of surface soil moisture distribution across small scale tomato fields using L band SAR data”, EGU General Assembly 2020, Online, 4–8 May 2020, EGU2020-623. <https://doi.org/10.5194/egusphere-egu2020-623>.

- 4 Punithraj Gururaj, Liya Mary, Pruthviraj umesh and Amba shetty (2020)
"Quantitative retrieval of surface soil moisture using ALOS PALSAR-2
polarimetric data in small scale farm fields" National conference on innovative
research advances in engineering applications and processes, Jyothy institute of
technology, Bangalore, 28 Aug 2020 (Virtual).

CURRICULUM VITAE



Name:	PUNITHRAJ G
--------------	--------------------

Permanent Address:	S/o Gururaj M D, Door no. 339, 4 th Cross, Siddhartha nagar Malavalli, Mandya, Karnataka - 571430
---------------------------	--

EDUCATION:	MASTER OF ENGINEERING (2014-16) <i>Discipline:</i> Water Resources Engineering University Visvesvaraya College of Engineering, Bengaluru Karnataka <i>Affiliated to:</i> Bangalore University, Bangalore.
	BACHELOR OF ENGINEERING (2010-2014) <i>Discipline:</i> Civil Engineering University Visvesvaraya College of Engineering, Bengaluru Karnataka <i>Affiliated to:</i> Bangalore University, Bangalore.

Contact No.:	+91-9740309708
---------------------	----------------

Email ID:	puniththeraj@gmail.com
------------------	------------------------

SCOPUS ID:	57214089414
-------------------	-------------
